EFFECTS OF VOLTAGE UNBALANCED SUPPLIES ON ENERGY-EFFICIENT MOTORS

A Thesis is submitted to the University of Cape Town in full fulfillment of the academic requirements for the Degree of Master of Science in Electrical Engineering.

Prepared by: Mr Ashwill Louis Van Wyk

Supervised by: Dr M.A. Khan
Co-Supervised by: Dr P.S. Barendse

Date: 1 November 2010

DECLARATION

I, **Ashwill Louis Van Wyk,** declare that this dissertation is my own work. All information that is not of my own has been referenced. I declare that this thesis has not been presented and will not be presented to any other University for a similar or any other degree award.

Signature……

Date: ……

University of Cape Town, Cape Town

Acknowledgements

The author would like to thank the following:

- God Almighty for really spoiling me with so many blessings throughout my academic career to Him be all the praise and the glory;
- My parents for their unconditional love and support;
- My supervisor, Dr Azeem Khan for his advice and guidance for the duration of this thesis;
- My friends and colleagues; Ms Barbara Herndler, Mr Hartmut Jagau, Mr Ernest Ohene Anyang, Mr Wanjiku Gitonga, Mr Jaques De La Bat, Mr Henry Po-Heng and Dr Richard Okou for their assistance;
- Dr Marubini Manyage for his advise
- The lab supervisor, Mr Chris Wozniak for his advise and Mr Phillip Titus, for his technical support;
- And finally, Eskom and the NRF for the financial support.

CONTENTS Page

LIST OF FIGURES

EXECUTIVE SUMMARY

UNBALANCED OPERATION OF ENERGY EFFICIENT MOTORS

OVERVIEW

Eskom DSM has recently introduced an Energy Efficiency (EE) Motor program, which provides incentives to industrial customers to retrofit standard motors with EE motors. The main objective of the program is to realize energy savings through the replacement of standard (STD) induction motors with higher efficiency EE motors. Although the principle of the program is correct, there are several significant power quality and performance issues with EE motors. These issues need to be thoroughly investigated in order to achieve the overall energy saving objectives of program. This research report addresses some of these issues through detailed testing, analysis and comparison of standard and EE motors. This will ultimately ensure the success of Eskom DSM's EE motor program.

BACKGROUND

The depletion of natural resources and the negative impact of green house gases (GHG) on the environment have resulted in a global focus on energy conservation and energy efficiency. Induction motors are widely used in industry and drive the largest percentage of loads. In South Africa (SA), motorized systems account for up to 60% of the consumed electricity in the industrial sector. Small improvements in motor efficiency can therefore yield significant energy savings, which could delay the need for additional generating capacity. Most electric motors imported into South Africa are still of the standard efficiency type. New energy efficient (EE) motors are currently being endorsed and incentivised by Eskom Demand Side Management (DSM) through their EE motor program. This research project addresses issues relating to EE motors.

OBJECTIVES

The main objectives of this research project include:

- Development and commissioning of a flexible 22kW test rig for testing standard and non-standard motor frame designs. This rig includes a flexible supply that can emulate various supply voltage unbalances.

- Comparing the design and performance differences between STD and EE motors,
- Quantifying the differences in efficiency between STD and EE motors,
- Assessing the impact of supply voltage unbalance in combination with over-voltages or under-voltages on the efficiency, and
- Temperature rise of EE motors.
- Perform an error analysis of the efficiency results

APPROACH

Several STD and EE motors were procured for the purposes of this research project. The investigation was limited to four STD and four EE motors, each group with ratings of 3kW, 7.5kW, 11kW and 15kW. The motors were LV (380V), 4-pole, 50Hz machines, and were procured from the same vendor. The motors were tested in accordance with the three main international standards for testing induction motors. These included: the IEEE 112-B, the IEC 60034-2 and the IEC 60034-2-1. Several tests were performed at rated, unbalanced, over- and under-voltage supply conditions per motor and numerical averaging applied to obtain a representative response of the motor. Detailed analysis of the test results were performed with the aid software programs written in MATLAB. In depth comparisons were made between the results obtained for the standard and EE motors.

RESULTS

The design and operational differences between STD and EE motors were investigated. It was found that the main improvements implemented to increase the efficiency of EE motors includes: use of better lamination steel, over-sizing the stator conductors in order to reduce the stator copper losses, over-sizing the rotor conductors in order to reduce the rotor joule losses and smaller cooling fans to reduce the windage loss on EE motors.

The differences between international standards for testing induction motors were investigated. It was found that the efficiency results of the same motor vary depending on the standard used to test the motor. This is primarily due to the difference in the treatment of stray load losses between the standards. The catalogue efficiency values are often different to that predicted by the standards.

The efficiency differences between standard and EE motors vary between 2 to 4% across the load range of the motors. It was found that the EE motors generally exhibit a flatter efficiency vs. load profile. The peak efficiencies of the STD and EE motors also occurs at different loadings.

The impact of voltage unbalance on EE motors was also assessed. The definitions of voltage unbalance were first assessed before a suitable definition could be used for the purpose of the research project. The range of standard and EE motors under consideration were then subjected to unbalanced supply voltage conditions of 0%, 2.5% and 5%. The voltage unbalance was introduced in turn with average rating (380V) across the machine; with the average line voltage at 10% above rated and finally with the average at 10% below rated voltage. It was found that the voltage unbalance results in a larger % current unbalance in EE motors. This is primarily due to the lower negative sequence impedance associated with EE motors. Furthermore, the presence of a negative sequence current in a motor results in a negative sequence torque, which ultimately leads to a lower resultant shaft torque.

When subjected to the supply voltage unbalance, it was observed the EE motors experience a larger % temperature increase. However, these % temperature increases result in lower final operating temperatures than that reached by corresponding STD motors which were subjected to the same unbalance supply conditions.

The efficiency of STD and EE motors are adversely affected by supply voltage unbalance. The greatest drop in efficiency is experience during under voltage conditions with unbalance.

CONCLUSIONS

Based on the findings presented in this report the following conclusions can be drawn:

The efficiency of a motor is not an absolute value. It is largely dependent on the international testing standard used. The catalogue efficiency provided by the supplier (for all motors tested) showed no correlation with any of the efficiency results obtained from tests according to the standards.

The EE motors are approximately 2 – 4% more efficient than STD motors, and also exhibit a relatively flat efficiency versus load curve.

The IP rating has significant effects on the friction and windage loss. The higher IP rating found on the energy efficient motors increases the friction and windage losses to up to four times than that of the standard motors.

EE motors produce less core loss because of the type of core material used and the thinner laminations.

EE motors operate at a lower slip when retrofitted with a standard motor on a centrifugal pump load system. This could lead to higher output power delivered to the pump and marginally less input power drawn from the supply.

Separate stator and rotor thermal model circuits were adopted. Tests were performed to determine thermal parameters from tests rather than from motor design data. The developed thermal model was able to predict the steady state temperatures to a maximum deviation of less than 4°C from the measured values.

The definitions of voltage unbalance developed by NEMA, IEEE and IEC have been studied. The IEEE uses a similar definition of voltage unbalance as NEMA, the only difference being that the IEEE uses phase voltages rather than line-to-line voltages. The phase angle information for these two definitions is lost since only magnitudes are considered. The IEC definition, referred to as the 'true' definition, involves both magnitude and angles when calculating the positive and negative sequence voltage components. Two formulas that avoid the use of complex algebra were also presented.

The IEEE standard 112-A was adopted to test and investigate the effects of voltage unbalance on standard and energy efficient motors. This method, also known as the direct method, was used since the absolute efficiency values of the motors aren't considered important and was merely used to compare trends.

Unbalanced supply conditions are detrimental to the efficiency of STD and EE motors. A higher % current unbalance is produced in EE motors compared to STD motors for the same

unbalanced supply voltage conditions. The negative sequence current present during voltage unbalance produces a negative sequence torque, which results in a lower shaft torque. The % temperature rise is greater for EE motors subjected to the same voltage unbalance as STD motors. However, EE motors run, on average 18.2°C cooler because they generate less I^2R heat, thus producing less stress on the windings.

RECOMMENDATIONS

Based on the findings in this report the following recommendation can be made:

A comprehensive study was done on the steady state differences between STD and EE motors. However, work needs to be done on the transient performance of EE motors. This includes start-up current analysis, start-up and breakdown torque performance, etc. The high inrush current drawn by energy efficient motors could have serious implications on protection systems and cables in a retrofit application. This is known to cause nuisance tripping of circuit breakers and needs to be investigated.

A new derating curve for energy efficient motors should be developed which includes a combination of over or under voltages with unbalanced voltages. The NEMA derating curve that exists was developed for standard motors and may or may not be conservative when applied to EE motors. The new derating curve will provide guidelines on how to "derate" an EE motor to avoid overheating and loss of life when the motor is operating in the presence of voltage unbalance with a combination of over or under voltages.

For the purpose of this thesis four motor ratings were considered. However, to obtain more representative results more motors from several manufacturers should be tested and analysed.

The motor temperature should be allowed to stabilize for every supply condition implemented for efficiency testing.

EE motors operate at a lower slip when replacing a standard motor on a centrifugal pump load system. The higher output power delivered to the pump and hence the marginally lower input power drawn from the supply could result in negligible savings to the user. This phenomenon

should thoroughly be investigated with several load and EE motor types. This could represent a serious threat to the success of Eskom DSM's EE motor program.

INDUSTRY PERSPECTIVE

This research supports Eskom DSM's EE motor program directly. A better understanding of the steady-state performance of EE motors was developed. The ultimate objective of this research and subsequent proposal is to develop a guideline for the effective retrofitting of STD motors with EE motors. This, together with the current subsidy associated with the EE motor program will ensure the envisaged saving in electricity demand and the ultimate success of the EE motor program.

KEYWORDS

energy efficient motor, efficiency, voltage unbalance, error analysis.

FUTURE REVIEW

Due to the results from this study, it is imperative for the results to be verified and the tests to be repeated for other motor ratings and manufacturers. This is critical as it could have implications on the current DSM EE Motor Programme.

CHAPTER 1

1. INTRODUCTION

The depletion of natural resources, the negative impact of green house gases (GHG) on the environment and the security of electricity supply have resulted in a global focus on energy conservation, energy efficiency and renewable energy.

In March 2005, the South African (SA) Cabinet approved the Department of Minerals and Energy (DME) Energy Efficiency Strategy target to reduce the total electricity demand by 12% by 2015. Eskom Demand Side Management (DSM) has also been investing considerable resources in energy efficiency initiatives to reduce electrical energy demand by 3GW before 2012.

In South Africa, the industrial sector accounts for over two-thirds of the country's national electricity consumption. Motorized systems in South Africa currently account for approximately 57% of the peak electricity demand. Induction motors in particular are widely used in industry and drive the largest percentage of loads. The recent power crisis in SA has highlighted the need for motor efficiency optimization. Improvements in motor efficiency can yield significant energy savings and therefore delay the need for additional generating capacity.

Most electric motors imported into South Africa are still of the standard efficiency type. Eskom DSM has recently introduced an Energy-Efficient (EE) motor program, which provides incentives to industrial customers to retrofit standard motors with EE motors. The main objective of the program is to realize energy savings through the replacement of standard induction motors with more efficient EE motors. Although the principle of the program is correct, there are several significant power quality and performance issues with EE motors. These issues need to be thoroughly investigated in order to achieve the overall energy saving objective of the program. This thesis addresses some of these issues through detailed testing, analysis and comparison of standard and EE

motors. The findings presented in this thesis will assist in ensuring the success of Eskom's DSM EE motor program.

1.1 BACKGROUND

Globally, electric motors and their associate systems consume 40% of the electricity consumption. Motorized systems in South Africa currently account for approximately 57% of the peak electricity demand. There are more than 17,500 motors running in SA, with power ratings from 0.15kW up to 36MW. Together, these motors represent 10GW of installed capacity.

Eskom DSM introduced an EE motor program to industry in 2008, which provides incentives to industrial customers to retrofit standard motors with EE motors. The main objective of the program is to realize energy savings through the replacement of standard induction motors with higher efficiency EE motors. Motors in the range from 0.75-90kW are included in the program.

In general, a 1% voltage unbalanced applied to standard induction motors results in a greater current unbalance, typically 5-6%. Furthermore, the lower stator and rotor resistances associated with EE motors results in even greater percentage current unbalance in EE motors. This may lead to a more decreased efficiency and a more increased temperature rise in EE motors that are retrofitted in industries where these power quality problems are prevalent. Furthermore, the variability of EE motor designs and manufacturing techniques from Eskom's DSM approved EE motor distributors, will further complicate the assessment of the impact of these power quality problems on EE motors. The effects of voltage unbalance on EE motors in South Africa is not known and should be investigated to ensure the success of Eskom DSM's EE motor program.

1.2 SCOPE

This thesis investigates power quality and performance issues with EE motors. The power quality issues will include the impact of voltage unbalance in combination with over-voltages or under-voltages on the efficiency of a range of EE motors.

1.3 OBJECTIVES

The main objectives of this thesis include:

- Development and commissioning of a flexible 22kW test rig for testing standard and non-standard motor frame designs. This rig includes a flexible supply that can emulate various supply voltage unbalances.
- Comparing the design and steady-state operational performance differences between STD and EE motors.
- Quantifying the efficiency differences between STD and EE motors.
- Assessing the impact of supply voltage unbalance, in combination with over-voltages or under-voltages, on the efficiency and temperature rise of STD and EE motors.
- Perform an error analysis on the efficiency results.

1.4 RESEARCH QUESTIONS

The research questions considered in this thesis include:

1. What are the design and steady-state operational differences between STD and EE motors?

2. Can the efficiency differences between STD and EE motors be quantified?

3. What is the impact of supply voltage unbalance, in combination with over-voltages or under-voltages, on the efficiency of STD and EE motors of four different sizes?

1.5 METHODOLOGY

The methodology associated with this research is mainly analytical and experimental. Several STD and EE motors were procured for the purposes of this research project. The investigation was limited to four STD and four EE (Premium Plus)motors, each group with ratings of 3kW, 7.5kW, 11kW and 15kW. The motors were LV (380V), 4-pole, 50Hz machines, and were procured from the same vendor. The motors were tested in accordance with the three main international standards for testing induction motors. These included: the IEEE 112-B, the IEC 60034-2 and the IEC 60034-2-1. Several tests were performed at rated, unbalanced, over- and under-voltage supply conditions, on each motor and numerical averaging applied to obtain a representative performance of the motor. Detailed analysis of the test results were performed with the aid programs written in MATLAB. In-depth comparisons were made between the results obtained for the standard and EE motors.

1.6 LIMITATIONS

The experimental work is limited to standard and EE motors from the same vendor. The range of motors included in the study is: 3kW, 7.5kW, 11kW and 15kW. The general ratings of the machines are: 4-pole, 380V, 50Hz.

1.7 THESIS STRUCTURE

Chapter 1 describes the background to this thesis, the problem description, objectives and scope and limitations are all presented along with a short introduction.

Chapter 2 discusses the some of the existing motor efficiency classification schemes and presents a cost analysis in the South African context.

Chapter 3 deals with the analytical modelling of induction motors and a discussion of the various definitions of voltage unbalance.

Chapter 4 outlines the laboratory setup of the instrumentation and equipment required for the experimental procedures; the testing process is also explained in its entirety.

Chapter 5 discusses some design differences between STD and EE motors. It then presents the steady state and dynamic performance differences between STD and EE motors.

Chapter 6 presents the current and voltage unbalance experimental results.

Chapter 7 involves a comprehensive error analysis of the estimated efficiencies obtained by the three methods presented in this thesis**.**

Chapter 8 presents the conclusions and recommendations.

CHAPTER 2

2. INDUCTION MOTOR EFFICIENCY CLASSES

This chapter discusses the different efficiency classification schemes for induction motors that exist worldwide. It then refers to ESKOM's motor subsidy program before looking at the cost differential of STD and EE motors before and after the rebate is taken in into account.

2.1 EFFICIENCY CLASSIFICATION SYSTEMS

Until the energy crises in the 1970s, most general-purpose motors were designed to provide rated output and operating characteristics at reasonable cost. Efficient operation was at best a secondary consideration. However, as energy prices began rising, manufacturers began promoting improved efficiency motors which they branded as "high-efficiency" and "energy-efficient", despite the fact that these terms were not specifically defined at the time. [1]

In 1992 the US Congress enacted the Energy Policy Act. Several years later in 1997, did this Energy Policy Act set minimum efficiency standards for certain classes of electric motors in USA. There are many different motor efficiency classification standards that exist worldwide today. The most important are listed below [2]:

- 1992 – USA – *Energy Policy Act (EPAct)*
- 1997 – USA – *Mandatory Minimum Efficiency Levels (NEMA Standard MG-1-1993)*
- 2001 – USA – *NEMA Premium Motors Standards (Voluntary)*
- 2001 – Europe – *CEMEP* Motors Standards (Eff1, Eff2, Eff3)
- 2002 – Brazil – Mandatory *Minimum Efficiency Levels (Standard and High-Efficiency)*
- 2005 – Brazil – *Mandatory Minimum Efficiency Levels (High Efficiency)* from 2010
- 2009 – Europe – *IEC establishes standards* IE1 (Standard Efficiency), IE2 (High Efficiency), IE3 (Premium Efficiency)

The commonly used standards in South Africa are the NEMA (National Electrical Manufacturers Association), CEMEP (Comité Européen de Constructeurs de Machines Electriques et d'Electronique de Puissance) and recently the IEC (International Electrotechnical Commission) efficiency standards. Notably, Eskom currently only considers the CEMEP standard, which has recently been succeeded by the IEC 60034-30 standard. The afore-mentioned three standards will be discussed further due to their relevance to South Africa.

2.1.1 NEMA Standard (EPAct)

EPAct was established in 1992 and only came into effect in 1997 and was later improved in 2001. According to the Act, motors in a specific range that are manufactured after October 24, 1997 must meet a specific full-load nominal efficiency that is consistent with the NEMA standard. EPAct dictates that the nominal full load efficiency standards for the open and enclosed 2, 4, 6 pole motors are consistent with NEMA Standard energy efficient table and with testing procedures conducted after IEEE STD 112 Method B. Figure 1 shows the minimal ($NEMA_{min}$) and the nominal ($NEMA_N$) energy efficiency range which motors need to comply with. [1]

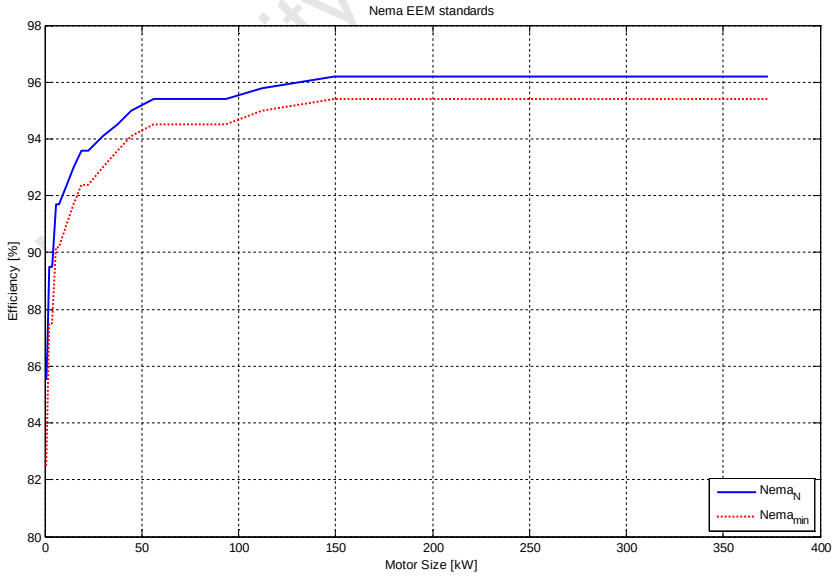

Figure 1: NEMA EEM Standard

2.1.2 The CEMEP Standard

CEMEP represents the European Manufacturers of Electrical Machines and Power electronics equipment and systems. It was founded on the 1st of January 1991 succeeding the two section committees COMEL and COCOS, which were disbanded on the 31st of December 1990. [3]

The agreement defined three efficiency classes (Eff1, Eff2 and Eff3) for low-voltage three-phase motors. The motors included in this scheme are defined as totally enclosed fan ventilation (IP 54 or IP 55) three phase A.C. squirrel cage induction motors in the range 1.1 to 90kW, having 2- or 4-poles, rated for 400V line, 50Hz, S1 duty class, in standard design. (Standard design can be interpreted as Design N according to IEC 60034-12 and IEC 50347). Efficiency values are determined on the basis of the summation of losses method in accordance to IEC 60034-2.

The efficiency classification system has been introduced and successfully adopted in many countries worldwide. The CEMEP standard was interpreted differently by individual countries, which lead the IEC to develop and publish an energy efficiency standard which addressed all the different national issues. In parallel, IEC developed and issued a new standard for the determination of motor efficiencies. The new standard IEC 60034-30 defines and harmonizes worldwide the efficiency classes IE1, IE2 and IE3 for low-voltage three-phase motors. Figure 2 illustrates the efficiency regions of the CEMEP standard. [3]

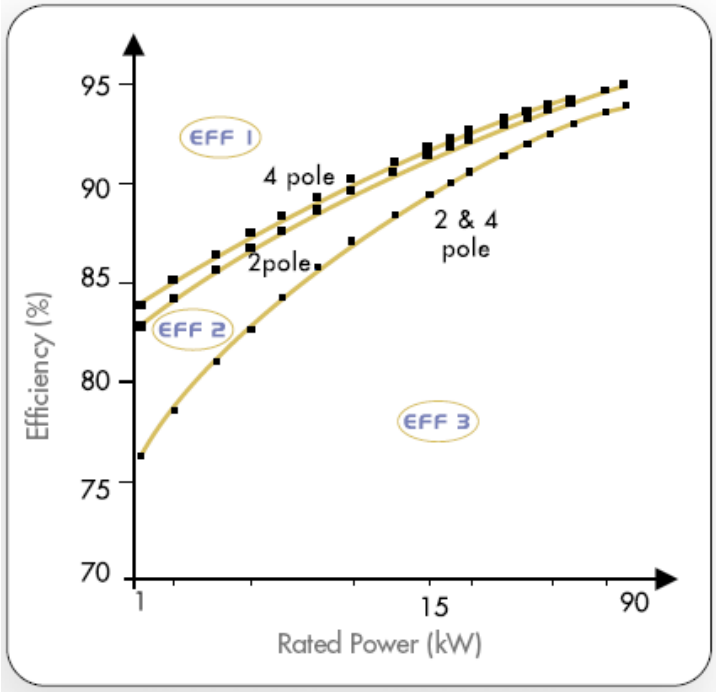

Figure 2: CEMEP EEM Standard IEC Standard

The IEC standard for energy efficient motors (EEM) is found in the IEC 60034-30. Currently there are three types of EEM classes, namely:

- IE1: Standard Efficiency
- IE2: High Efficiency
- IE3: Premium Efficiency
- IE4: Super Premium Efficiency

The fourth EE motor class (IE4) is envisaged, but is not yet part of the IEC standard as more experience with such products is required before standardization [5].

In this standard, the nominal 50Hz limitations of Standard (IE1) and High Efficiency (IE2) are based on the well-known CEMEP Eff2 and Eff1 limits respectfully, which can also be seen in Figure 2. However, they have been adjusted to take the different test procedures into account. The method for measuring the efficiency of low-voltage three-

phase asynchronous motors was revised with the new IEC 60034-2-1 (2007-09) standard, which replaced the previous standard IEC 60034-2 (1996). The new standard significantly increases the accuracy under defined laboratory conditions. CEMEP assumed fixed stray load losses (*SLL)* of 0.5% of the input power at rated load. For the revised IEC standard, the *SLL* is determined from tests performed under laboratory conditions [4]. Table 1 illustrates the adapted measuring standard.

Table 1: Methods for measuring efficiency [4]

Measuring efficiency for the European classification scheme	
Old efficiency testing standard EN / IEC 60034-2: 1996	**New efficiency testing standard IEC 60034-2-1: 2007-09**
Direct method	Direct method
Indirect method:	Indirect method:
• SLL estimated at 0.5% of input power at rated load	• SLL determined from measurement
	• SLL estimated at 2.5% - 0.5% of input power at rated load
	• Eh star – alternative indirect method with mathematical calculation of SSL
Winding losses in stator and rotor determined at 95 °C	Winding losses in stator and rotor determined at [25 °C + temperature rise measured]

In a direct comparison of both measuring methods applied to the same motor, it is expected that the efficiency levels determined according to the new method are up to a few percentage points lower than the efficiency obtained using the old method. To achieve compatibility with the old Eff1 and Eff2 classes, the limit values of IE2 and IE1 classes were lowered slightly. For example, a 11 kW, 4-pole Eff1 motor with 91.0% efficiency is identical with a new IE2 motor with 89.8% efficiency. The motor has not physically changed but was measured using two different methods. Table 2 compares the three different standards discussed above [1]. A comparison of a range of EE motor efficiencies according to the CEMP and IEC standards are in Figure 3.

Table 2: Overview of EE Motor standards [*Source: www.abb.com*]

IEC 60034-30	**EU MEPS**	**CEMEP**	**US EPAct**	**Other, similar local regulations**
IE3 Premium efficiency	IE3 Premium efficiency		Identical to NEMA Premium efficiency	
IE2 High efficiency	IE2 High efficiency	Comparable to EFF1	Identical to NEMA Premium efficiency / EPACT	Canada Mexico Australia New Zealand Brazil 2009 China 2011 Switzerland 2012
IE1 Standard efficiency		Comparable to EFF2	Below standard efficiency	China Brazil Costa Rica Israel Taiwan Switzerland 2010

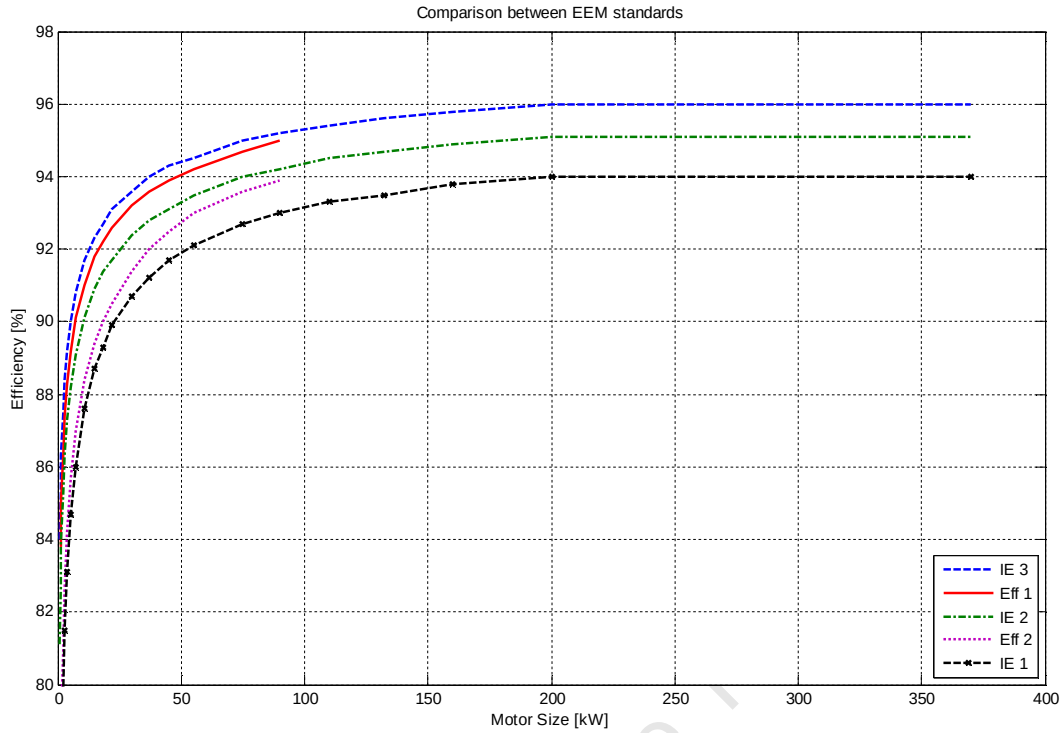

Figure 3: Comparison between the different EE motor standards (4-pole) [3], [4]

2.2 ESKOM DSM'S EE MOTOR PROGRAM

Eskom DSM introduced an EE motor program in 2008. The main objective of the program is to incentivize the replacement of standard induction motors with EE motors. Motors in the range from 0.75-90kW are included in the program. Financial incentives are offered for the replacement of standard motors with EE motors procured from vendors approved by Eskom DSM.

DSM involves technical and behavioural measures driven by a utility in order to influence the demand for electricity. In the short term, DSM is an effective measure to reduce load shedding incidents and to reduce the cost of operating expensive peaking plants. In the long term, DSM is often a favourable alternative to supply-side investments as the electricity demand is being managed. [5]

Eskom's DSM consists of many programs targeting energy efficiency, such as the EEM program. Globally, electric motors and their associate systems consume 40% of the electricity consumption. In South Africa this amounts to 60%. There are more than 17,500 motors running in SA, with power ratings from 0.15kW up to 36MW. Together, these motors represent 10GW of installed capacity. The program is designed to create awareness for the vital contribution these motors can make to increasing national electrical savings.

Eskom's policy is to subsidize all purchases of motors ranging from 1.1kW up to 90kW, which amounts to R400 – R3,500 respectively (see Table 3). The efficient motors available on the program are rated according to the European Union efficiency definitions CEMEP, Eff1 (premium efficiency) and Eff2 (improved efficiency). As the new IEC standard for EEM motors has been launched, Eskom needs to adapt their EEM program to meet the IEC standard. The Eff1 motor is comparable to the IE2 motor and the Eff2 to IE1. [5]

Table 3: Overview of Eskom's DSM Subsidy

kW Rating	4-pole Eff 1	2-pole Eff 1	DSM Subsidy
	Eff(%)		
1.1	≥83.8	≥82.2	R400
1.5	≥85	≥84.1	R400
2.2	≥86.4	≥85.6	R500
3	≥87.4	≥86.7	R500
4	≥88.3	≥87.6	R500
5.5	≥89.2	≥88.5	R700
7.5	≥90.1	≥89.5	R700
11	≥91	≥90.6	R700
15	≥91.8	≥91.3	R700
18.5	≥92.2	≥91.8	R1000
22	≥92.6	≥92.2	R1300
30	≥93.2	≥92.9	R1400
37	≥93.6	≥93.3	R1700
45	≥93.9	≥93.7	R2200
55	≥94.2	≥94	R2600
75	≥94.7	≥94.6	R3000
90	≥95	≥94.6	R3500

Source: www.eskomdsm.co.za

2.3 COST DIFFERENCES BETWEEN STANDARD AND EE MOTORS

There are currently five registered vendors on Eskom DSM's EE motor program. These include [5]:

1. CMG Motors Pty (Ltd)
2. BMG
3. ABB South Africa (Pty) Ltd
4. Indusquip Marketing CC
5. ZEST Electric Motors Pty (Ltd)

The list prices of standard and EE motors from an Eskom DSM approved vendor is presented in this section.

Table 4 shows the purchase cost of the most commonly used motors and illustrates the price difference between the standard efficiency and premium efficiency motor. Prices are taken from the ZEST manufacturer and are all 4 pole motors running at a nominal speed of slightly less than 1,500rpm.

Table 4: Price Comparison between IE1 and IE2 EE Motors

Power Rating [kW]	Price of STD Efficiency (IE1) [ZAR]	Price of High Efficiency (IE2) [ZAR]	Price Difference Without Subsidy [%]	Price Difference With Subsidy [%]
3	4,101	4,716	15.00	2.80
7.5	6,947	7,990	15.01	4.94
11	10,950	12,595	15.02	8.63
15	14,315	16,464	15.01	10.12
22	21,234	24,423	15.02	8.90
37	34,844	40,078	15.02	10.14
45	40,545	46,633	15.02	9.59
55	52,188	60,024	15.01	10.03

It can be seen that there is a consistent 15% price difference between standard and energy efficient motors, when subsidies are not accounted for. Notably this increase is independent of motor size. In contrast, the price increase differs greatly when subsidies are taking into account and are dependent on the size of the motor.

CHAPTER 3

3. ANALYTICAL MODELLING OF INDUCTION MOTORS

This chapter deals with the modelling and performance analysis of induction motors on a per phase basis.

3.1 SYMMETRICAL COMPONENTS

Symmetrical components can be used in order to analyse an unbalanced supplied induction motor on a per phase basis. The symmetrical components theory was developed in 1918 by Charles L. Fortescue [6] which essentially converts any poly-phase unbalanced system into independent symmetrical systems. Thus, an unbalanced three-phase network can be resolved into two balanced systems and a zero sequence component. These balanced systems are known as the positive and negative sequence components.

The zero sequence components are equal in magnitude and have no phase displacement. However, it can be eliminated since induction motors are typically connected in delta or ungrounded star, hence no zero sequence currents will flow, except in a fault condition [7],[8].

The sequence components can be found from the phase components by applying a transformation matrix as shown below:

$$\begin{matrix} V \\ V \\ V \end{matrix} = - \begin{matrix} 1 & 1 & 1 \\ 1 & a & a \\ 1 & a & a \end{matrix} \begin{matrix} V \\ V \\ V \end{matrix} \qquad (1)$$

Where:

phasor operator $a = e^{j\frac{2}{3}\pi}$.

3.1.1 Positive Sequence Network

The positive sequence network consists of three phasors, equal in magnitude with phase displacements of 120° and positive sequence rotation as depicted in Figure 4.

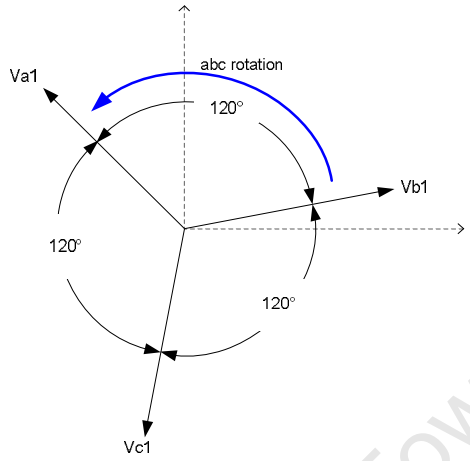

Figure 4: Positive sequence network

3.1.2 Negative Sequence Network

The negative sequence network also consists of three equal in magnitude phasors with a phase displacement of 120°, but has a negative sequence as shown in Figure 5.

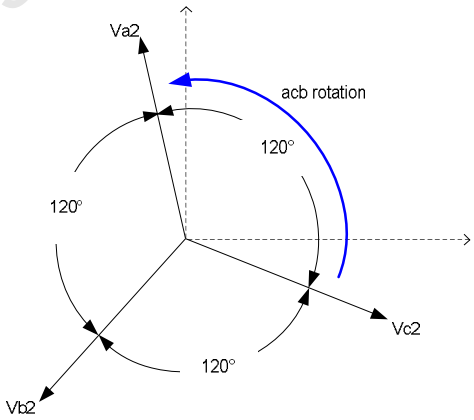

Figure 5: Negative sequence network

The negative sequence can effectively be obtained by interchanging two leads applied to the stator terminal. The rotating field in the air gap established in this circuit rotates at synchronous speed but in the opposite direction to that of the positive sequence [9]. The negative sequence slip is given by [9]:

$$s_n = 2 - s \tag{2}$$

3.1.3 Zero Sequence Network

As can be seen from Figure 6, the zero sequence network consists of three phasors with equal magnitudes and no phase displacement i.e. Va0=Vb0=Vc0.

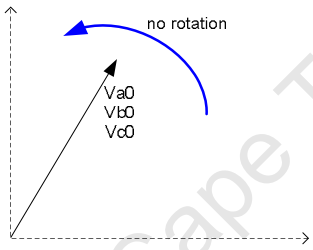

Figure 6: Zero sequence network

3.1.4 Symmetrical Components to ABC conversion

Similarly the ABC network can be reconstructed from the sequence component using the matrix below:

$$\begin{matrix} V \\ V \\ V \end{matrix} = \begin{matrix} 1 & 1 & 1 \\ 1 & a & a \\ 1 & a & a \end{matrix} \begin{matrix} V \\ V \\ V \end{matrix} \tag{3}$$

From the above matrix it is clear that for example V_a is the summation of the three sequence components and can graphically be illustrated as in Figure 7.

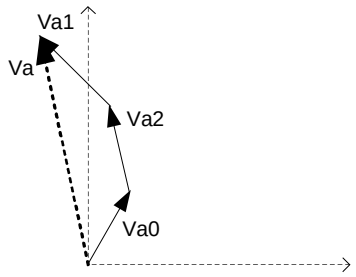

Figure 7: Conversion between ABC and sequence domain

The transformation in the matrix equation 1&3 can also be applied to the current phasors as can be seen in chapter 6.

3.2 DEFINITIONS OF VOLTAGE UNBALANCE

The term voltage unbalance is not uniquely defined. A specific voltage condition can be expressed in different percentages depending on which definition is used. In this section, four of the most commonly used definitions are discussed.

3.2.1 NEMA

The NEMA definition of voltage unbalance, also known as the line voltage unbalance rate (LVUR) [10,11,16] is given by:

$$LVUR = \frac{\cdot \qquad \cdot}{\cdot} \times 100\ [\%] \qquad (4)$$

The NEMA definition requires only magnitudes of the line voltages and the phase angles are not included. Obviously this definition is easy to use as little more than a Digital Multi Meter (DMM) is needed. For this reason the NEMA definition is widely adopted in industry and it is on this basis that it was used throughout this thesis.

3.2.2 IEEE

The IEEE definition of voltage unbalance, also known as the phase voltage unbalance rate (PVUR) [11,16], is given by:

$$PVUR = \frac{\cdot \qquad \cdot}{\cdot} \times 100\ [\%] \qquad (5)$$

The IEEE defines voltage unbalance in a similar way as the NEMA definition. However, the IEEE uses phase voltages rather than line-to-line voltages. As for the NEMA definition, phase angle information is not required.

3.2.3 Approximation Formula

This equation gives a good approximation of the true definition is given by[16]:

$$VU = \frac{\qquad}{\cdot} \qquad (6)$$

Where:

V_{abe} = difference between the line voltage V_{ab} and the average line voltage, etc

.

3.2.4 IEC ("True Definition")

The IEC or the 'true' definition of voltage unbalance is defined as the ratio of the negative sequence voltage component to the positive sequence voltage component. The voltage unbalance factor (VUF) is given by [11,16]:

$$= — \times 100\% \qquad (7)$$

Phase or line voltages can be used for this definition. The positive and negative sequence components can be obtained by decomposing any three phase supply into symmetrical components. The positive and negative sequence components are calculated using the matrix equation 1.

The true definition involves both magnitude and angles when calculating the positive and negative sequence voltage components.

3.3 PER-PHASE EQUVALENT CIRCUIT MODELS

The motor equivalent circuit parameters are based on the IEEE and the IEC standards and are derived from the test data recorded from the no load test and the locked rotor test as described in chapter 4. The equivalent circuit characterises one of the three phases of an induction motor connected in star or even for a delta connected [12] motor. This was the case for the 15 kW, 11 kW and 7.5 kW motors. All parameters are referred to the primary (stator) side and the reactance and impedances are determined at the temperature during the test. The resistances were corrected to the specified temperature.

3.3.1 Positive Sequence Equivalent Circuit.

Figure 8 shows the per phase steady state equivalent circuit. It is worth mentioning that the circuit contains a shunt core loss resistance R that is a representation of the core loss at rated voltage and were calculated using equation 14 according to [12],[13]. The stator resistance R and its leakage reactance X are represented on the left of R and the magnetizing reactance X . On the right, the rotor representation is shown with the rotor leakage reactance X and the slip dependent rotor resistance R /s.

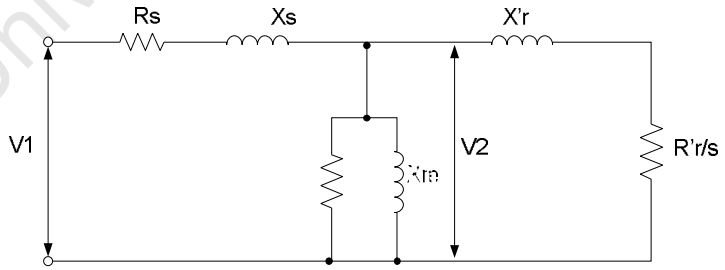

Figure 8: Positive sequence equivalent circuit of induction motor (per-phase)

The reactive power of the complete motor at no load and during the blocked rotor tests were calculated using equations 8 and 9, respectively below:

$$= \overline{\qquad\qquad} \; -$$

$$= \overline{\qquad\qquad\qquad} \quad (8)$$

And:

$$Q = \overline{\qquad\qquad} \; S \; - P$$

$$= \overline{\qquad\qquad\qquad} \quad (9)$$

The magnetizing reactance and stator leakage reactance can be calculated [12],[13] using the non linear equations 10 and 12 by initially assuming a value for — and X and recalculating until X and X deviates by less than 0.1% of the preceding value. To perform this calculation the iteration loop was coded in MATLAB.

The magnetizing reactance is calculated by equation 10 below:

$$= \frac{\qquad}{(\qquad)} \times \frac{\qquad}{(\quad —)} \quad (10)$$

The stator leakage reactance at the test frequency is given by equation 11

$$= \frac{\qquad\qquad}{— \quad —} \times \quad — \; + \; — \quad (11)$$

The stator leakage reactance at rated frequency is given by equation 12.

$$= \frac{}{——} \times X \quad (12)$$

Since all the motors that were tested are of NEMA design B type (or IEC type N), — is equal to 1. The per phase equivalent core loss resistance is derived from the core loss at rated voltage and core loss from the no load test using equation 13:

$$= \frac{\quad}{\quad} \times \frac{\quad}{\quad} \tag{13}$$

The rotor resistance at the time of the test is calculated using equation 14:

$$= \quad - \quad \times \quad 1 + \quad - \quad \times \quad \tag{14}$$

3.3.2 Negative Sequence Equivalent Circuit

The negative sequence equivalent circuit is shown in Figure 9. The form of the equivalent circuit is similar to that of the positive sequence circuit. However, the voltages and currents are negative sequence values, whilst the slip is 2-S.

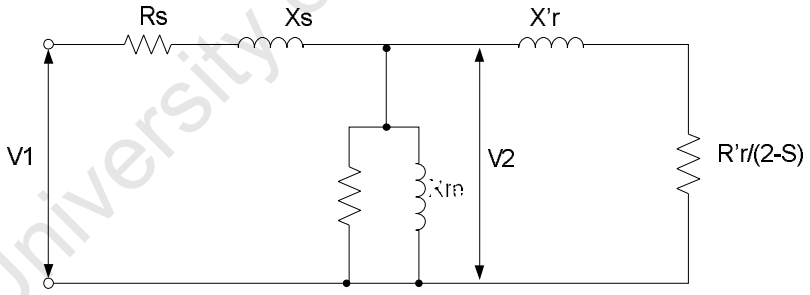

Figure 9: Negative sequence equivalent circuit of an induction motor (Per-phase)

3.3.3 Zero Sequence Equivalent Circuit

Since three-phase motors windings are normally connected in Delta (Δ) or ungrounded star (Y,), no zero sequence currents will flow. For this reason the zero sequence

equivalent circuit can be omitted and will hence have no influence on the motor developed power.

3.3.4 Resistance Correction to Specified Temperature

The resistances, R & R of the stator and rotor winding are corrected to that corresponding to specific temperature [12], T with a known winding resistance, R at temperature, T using the formula in equation 16. This is based on the assumption that the rotor is at the same temperature of that recorded by the thermocouples placed on the stator winding. The specific temperature is equal to the measured temperature rise at rated load of the motor obtained from the temperature plus 25°C [14].

$$= \frac{(\quad .)}{.} \tag{15}$$

3.3.5 Effects of Negative Sequence Component on Developed Torque and Power

An unbalanced three-phase voltage supply connected to a motor causes the motor to draw unbalanced currents of multiple times the voltage unbalance. The rule of thumb is that for every one percent of voltage unbalance, a standard motor will draw about five to six times as much current unbalance. The degree of current unbalance for a given voltage unbalance varies a great deal because of the variations in design and manufacturing techniques of EE motors. According to [15], the current unbalance can be as high as nine times the voltage unbalance for some small EE motors.

The positive and negative sequence equivalent circuits of induction motors in Figure 8 and Figure 9 are used to explain this further.

Due to the positive and negative sequence circuits, the induction motor behaves as two machines operating in opposite directions, one with voltage V_{pos} and slip s, and another with voltage V_{neg} and negative sequence slip (2-s) [16]. The effect of the reduction in negative sequence impedance in EE motors is an increase in negative sequence current

under unbalanced voltage conditions. This can result in additional heating of the rotor and vibration of twice the supply frequency. In addition to that, EE motors operate at slightly higher speeds, and may result in increased power delivered to the load causing further overheating of the motor [17]. Current unbalance can be defined by equation 16 below:

$$CUF = \frac{I_{neg}}{I_{pos}} \times 100\% \tag{16}$$

Where:

CUF is the percentage current unbalance

I_{pos} and I_{neg} is the positive and negative sequence current respectively.

As can be seen from the equivalent circuits in, the positive and negative sequence currents are proportional to the following:

$$I_{pos} \ \alpha \ \frac{s}{R'_{rot(pos)}} \tag{17}$$

$$I_{neg} \ \alpha \ \frac{2-s}{R'_{rot(neg)}} \tag{18}$$

Using the equation in 17 and 18 and combining it into the current unbalance equation in 16, the following proportionality expression can be made:

$$CUF \ \alpha \ \frac{2-s}{s} \tag{19}$$

Therefore, since EE motors operate at lower slip values, the current unbalance generated for a specific voltage unbalance is higher than standard motors.

As shown in Figure 10, the negative sequence current causes a torque in the opposite direction of the torque developed by the positive sequence current. The effective torque delivered by the motor is the summation of the two, which is less than the positive torque.

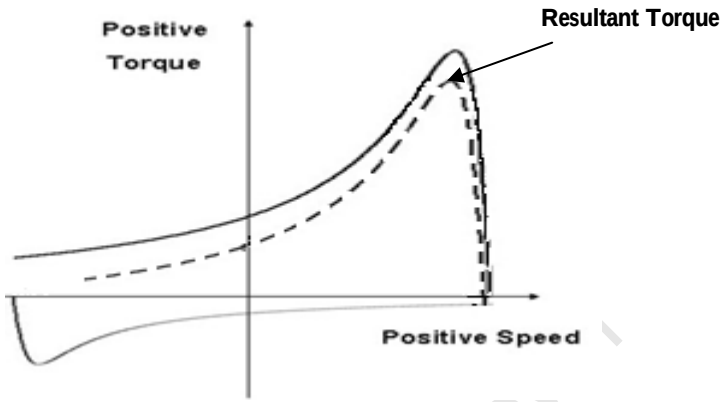

Figure 10: Positive, negative and resultant developed torque of voltage unbalanced supplied induction motor

Since EE motors draw higher negative sequence currents for a particular voltage unbalance, the percentage reduction of the developed torque is higher than the same size standard motor. Subsequently, the percentage increase in slip for the EE motors is higher as will be shown in chapter 6. Motors that are continuously operating under unbalanced conditions will experience a decrease in efficiency due to the increase in the current and winding resistance [18].

The flow of negative sequence current results in the reduction of power P_m and resultant torque, T_m as indicated in equations 20 and 21 respectively:

$$= \quad \times \quad \times \frac{\quad}{\quad} - \quad \times \quad \times \frac{\quad}{\quad} \quad [W] \qquad (20)$$

Where:

$I^{2\prime}_{rp}$ and $I^{2\prime}_{rn}$ are the positive and negative sequence rotor currents respectively.

The total torque can be expressed as:

$$= \times \times \frac{}{} - \times \times \frac{}{(\quad)} \text{ [Nm]} \tag{21}$$

Where:

ω_0 is the synchronous speed in radians per second.

The positive and negative sequence rotor currents can be obtained from equations 22 and 23 provided the slip and motor parameters are known.

$$= \frac{}{} [\ ] \quad h \tag{22}$$

$$= \frac{}{} [\ ] \quad h \tag{23}$$

Where E_p and E_n are positive and negative sequence air gap voltages

Equations 20 and 21 show that the total mechanical power and torque are reduced by the presence of negative sequence currents. The positive and negative sequence equivalent circuits, core loss curves and the above equations, can be used to determine the motor performance when it is supplied with a combination of over or under voltages with unbalanced voltages.

3.4 THERMAL MODELING OF INDUCTION MOTORS

The thermal models from [19] were used to predict the transient and steady state thermal behaviour of the induction motor. The temperature prediction was needed to compare the temperature rises of the STD and EE motors under voltage unbalance supply conditions. The thermal model was used because it does not require the physical

dimension data for parameter estimation, which are generally not supplied with the motor. Through simple heat run tests, the parameters of the motor can be determined.

The models were based on the assumption that the rotor heat does not conduct through the stator to the ambient but via the shaft to the ambient [19]. This means that the stator and rotor thermal circuits are isolated and can be used independently. In this thesis it was focused on the stator winding temperature, and the rotor model was therefore not needed. Figure 11 shows the process followed to predict the stator winding temperature.

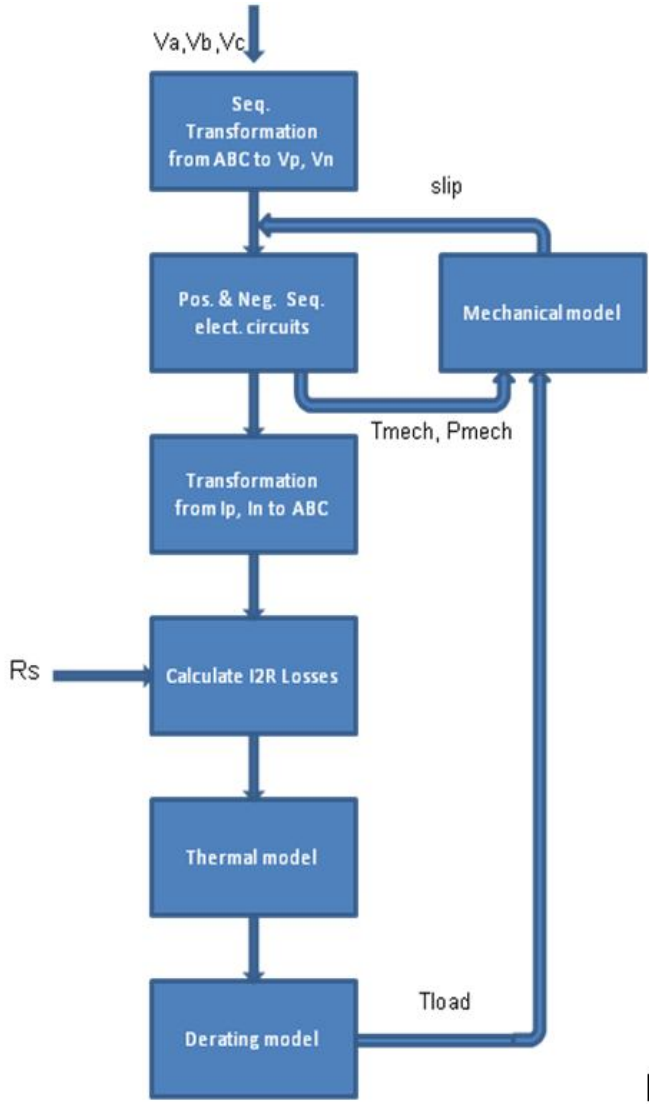

Figure 11: Thermal model development process

3.4.1 Lumped Parameter Stator Thermal Model

Figure 12 shows the stator thermal model circuit of an induction motor [19]. This model contains heat sources, thermal capacitance and thermal conductance. The heat sources represent the three phase stator winding copper losses and the core loss. The thermal capacitance can be seen as the ability of the material (windings, core etc.) to store the heat. The thermal conductance is the ability of the material to conduct the heat away. Each one of the phases is represented by a heat source and three conductances. Two of the conductances connect it to the other phases and one conductance connects it to the core.

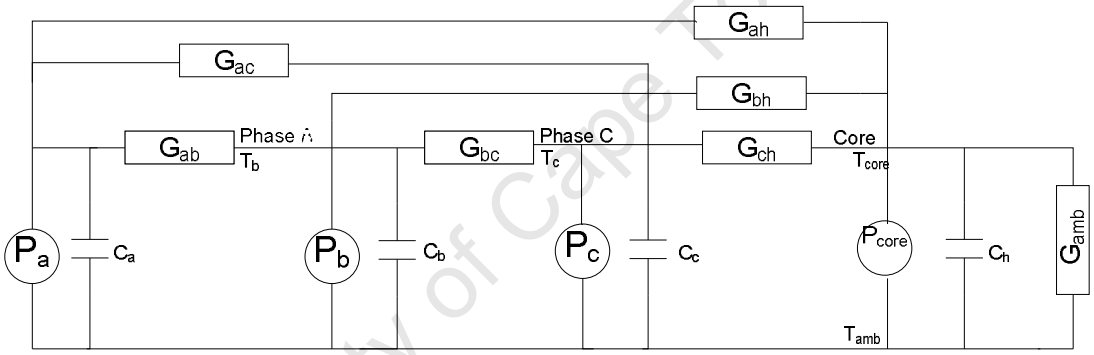

Figure 12: Stator Thermal Model Circuit

Where:

P_a, P_b, P_c	= stator copper loss of phase A, B and C (W)
P_{core}	= stator core loss
G_{ab}, G_{bc}, G_{ac}	= thermal conductance between two phases, (w/°C)
G_{ah}, G_{bh}, G_{ch}	= thermal conductance between phase and core
G_{amb}	= thermal conductances between core and ambient
T_a, T_b, T_c	= phase A,B,C stator winding temperature, respectively
T_{core}, T_{amb}	= core and ambient temperature (°C)
C_a, C_b, C_c, C_h	= thermal capacitance (Ws/°C)

CHAPTER 4

4. DETERMINATION OF INDUCTION MOTOR EFFICIENCY

This chapter deals with the various international testing standards used to determine the efficiency of induction motors. A thorough comparison of all the standards is performed before the test setup is discussed.

4.1 DEFINITION OF EFFICIENCY

The efficiency of any machine is defined as the ratio of the useful output power to the total input power. This can be expressed as:

$$= \frac{\quad}{\quad} = \frac{\quad}{+ \sum}$$

Where, is the power delivered to the shaft of the motor and P is the electrical power absorbed by the motor. The difference between the electrical power and the mechanical power is the sum of the total losses. In practice, the direct ratio of the output power to the input power is inaccurate, since small errors in measuring the input and output power can result in large errors in efficiency as will be shown in chapter 7.

4.2 INTERNATIONAL INDUCTION MOTOR TESTING STANDARDS

Several standards for testing electrical machinery exist worldwide. The most important standards for testing induction motors are the IEEE 112-B [12], IEC34-2 [20] and JEC3. More recently the IEC 34-2-1 [13] standard was introduced. The IEEE standard is primarily used in North America, which is known as C390 in Canada, whereas the IEC34-2 is mainly used in Europe [21]. These standards recommend different measurement and calculation methodologies in determining motor efficiency specifically in the copper loss temperature correction and the evaluation of the stray

load loss [21]. The Japanese Standard (JEC) merely neglects the stray load loss [21], [22] and will undoubtedly yield higher efficiencies than all the other standards under discussion in this section. In 2002, the IEC 61972 was released and is similar to the IEEE standard. A summary of the main differences between the IEEE and the IEC standards are shown in Table 5 [23].

Table 5: Summary of the differences and similarities of the IEEE 112-B, IEC 34-2 and the IEC 61972. [23]

		IEC 34 – 2 (Indirect Method)	**IEEE 112 – B**	**IEC 61972 (Direct Method)**
Type of measurement		Summation of losses	Direct	Direct
Segregation of losses		Yes	Yes	Yes
Core losses with voltage drop compensation		No	No	Yes
SLL using regression analysis		No	Yes	Yes
Temperature correct winding (I^2R) losses (both in the rotor and in the stator)		No	Yes	Yes
Thermal equilibrium at rated load		No	Yes	Yes
Stabilization of no-load losses		No	Yes	Yes
Dynamometer torque correction		No	Yes	Yes
Instrumentation accuracy (+/- % of full scale)	Electrical	1.0	0.2	0.2
	Instrument transform	1.0	0.2	0.2
	Frequency	1.0	0.1	0.1
	Speed	1.0	1 rpm	0.1
	Torque	1.0	0.2	0.2
	Resistance	0.5	**0.2**	0.2

The above-mentioned standards with the exception of the JEC will be discussed in more detail in the following subsections.

4.2.1 The IEEE 112 – 2004

The IEEE 112 [12] standard essentially consist of five methods of calculating motor efficiency namely method A, B, C, D, E, and F. Method A determines the motor efficiency directly by taking the ratio of the measured output to the input power. Method B requires the segregation of losses and the direct measurement of the stray load loss. Method F uses the equivalent circuit to determine the efficiency with direct measurement of the stray load loss. The IEEE 112-B directly measures the stray load loss based on an output power measurement. When performing the load test, the IEEE 112-B requires the winding temperature to be within 10°C of the highest winding temperature recorded during the rated load temperature test. This is significantly higher than the 5°C margin required by the IEC 34-2-1 and the IEC 61972 standards. The IEEE 112 standard does not compensate for the voltage drop in the stator winding in determining the core loss, which essentially means that the no load core loss is the same as the core loss under load conditions. This can undoubtedly lead to higher calculated core loss especially at higher load levels since the volt drop increases with load current. The correlation factor when performing a linear regression on the measured stray load loss must be greater than 0.9. The correlation factor that, is in essence a quality factor [21] and an indication of the error in test measurements and instrumentation, is significantly worse than the minimum correlation factor of 0.95 required by the IEC34-2-1 and IEC 61927.

4.2.2 The IEC 60034-2-1 and IEC 60034-2

The IEC 34-2-1 [13] and the IEC 34-2 [20] also utilises the segregation of losses to determine the efficiency of a motor. The IEC 34-2 (1972) however, is quite different from the [12], [13] and [24] in many aspects. It does not compensate for the voltage drop in the stator winding when determining the core loss. It also does not require a temperature correction of the copper loss to the specific temperature and for this reason no rated temperature test is required. The most important discrepancy of the IEC34-2 is the way in which the stray load loss is determined. The stray load loss is

indirectly calculated by attributing 0.5% of the input power absorbed by the motor. Another critical aspect of the IEC 34-2 is that it does not require the friction loss in the bearings to stabilise at the operating condition before the no load test is performed. Previous research has shown that the expected difference between the efficiency results of the IEEE and the IEC34-2 was about 1% [23]. The new IEC standard, the IEC 34-2-1(2007) [13], is similar to [12] in particular in the manner by which the stray load loss is dealt with. This standard does however compensate for the voltage drop in the stator winding in determining the core loss.

4.2.3 The IEC 61972

The IEC 61972 [24] as previously mentioned is similar to the IEEE and is now known as the IEC 34-2-1. It gives two methods of evaluating the stray load loss. It can either be obtained directly as is the case for the IEEE 112-B and IEC34-2-1 standards, or indirectly by attributing a fixed amount from a predefined curve based on the power rating of the motor [23] [22].

4.3 LABORATORY SETUP FOR INDUCTION MOTOR TESTING

The laboratory setup, instrumentation and test procedures for testing the range of induction motors are described in this section. The laboratory setup is configured to ensure conformity with the international induction motor testing standards.

4.3.1 Specifications of Squirrel-Cage Induction Motors Tested

The motors that were studied are standard and premium plus motor with output power ratings of: 3kW, 7.5kW, 11kW and 15kW. All the motors were totally enclosed fan cooled (TEFC), four-pole, 380/400V, 50Hz type. Some of the differences in the nameplate ratings of the motors are outlined below:

Standard motors	EE Motor (Premium Plus Eff)
IP 55 Class F insulation	IP 66 Class H insulation
1 Service Factor	1.15 Service Factor
1450rpm (15kW, 11kW, 7.5kW)	1460 rpm (15kW, 11kW, 7.5kW)
1390rpm (3kW)	1425 rpm (3kW)

4.3.2 Laboratory Generator System

Power is generated by a 520 kW 6 pole three phase synchronous generator to comply with the maximum voltage unbalance and total harmonic distortion (THD) of 0.5% and 5% respectively. The frequency was kept within ±0.1% of 50Hz by controlling the speed of generator. The generator generates 6.6kV at its terminals with the voltage being stepped down by a 6.6kV/400V transformer. The synchronous machine is driven by a 250kW DC motor and/or a 75kW AC induction motor.

4.3.3 Test Rig Dynamometer system

Two test rigs were used for the motor sample. A 3.6hp (2.6kW) test rig was used for the 3kW motors whilst the rest of the motors were tested on the 16hp (11kW) rig shown in Figure 13. Each motor were coupled to a separately excited DC machine. The DC machine is run as a generator (dynamometer) and the torque is controlled by adjusting the machine's armature current (since Torque α armature Current). The armature current is controlled by a three phase four-quadrant rectifier/inverter feeding the energy back to the grid. Therefore, only the power losses associated with the drive train is wasted. An external resistor bank was occasionally needed to dissipate some of the power that cannot be absorbed by the 15hp drive in the case of the 11kW and 15kW motors.

4.3.4 Old Machine Mounting System

The DC machine shown in Figure 13 was cradled on a double bearing gimble system. The stator of the machine in this configuration is free to rotate with the rotor and was only tied to a 200kg load cell that was bolted to the base platform. The reaction torque was measured by relating it to the reaction force exerted on the load cell.

Figure 13: 15kW Test rig – Dynamometer coupled to a standard induction motor

The Motor Under Test (MUT) was bolted down on riser blocks machined to be able to accommodate three motor frame sizes. The short comings of this system are that a limited number of motors could be fitted on it and a precise height adjustment is intricate. A Fenner coupling was used for this system that suffers from backlash. Furthermore, the fact that the load machine was gimbled, introduced considerable noise in the load cell torque signal.

4.4 FLEXIBLE 22KW TEST RIG

Due to the short comings mentioned in the previous section, as well as accuracy concerns, a decision was made to design and construct a new, more accurate test rig.

4.4.1 Flexible Supply System

A flexible power supply system was also designed and commissioned. Unbalanced supply voltages are created by means of a three-phase variac and three single-phase variacs. The single-phase variacs are shown in Figure 14.

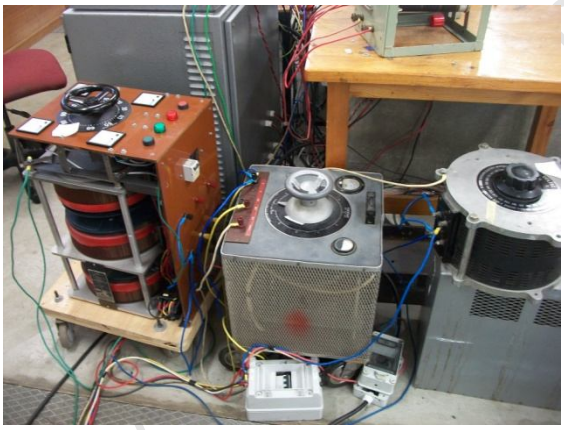

Figure 14: Three single phase- low kVA variacs

A three phase, 64A variac shown in Figure 15 is used to supply the motors with up to 150% full load current.

Figure 15: 40kVA three-phase series connected variac

Three single phase variacs, with low kVA ratings are used in conjunction with the 64 A variac, to give independent voltage control from each phase. The brush voltage of the low kVA variacs (G1) are fed into the winding of the larger variac (G2) to control its brush (output) voltage as shown in Figure 16.

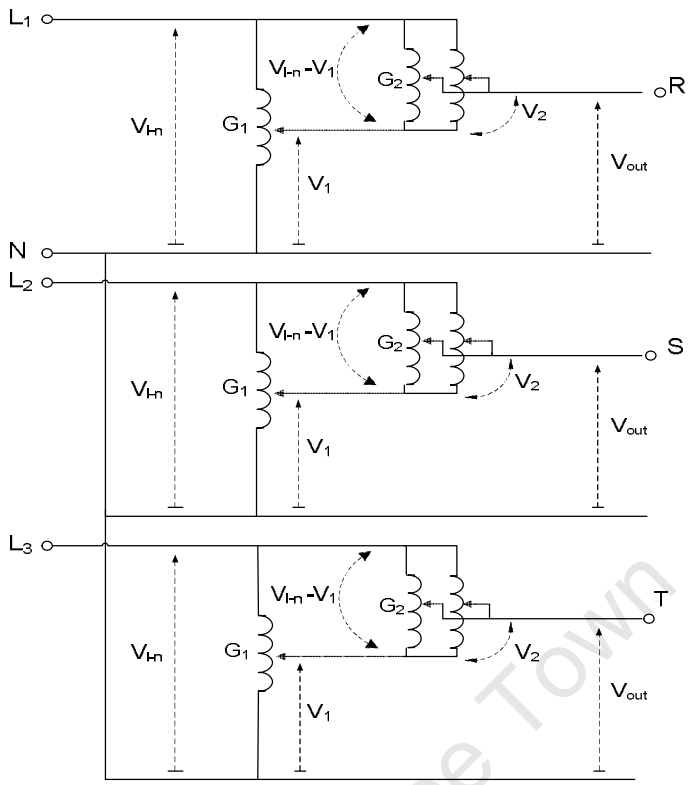

Figure 16: Variac configuration for implementing voltage control with high current capability

It should be noted that the high power variac can easily be replaced with three single phase transformers. Each transformer can be connected with its secondary side in series with then load and its primary across one of the lines and the brush of the single phase variac. The transformer may only be a few kVA since the secondary voltage will only be about 20V at the load current. This ought to be a much more viable solution than using a high-power three-phase variac.

4.4.2 Mounting blocks

One of the objectives of this thesis was to upgrade the mounting platform of the test motor (drive) and the load machine. Together with this an inline torque transducer was procured and so a riser block for it was also needed.

The instructions were clear:

- The mounting blocks must be adjustable in order to mount any non-standard motor within a specified range.
- It must be rigid.

In Figure 17 the adjusting nuts can seen as well as the T-slots and T-nuts for bolting down the test motor. This arrangement has the capability of a three-dimensional (3D) alignment. The T-slots on the base plate allows for axial movement to accommodate motors of practically any foot mounting pitch and shaft length. The threaded rots and nuts allow for up and down adjustments where the T-slots on the riser blocks takes care of radial pitch of the motors foot mountings.

Figure 17: Motor adjustable riser blocks

Figure 18 shows the drive train after it was precision aligned. Every element of the drive train assembly is meticulously aligned and the couplings are a fundamental component.

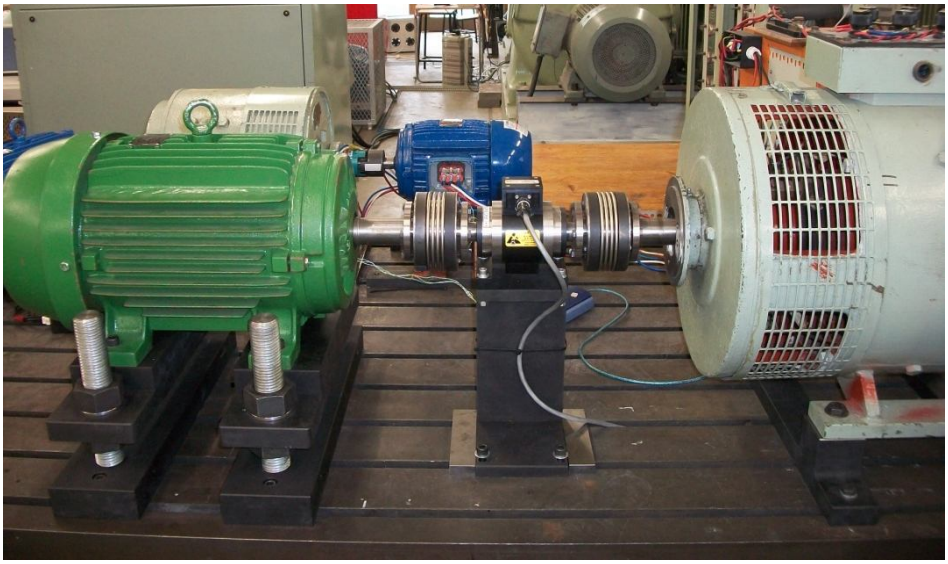

Figure 18: Newly constructed 22kW flexible motor test rig

4.4.3 Magtrol Torque Transducer

It was decided to opt for an inline TM 312 (high accuracy) torque transducer with speed sensing. The torque transducer falls in a 0.1% accuracy class and is rated 200 Nm with a 100% overrated capability. The measuring system, based on the principle of a variable, torque-proportional transformer coupling, consists of two concentric cylinders shrunk on the shaft on each side of the shaft's deformation zone, and two concentric coils attached to the housing. Both cylinders have a circularly disposed coinciding row of slots and rotate with the shaft inside the coils. An alternating current with the frequency of 20 kHz flows through the primary coil. When no torque is applied, the slots on the two cylinders fail to overlap. When torque is applied, the deformation zone undergoes an angular deformation and the slots begin to overlap. Thus a torque-proportional voltage is on the secondary coil. The integrated conditioning electronic module outputs a full scale analog voltage of ±5V. Non-contact differential transformer torque measuring technology is used. This means that no electronic components rotate during operation. Speed is taken from an open collector pin and a 10 kΩ pull-up resistor is used. An optical sensor reads the speed on a toothed wheel. The electronic conditioner outputs a frequency signal proportional to the rotational speed of the shaft. An active

circuit compensates the zero offset and temperature sensitivity drifts within a tolerance of 0.1% / 10K.

4.4.4 Vibration Mitigation

Excessive vibration can cause energy to be lost in the drive train which would result in reduced efficiency measurements. Vibration introduces noise in the torque and speed signals and therefore causes larger uncertainty in the measurement. Two bellows couplings were utilised on either side of the inline torque transducer in order to mitigate vibration as shown in Figure 18. These couplings are backlash free which is important for dynamic and low torque measurements. The radial misalignment tolerance is 0.3 mm and an angular misalignment of 1°. To ensure that this criteria is met, an alignment clock is used as shown in Figure 19.

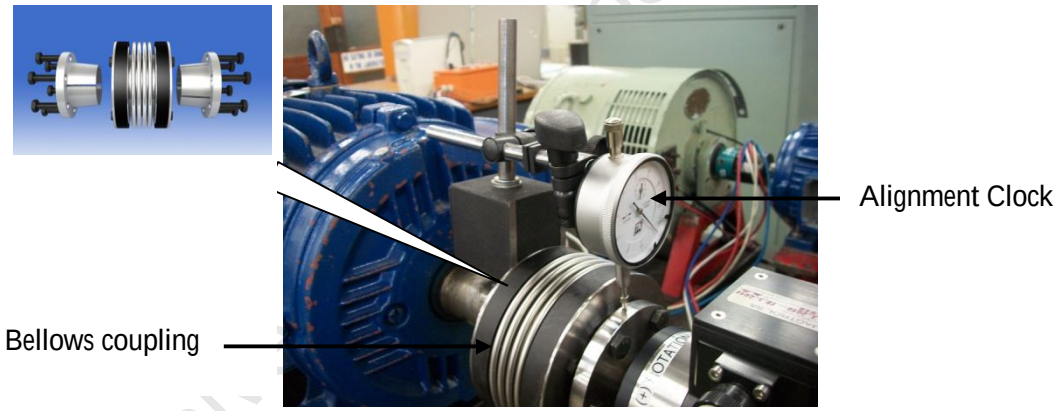

Figure 19: Alignment procedure to minimize vibration

The magnetic base of the clock is placed on the shaft of the motor with the plunger stem resting on the torque transducer shaft. Starting with it on top (12o'clock) and rotating the shafts 180°, the vertical and radial misalignment is measured. By turning the height adjustment nuts shown in Figure 18, any vertical misalignment is corrected. Similarly, the horizontal misalignment is measured by rotating the alignment clock on the shafts from the 9 o'clock position to 3 o'clock position or vice versa. This is

graphically illustrated in Figure 20. This alignment is corrected by shifting the motor parallel to the shaft along the mounting T-slots.

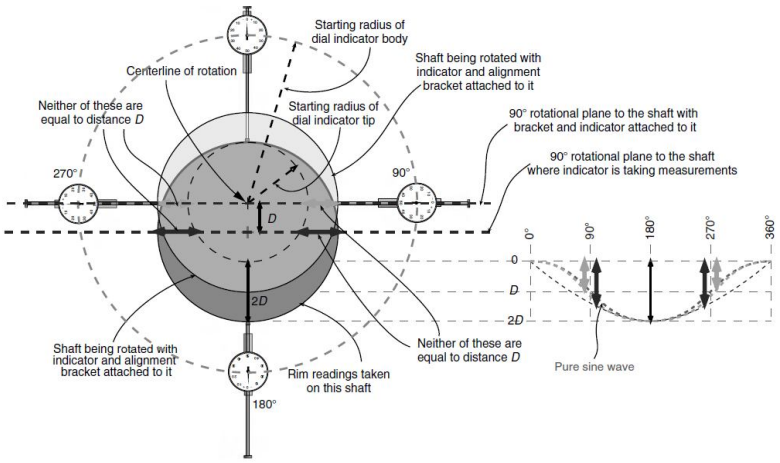

Figure 20: Axial view of Dial indicator vertical and horizontal positions [44].

A simple three dimensional on-line vibration sensing system could be implemented to the new 22kW test rig. This monitoring will ensure that cold and hot vibrations are always within limits during a test. It can also used for a structural analysis of the test bench under dynamic load conditions.

4.4.5 Yokogawa Power Analyser

A three phase power analyser shown in Figure 21 was connected in series with the generator supply to the tested induction motor. The average power, voltage current is logged by the power analyser and the electrical connections can be seen in Figure 22.

Figure 21: Yokogawa Digital Power Analyzer

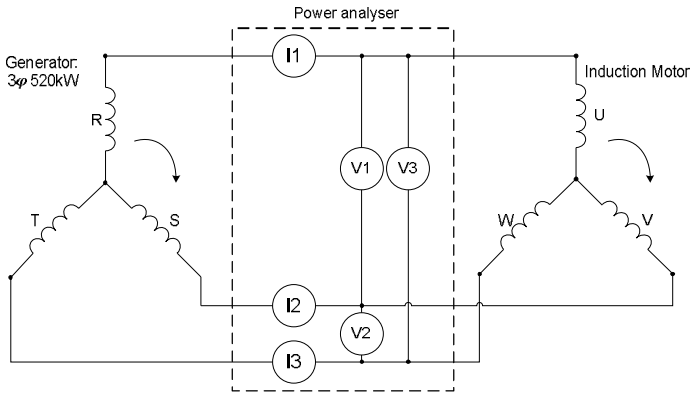

Figure 22: Electrical setup of instrumentation connected to the generator and motor in laboratory

The speed and torque from the transducers were also fed to the power analyser and recorded in synchronism with the power, voltage and current. The output power was obtained through the torque and speed measurements.

4.4.6 Winding Resistance Measurement

The Galvanometer shown in Figure 23 is under most circumstances the most accurate method of measuring winding resistance.

a) b)

Figure 23: a) Galvanometer and b) Digital Multi Meter for winding resistance measurement

Galvanometers basically consist of a Wheatstone Bridge with four resistance branches, a current source and a detector (meter) as shown in Figure 24. Three known resistances are matched with the unknown winding resistance for zero current in the detector at balance.

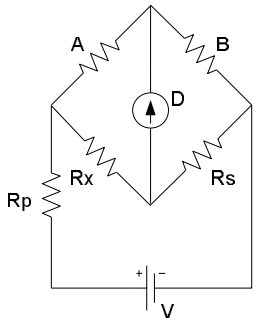

Figure 24: Basic Wheatstone Bridge

A Digital Multi Meter (DMM) shown in Figure 23 was also used for the same purpose. It gives a better resolution (6.5 digits) than the galvanometer. It utilizes the four wire method depicted in Figure 25 as described in the IEEE 118 Standard Test Code for Resistance Measurement.

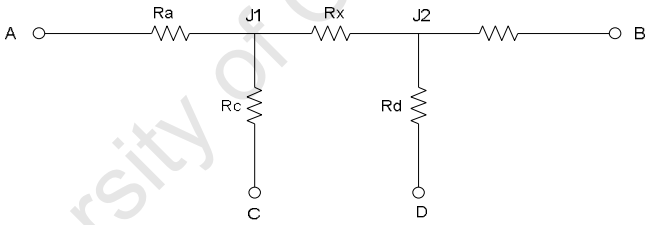

Figure 25: Four Terminal Representation of a Resistor

Where:

Ra, Rb, Rc and Rd are the lead resistances

Rx represents the unknown winding resistance

Terminals A and B are the current source input and output terminals. Terminals C and D represent the potential terminals. The advantage of the four wire method is that the four contact resistances and lead resistance can effectively be eliminated.

4.4.7 Temperature Measurement

Three K-type thermocouples are installed on the drive-end side (i.e. the opposite side of cooling fan) of the stator end windings. The thermocouples are located in close proximity to the parts where the highest temperature measurement of the windings was expected. The thermocouples are placed on the windings above and below the rotor and one on the side of the terminal box. All motors had the thermocouples placed at exactly the same place for comparison purposes. Great care was taken not to damage the insulation on the windings that might cause the motor to fail prematurely. Figure 26 shows the thermocouples mounted on a standard motor.

Figure 26: Thermocouple placement on stator end windings

An eight channel logger shown in Figure 27 was used to record the temperature in one second intervals. The data is sent via USB interface to a PC where it is stored in CSV format.

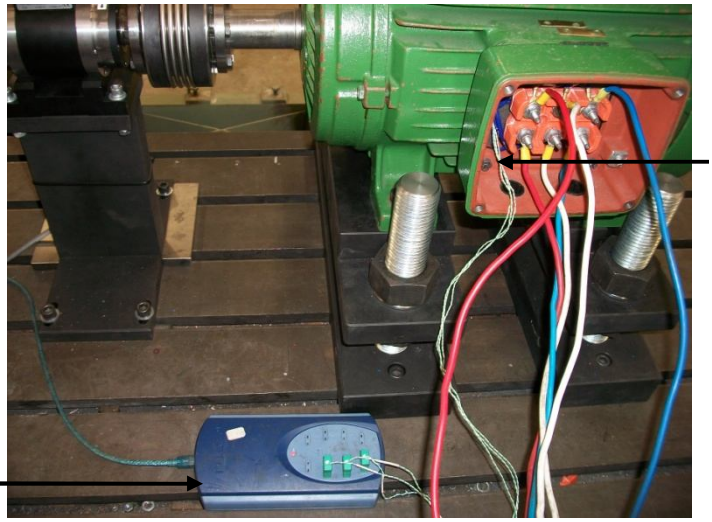

Figure 27: Eight channel temperature logger with USB interface

4.4.8 Torque Measurement and Load Cell Calibration

Torque is measured on the 15kW test rig by measuring the reaction torque of the dynamometer mounted on a gimbled bearing system. A load cell is used to measure the reaction force exerted on the frame (Stator) of the dynamometer, at a specific radius from its centre.

The load cell is calibrated by subjecting the frame of the dynamometer to known calibrated weights and calculating the correct amplification factor for the calculated torque using nominal length (*d*) of the torque arm. This can be expressed by the following equation:

$$= \times = \times$$

Where:

"*d*" is the length of the calibration arm,

"*g*" is the gravitational acceleration coefficient of Cape Town (9.796 m/s^2), and "*m*" is the calibrated mass.

Linearity and hysteresis effects associated with the load cell are assessed by loading and unloading the calibration arm with weights over its full range. A schematic of the torque measurement and load cell calibration system is shown in Figure 28.

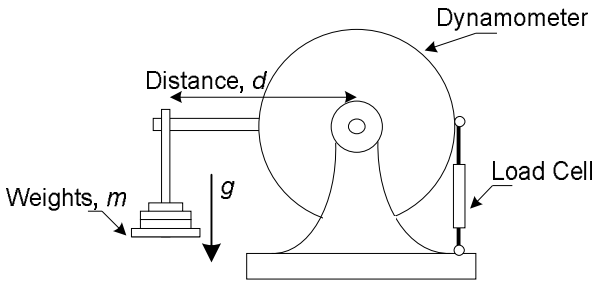

Figure 28: Torque measurement and load cell calibration system

One of the advantages of the new test rig is that calibration is only required on an annual basis. Although the new torque transducer was factory calibrated, another on site calibration was carried out for two reasons:

- To confirm the sensitivity of the transducer in case it was damaged during shipment.
- To check if the interfacing between the transducer and power metre display was done correctly.

The calibrated calibration arm shown in Figure 29 was manufactured to perform this task. The calibration arm was sent for calibration and is 509.81mm from centre to centre. By locking the shaft in place as shown in Figure 29 and hanging weights on to the cal-arm, a 5 Nm is displayed for every 1kg added.

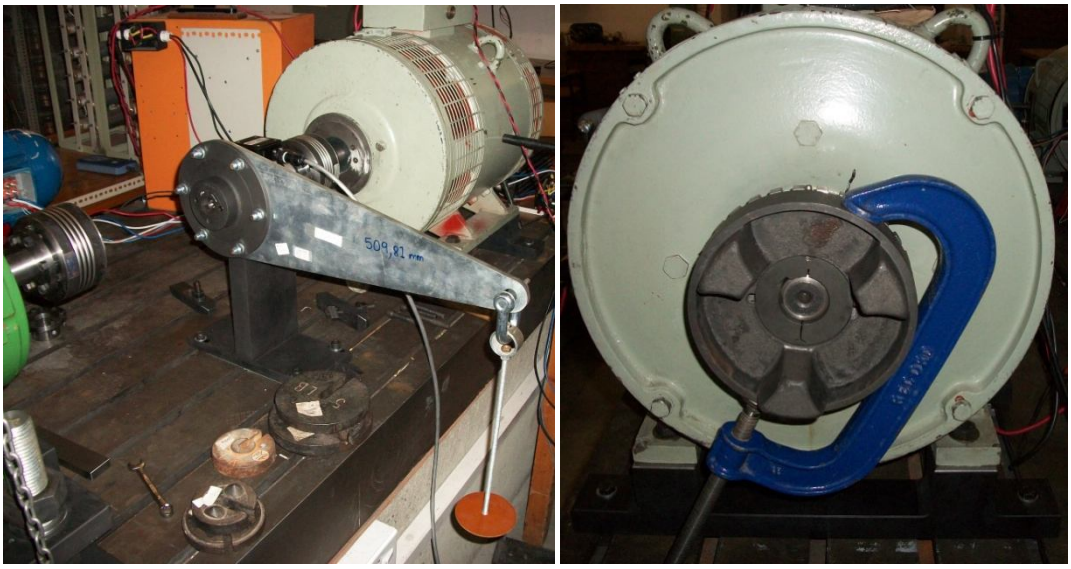

Figure 29: Torque calibration setup for the new 22kW test rig

4.4.9 Dynamometer Torque Correction

A dynamometer correction test was performed to compensate for the coupling and bearing friction losses of the DC machine, which was being used as the dynamometer. The induction motor being tested was coupled to the dynamometer and run at rated voltage and no field or armature current flowing in the DC machine. After the voltage, current, speed, torque and stator winding temperature were recorded the motor was uncoupled and the same measurements were taken except the torque.

The dynamometer correction is calculated as follow:

$$= — \times \frac{\quad'\quad}{\quad} — \qquad (24)$$

Where:

$$_{,} = \quad _{,} — \quad _{,} — \quad \times (1 — \ )$$

$$= (\quad _{\_} — \quad _{,} — \quad)$$

4.5 TEST PROCEDURE

4.5.1 Cold Winding temperature

The temperature of the stator windings is measured and recorded before the thermal test is performed. The ambient temperature is also recorded and the stator resistance measured.

4.5.2 Thermal Test at rated Load

The accuracy of the power losses that were measured was enhanced by letting the motor work at its full load and allowing it to stabilise at rated operating temperature according to [12],[13] and [20]. The motor that was coupled to the dynamometer is loaded to its rated torque and kept running until the temperature rise changes by no more than 2°C over a period of hour. Once thermal equilibrium is reached, the DC machine is de-energised as well as the three phase supply to the motor. Once the motor shaft had come to a complete standstill a galvanometer is connected to the stator winding terminals and resistance together with temperature is measured and recorded. The initial resistance is measured within 30 sec after the power to the motor is switched off. Since all the motors that were tested are continuously rated (S1), it is permissible by the standards to overload the motor by 25% to 50% during the preliminary heating period in order to shorten the time taken to reach the expected final temperature.

4.5.3 Variable Load Test

Prior to the variable load test measurements are recorded, it is required by the IEC standard that the winding temperature is within 5°C of the rated temperature (see thermal test). Although the IEEE standard requires up to a 10°C difference, the minimum of 5°C is adhered to if the data is used for calculating efficiencies with both standards. The motor is subjected to six loading conditions. The load is spaced in intervals of approximately 25%, between 25% and 150% of rated torque to obtain representative spread of efficiency over the load range of the motor. The test is carried out in descending order starting from 150% load. The voltage, current, power, speed, torque and stator winding temperature is recorded at each load condition. The test is

carried as quickly as possible to limit temperature changes that might influence the accuracy of the results.

4.5.4 No Load Test

The motor is run with the DC machine uncoupled from the shaft. The frequency is kept at rated frequency (50Hz) and the voltage is varied from 475V (125% of rated voltage) down to approximately 75V. The line-to-line voltage, line current, power, frequency and temperature are recorded. The no load test also gives the sum of the stator leakage reactance and magnetizing reactance for the equivalent circuit model.

4.5.5 Blocked Rotor Test

A blocked rotor test was conducted on each motor to obtain the leakage reactance and rotor resistance in the motor equivalent circuit. The shaft of the motor was clamped with a G-clamp. The voltage is slowly increased by means of a variac supply up to a point where the rated current of the motor is reached. The voltage, current and power is recorded during this experiment. This test is executed as quickly as possible not to overheat the windings of the motor.

CHAPTER 5

5. COMPARISON OF DIFFERENCES BETWEEN STD AND EE MOTORS

The design and operational differences between STD and EE motors are presented in this chapter.

5.1 DESIGN DIFFERENCES

This section deals with discussing some of the design differences between standard and energy efficient motors (also referred to as high efficiency motors). The purpose of this section is to discuss motor efficiency as it relates to motor design and application.
Motor manufacturers are currently developing new ranges of energy efficiency motors that requires an accurate motor design, the adoption of new and higher quality materials and innovative technologies [30].

5.1.1 Magnetic Core

One of the most common ways of improving the efficiency of a machine is to change the quality of the lamination steel of the core stack. The magnetic material plays a very important role in the improvement of the performance of the motor. Its main purposes are magnetic permeability and the specific losses per kg [31], [32]. Standard Motors use lower cost annealed steel which is more susceptible to temperature and environmental conditions. Table 6 shows watt losses for three types of electrical steels.

Table 6: Watt loss for various electrical steels [33]

Steel Grade	**Loss Breakdown**	**Watts Loss/lb @ 15kG 60 Hz**		
		29 ga	**26 ga**	**24 ga**
M1 Silicone	Hysteresis	1.10	1.21	1.36
	Eddy	0.50	0.52	0.60
	Total	1.60	1.73	1.96
M36 Silicone	Hysteresis	1.26	1.49	1.69
	Eddy	0.72	0.79	0.91
	Total	1.98	2.28	2.60
Carbon Steel	Hysteresis	-	2.17	2.67
	Eddy	-	1.37	1.62
	Total	-	3.54	4.29

The core of an EE Motor is made up of higher- grade silicone steels that are harder and more able to withstand high temperature conditions [34]. Newer magnetic steels are capable of operating at higher flux densities [35]. The magnetizing flux needs to be small to minimize the core losses, however this restricts the amount of breakdown torque and tends to reduce the starting torque [33].

5.1.2 Stator Copper Loss

The largest loss in induction motors (typically 35% of the total loss) is due to the finite resistance of the stator winding for a given current that produces heat. This loss can be reduced by increasing the cross sectional area of the copper by either increasing the slot fills or by using larger slots in the stator core. Figure 30 shows the difference between poor and good slot fill.

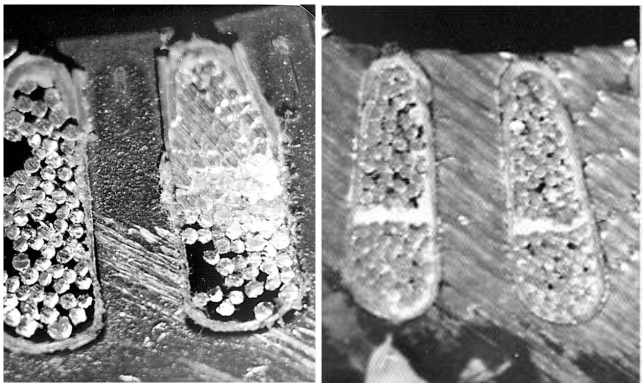

Poor slot fill *Good slot fill*

Figure 30: Increasing the slot fill reduces the current density in the conductor [16]

Larger slots however, reduce the volume of the magnetic circuit and will cause it to saturate and increase core loss. This can be counteracted by increasing the length of the magnetic core [35]. End windings must be kept as short and tight as possible to minimise the amount of inactive but loss-producing copper in the end windings. Manufacturing techniques were developed to incorporate multi-tier end windings [35].

5.1.3 Rotor Slip Loss

Larger rotor bars and end rings reduces the resistance loss in the rotor. However, to maximise the starting torque of the motor and to control the inrush current, the rotor resistance should be kept high [33].

5.1.4 Friction and Windage Loss

Energy efficient motors are designed principally with reduced windage and friction and stray load motor losses. The result is a much flatter efficiency curve versus loading condition, resulting in a motor that can operate at high efficiency levels even at loading conditions outside the ideal 50%-75% nominal full load range. Bearing grease has significantly been improved over the recent years and is still improving. This will certainly result in lower losses due to bearing friction loss [35]. Because energy efficient motors produce less heat than standard motors, smaller cooling fans can be used to reduce the friction and windage losses [31]. Using bearings that have ceramic balls

instead of steel balls further reduces friction loss. Ceramic bearings have the additional feature in that they isolate the shaft and prevent bearing fluting from circulating currents due to harmonics from VSD supplied motors. Bearing sizes are reduced in some cases to reduce the friction loss but that would limit the mechanical loading on the shaft, especially with belted loads [36].

5.1.5 Stray load Loss

Efficiency can be improved by keeping the stray load loss at a minimum. Often designers achieve that by increasing the air gap. However, in doing so, the magnetizing current increases which aggravates the power factor of the motor [28]. The stray load loss can also be limited by the skew of the stator and more commonly the rotor. However, this can create starting torque difficulties and electrical noise (harmonics) in the motor [28].

5.1.6 Cast Iron Casing

Newer energy-efficient designs have more ribs to increase the surface area as shown in Figure 31 [32]. The IEEE 841 motors specify cast – iron housings that are finned for better heat dissipation. The outer diameter of the stator lamination stack is fully round to provide increased thermal conductivity to the outer housing [36].

Figure 31: EE Motor casing with more ribs to improve surface area

5.2 EFFICIENCY DIFFERENCES

In this section, the differences between international motor testing standards are first illustrated. The efficiencies of four standard and four EE motors are then compared as a function of load. The efficiencies of the motors were determined using the IEEE 112 standard. Furthermore, rated supply conditions were maintained during all tests.

5.2.1 Efficiency Differences Between International Motor Testing Standards

In this subsection the efficiency results of the IEEE112-B, IEC34-2-1 and the IEC 34-2 will be compared as well the direct method. The efficiency versus load results obtained from testing the range of standard and EE motor with the afore-mentioned procedures are presented in Figure 32 to Figure 39. The catalogue efficiencies are also plotted on the graphs for comparison with the experimental data. From the figures it can be seen that the IEC 34-2 overestimates the efficiency in all cases by up to 2%. This is because the stray load loss is less than that of the other two standards. The IEEE 112 and IEC 34-2-1 give very similar results because the SLL are calculated in a similar manner. The direct method underestimates the efficiency when compared to the standards in all cases.

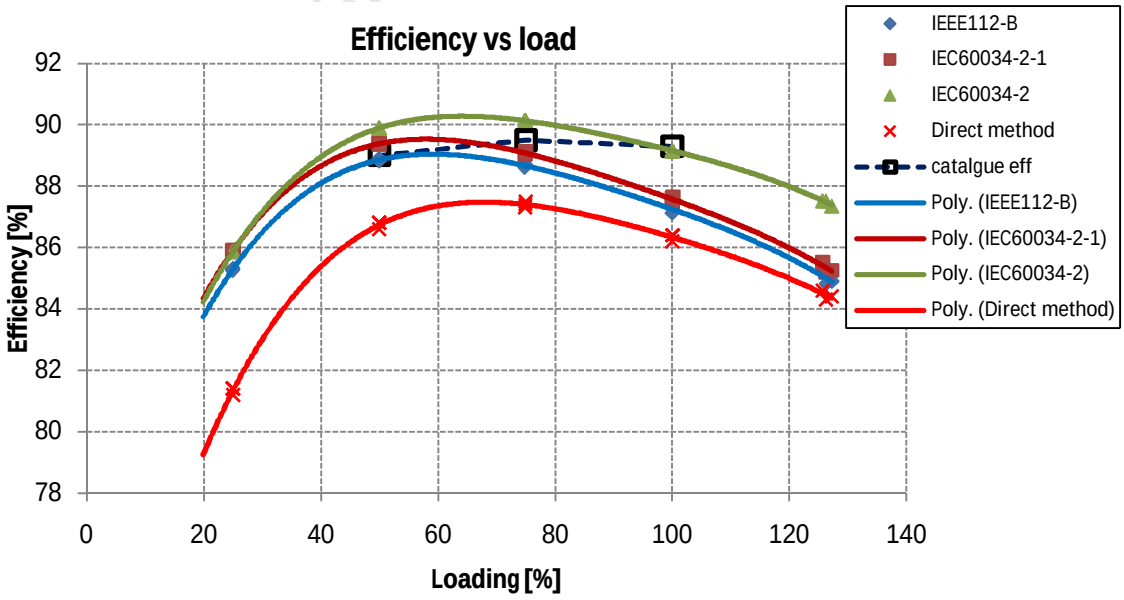

Figure 32: Efficiency of the 15kW standard motor obtained with different standards

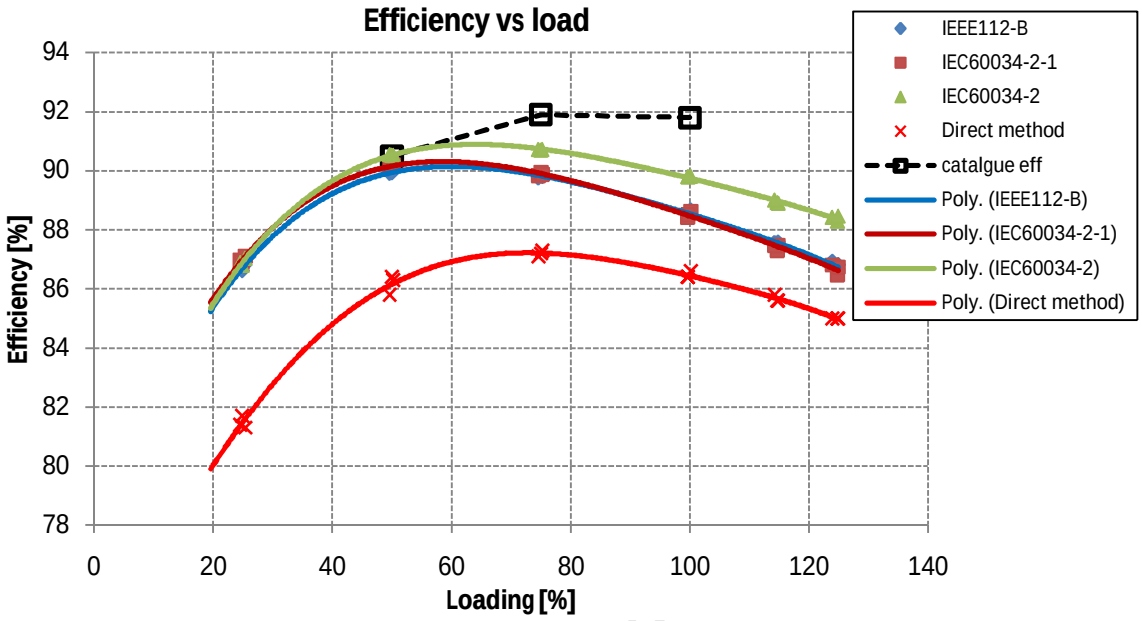

Figure 33: Efficiency of the 15kW EE motor obtained with different standards

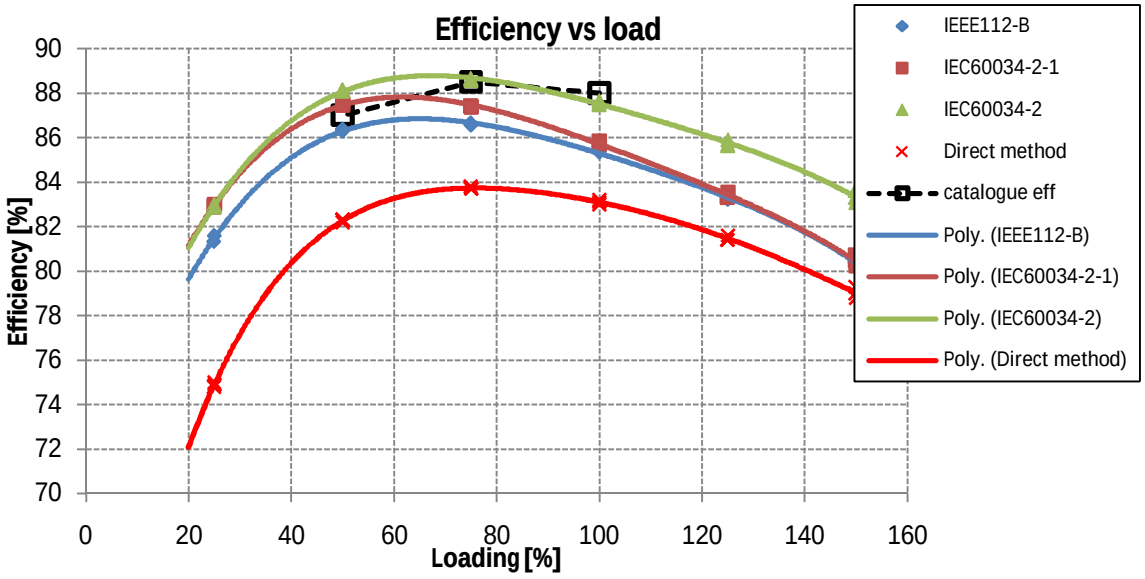

Figure 34: Efficiency of the 11kW standard motor obtained with different standards

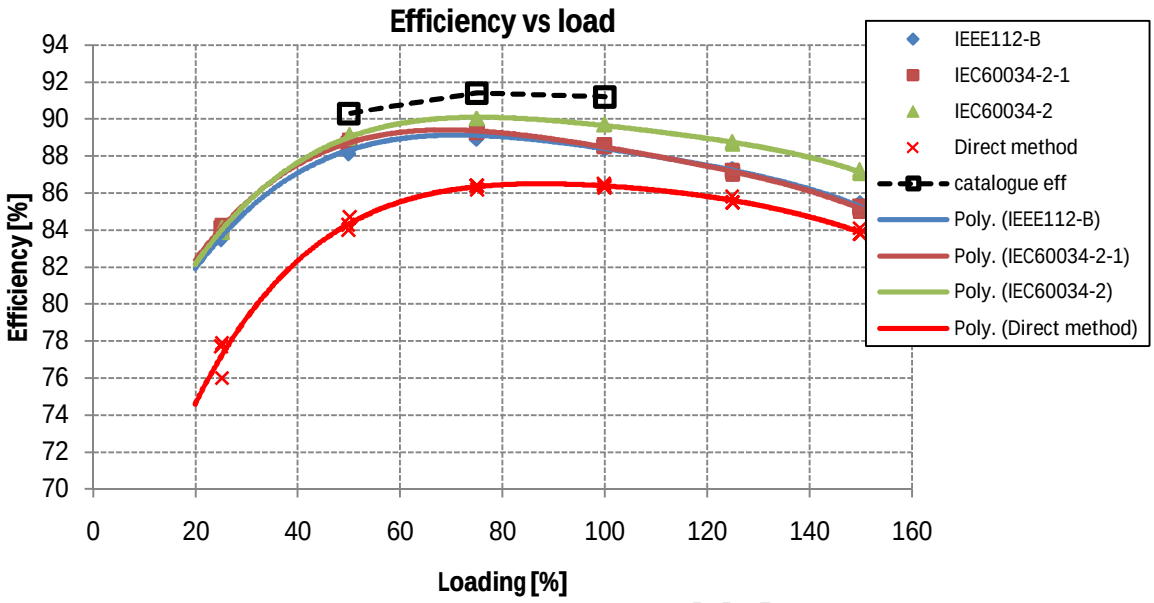

Figure 35: Efficiency of 11kW EE motor obtained with different standards

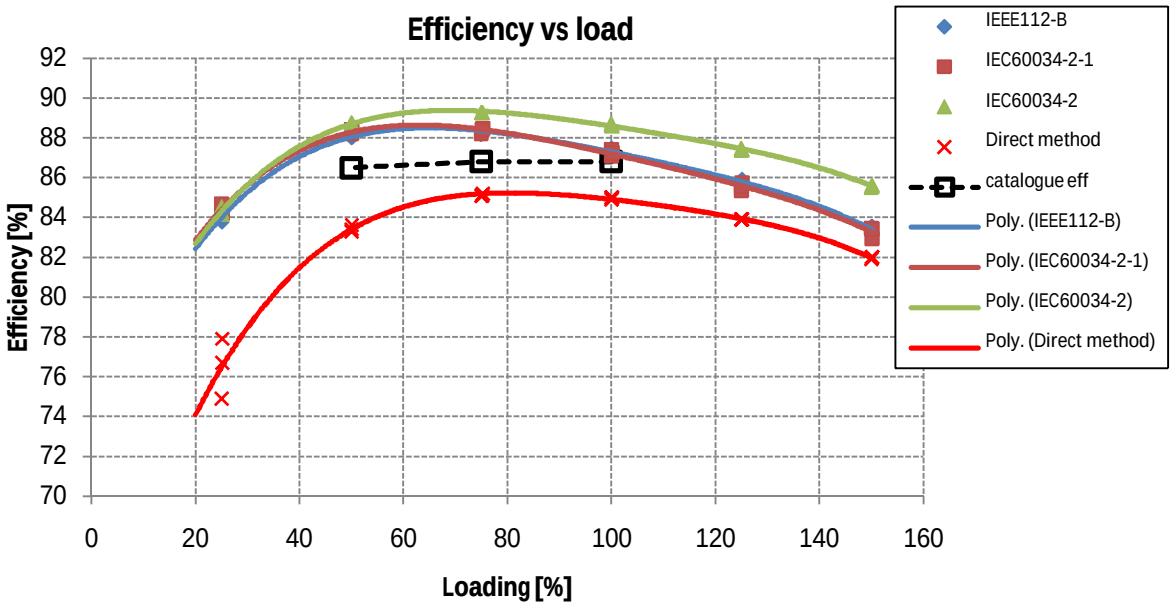

Figure 36: Efficiency of the 7.5kW standard motor obtained with different standards

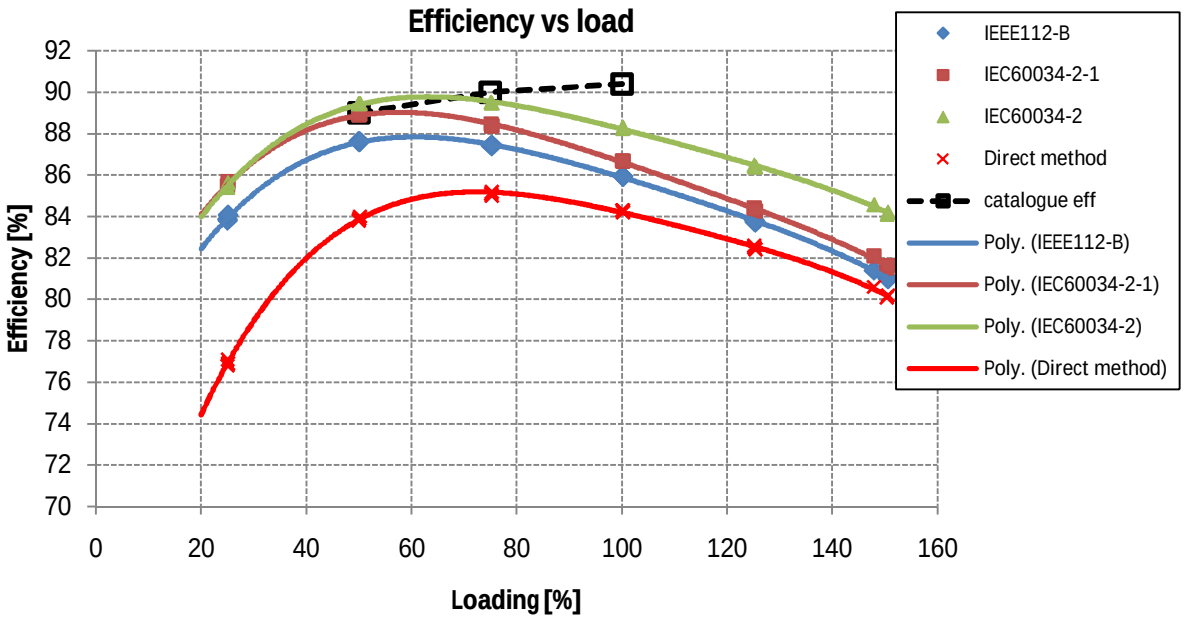

Figure 37: Efficiency of the 7.5kW EE motor obtained with different standards

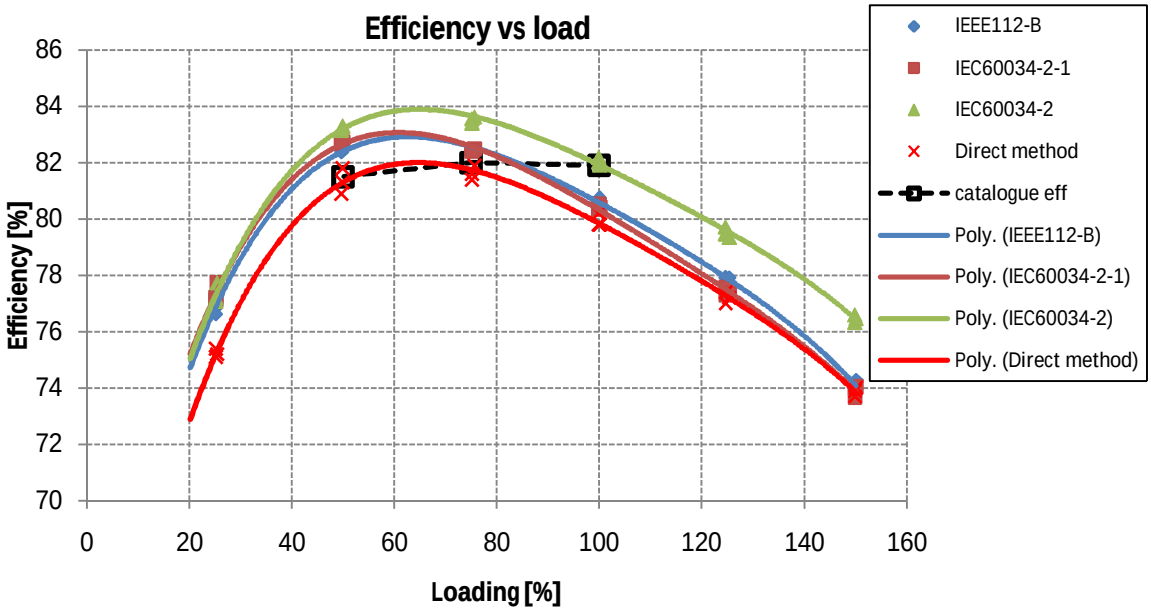

Figure 38: Efficiency of the 3kW standard motor obtained with different standards

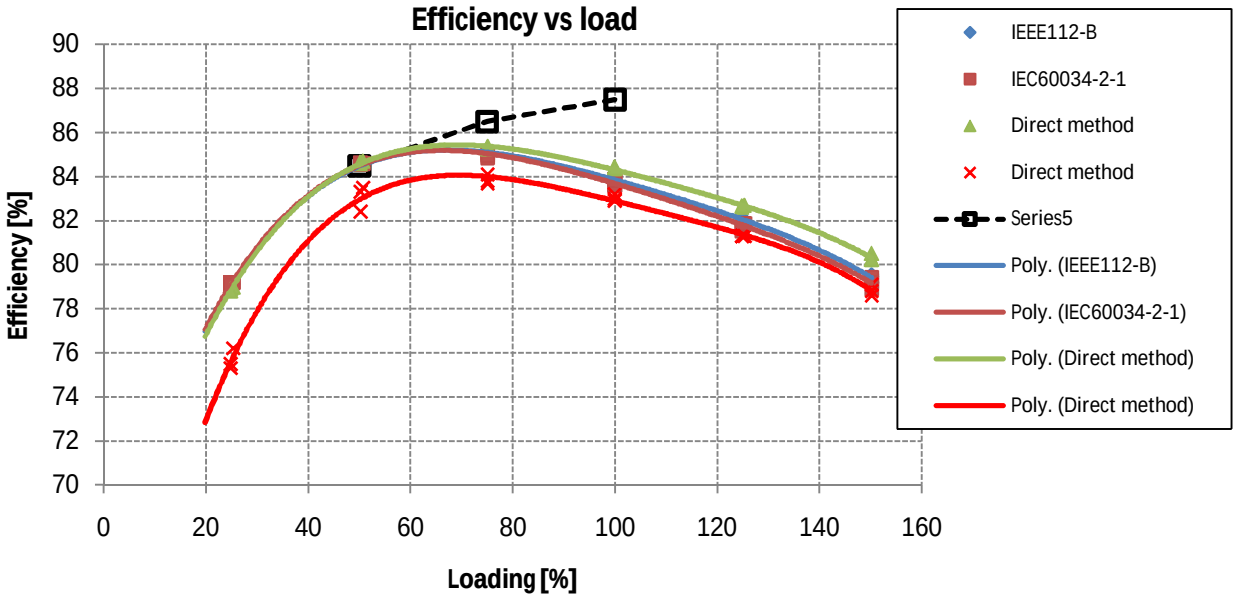

Figure 39: Efficiency of the 3kW EE motor obtained with different standards

5.2.2 Efficiency Differences between Standard and EE Motors

A minimum of three tests were performed on each motor and a regression is done on three efficiency curves to get the average efficiency curve of each motor. Figure 40 to Figure 43 show the efficiencies the energy efficient and standard motors according to the IEEE 112-B testing standard.

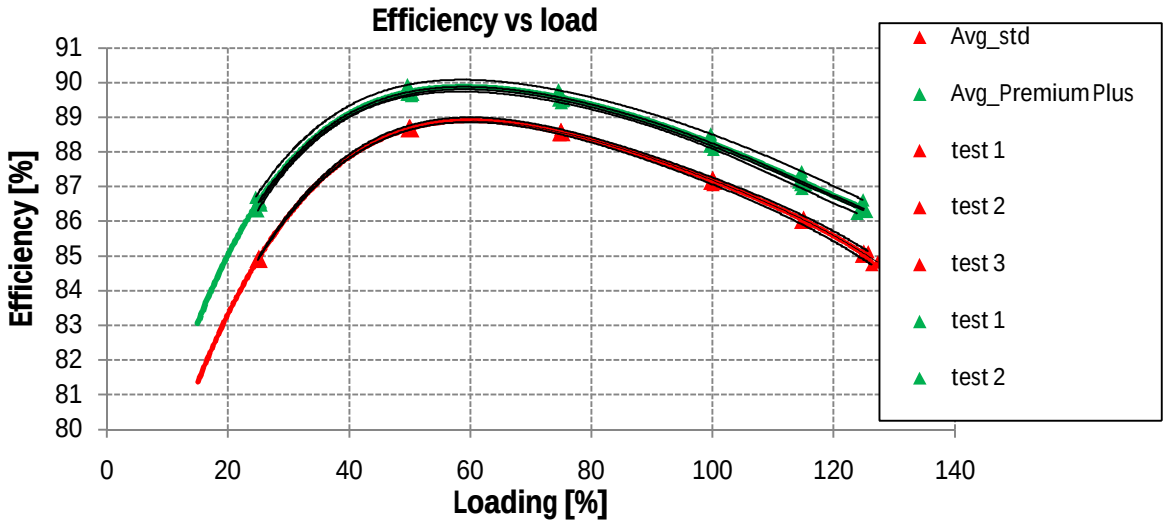

Figure 40: Efficiency vs load characteristics of 15kW standard and EE motors

The efficiency in Figure 40 of the 15kW EE motor has an approximately constant 1% higher efficiency than the standard motor. This is due to the lower overall losses associated with the EE motor. Both motors are designed to achieve maximum efficiency at around 60% loading.

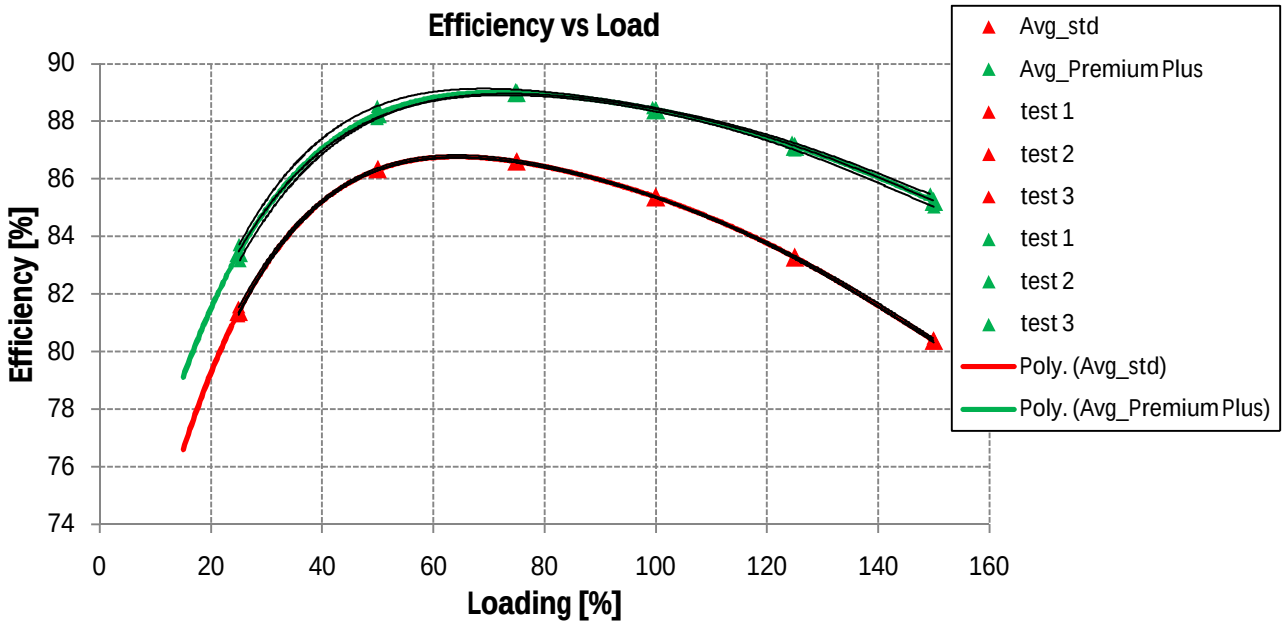

Figure 41: Efficiency vs. load characteristics of 11kW standard and EE motors

The 11kW EE motor in Figure 41 exhibits about a 3.5% higher efficiency at full load than the standard motor. It is evident from the figure that the premium motor has a flatter efficiency across the load range. Furthermore, the EE motor operates at maximum efficiency at approximately 75% of full load, whilst the standard motor reaches maximum efficiency at approximately 60%.

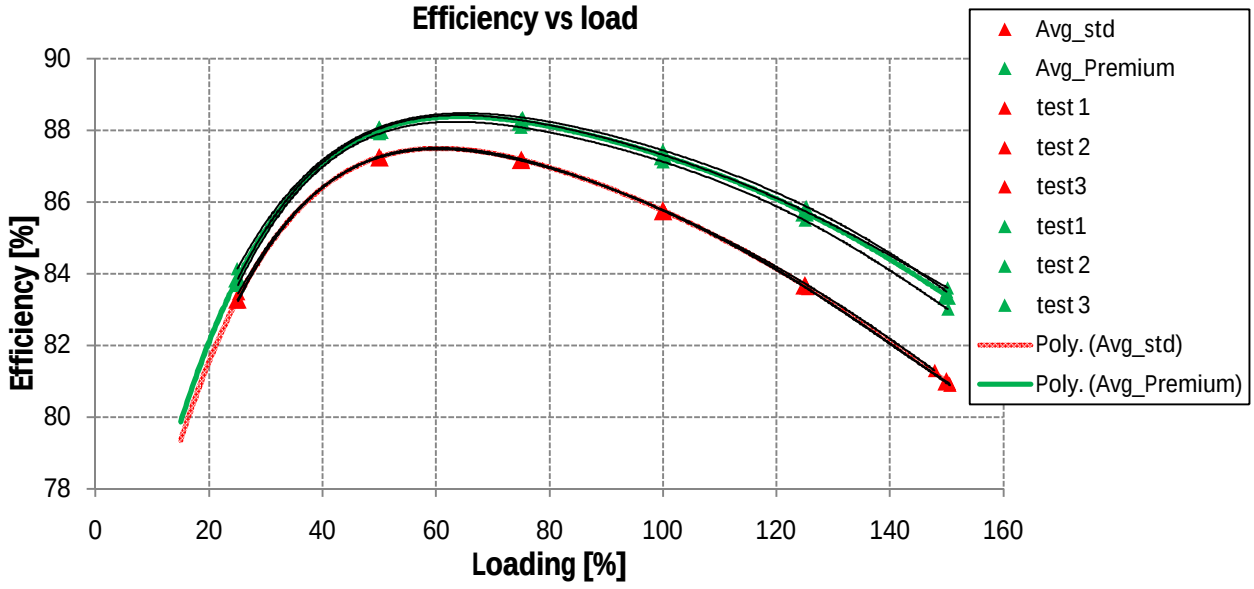

Figure 42: Efficiency vs. load characteristics of 7.5kW standard and EE motors

The 7.5kW EE motor in Figure 42 also has a flatter efficiency curve than the standard motor. The difference in efficiency at full load between the two motors is approximately 2%, with the premium plus motor being the highest. The premium plus maximum efficiency is 88.4% and 87.6% for the standard motor. The standard motor achieves maximum efficiency at 60%, whilst the premium plus motor achieves it at approximately 70%.

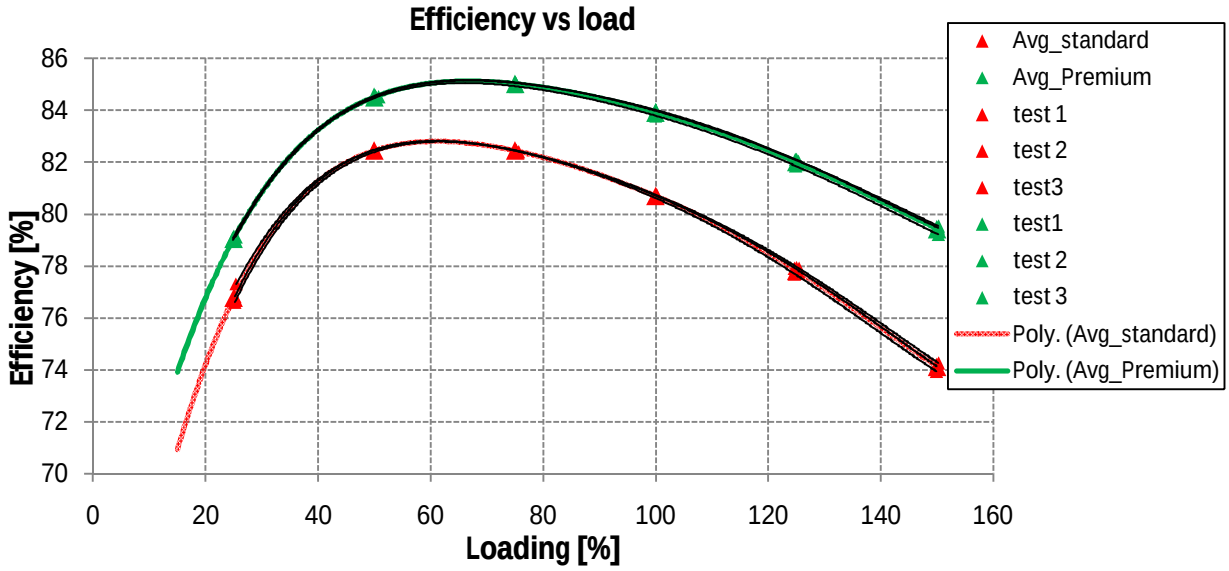

Figure 43: Efficiency vs. load characteristics of 3kW standard and premium plus motors

It is evident from Figure 43 that the 3kW premium plus motor reveals a higher efficiency than the standard motor. The premium plus motor is approximately 3.7% higher than the standard motor at full load. Maximum efficiency for the premium plus motor is 85% and 82.8% for the standard motor and is designed to be achieved at 70% and 60% for the premium plus and standard motors respectively.

5.3 OPERATING TEMPERATURE AND RESISTANCE DIFFERENCES

The operating temperature and winding resistance differences between the standard and EE motors are presented in this section.

5.3.1 Cold Temperature Results

Before the motors were energised, a dc test was performed to obtain the resistance on the stator winding and the temperature recorded. The resistance of each machine is shown in the Table 7:

Table 7: Motor cold stator winding resistances

	15kW	**11kW**	**7.5kW**	**3kW**
Standard	0.67 Ω	0.99 Ω	1.87 Ω	1.77 Ω
Premium Plus	0.605 Ω	0.796 Ω	1.575 Ω	1.46 Ω

5.3.2 Torque for Thermal Test Results

From the rated power and speed on the nameplate, the rated torque of each of the motors studied, was calculated using the equation below and is shown in Table 8.

$$= \frac{}{} \times \frac{60}{2}$$

Table 8: Motor Torque at rated power and speed

	15kW	**11kW**	**7.5kW**	**3kW**
Standard	98.45 Nm	72.45 Nm	49.23 Nm	20.61 Nm
Premium Plus	98.14 Nm	71.95 Nm	49.06 Nm	20.11 Nm

5.3.3 Operating Temperature

The motors were working at rated load and the temperature monitored every 30 min until it changed by no more than 1°C. On average, this took about 4 hours for each motor. The highest temperature measured at thermal equilibrium for each motor is shown in Table 9.

Table 9: Steady state motor temperatures

	15kW	**11kW**	**7.5kW**	**3kW**
Standard	117.12°C	118.78°C	115.8°C	110.44°C
Premium Plus	106.08°C	86.45°C	105.95°C	88.81°C

5.3.4 Steady state Resistance

Once this steady state condition was reached the motor was stopped and the resistance measured as quickly as possible to minimise a large temperature drop and hence a drop in resistance. The DC generator was left energized to bring the shaft quicker to a standstill. The per-phase resistance measured after the thermal equilibrium was reached is shown in Table 10:

Table 10: Motor steady state stator winding resistances

	15kW	**11kW**	**7.5kW**	**3kW**
Standard	0.87 Ω	1.4 Ω	2.407 Ω	2.26 Ω
Premium Plus	0.755 Ω	0.98 Ω	2.0 Ω	1.79 Ω

5.4 NO-LOAD TESTS

The no load test is carried out to obtain the core and friction and windage losses based on the assumption that they are independent of the load. The no load test was performed at input voltages ranging from approximately 475V to 76V and the resulting temperature, currents and power were recorded. The data recorded for the standard and the premium plus motors are given in Table 11 to Table 14, starting with the 15kW motors.

Table 11: No load data for 15kW Standard and Premium Plus motors respectively

Temp [°C]	Voltage [V]	Current [A]	Pin [W]	Temp [°C]	Voltage [V]	Current [A]	Pin [W]
68.97	472.3	21.32	1,575.22	61.38	472.54	20.92	1407.68
69.6	437.21	16.27	995.39	62.15	416.51	13.72	699.04
68.7	380.04	11.29	565.93	62.30	380.50	11.07	521.64
68.51	306.39	8.31	370.91	62.02	307.17	8.15	380.63
68.1	233.4	6.16	254.64	64.42	228.95	5.96	302.09
67.56	154.64	4.05	168.28	62.10	155.42	4.10	245.00
65.78	97.23	2.66	124.8	59.33	95.55	2.90	214.60

Table 12: No load data for 11kW Standard and Premium Plus motors respectively

Temp [°C]	Voltage [V]	Current [A]	Pin [W]	Temp [°C]	Voltage [V]	Current [A]	Pin [W]
72.57	461.51	18.37	1612.61	60.53	475.70	17.91	1356.32
73.89	417.96	12.80	889.53	61.13	419.36	11.67	692.52
73.44	380.43	9.55	565.48	60.97	380.39	9.15	502.23
72.35	303.64	6.39	323.34	60.67	301.04	6.55	364.82
70.69	166.06	3.36	149.40	59.82	152.54	3.35	250.75
69.39	92.75	2.00	98.28	59.31	96.97	2.57	224.95

Table 13: No load data for 7.5kW Standard and Premium Plus motors respectively

Temp [°C]	Voltage [V]	Current [A]	Pin [W]	Temp [°C]	Voltage [V]	Current [A]	Pin [W]
71.26	477.36	12.33	1201.94	52.32	476.18	8.79	686.64
73.04	413.35	7.08	480.61	52.82	416.36	5.83	400.74
72.69	383.04	5.47	322.52	53.19	381.05	4.92	335.99
71.50	308.06	3.53	180.86	52.27	300.96	3.64	254.89
70.43	204.10	2.22	105.92	52.32	150.80	1.88	170.98
69.78	113.34	1.28	68.96	51.22	88.55	1.54	151.74

Table 14: No load data for 3kW Standard and Premium Plus motors respectively

Temp [°C]	Voltage [V]	Current [A]	Pin [W]	Temp [°C]	Voltage [V]	Current [A]	Pin [W]
68.45	473.35	6.41	628.76	64.96	475.37	4.75	353.82
69.73	456.74	5.61	504.42	65.38	457.55	4.20	296.59
70.50	417.39	4.10	305.52	65.41	417.54	3.30	219.33
70.28	379.96	3.12	204.57	65.20	382.49	2.79	183.84
69.32	303.40	2.09	118.58	64.85	301.47	2.07	141.46
68.44	227.90	1.50	74.41	64.41	229.19	1.56	116.71
67.41	150.28	1.01	44.93	64.13	158.65	1.13	98.92
66.00	72.59	0.57	26.42	63.52	78.53	0.95	86.54

Since the bearing and seal friction losses of the tested energy efficient motors are higher, the no load losses are higher at reduced voltages as the bearing and seal friction losses are predominant at low voltages and speeds.

5.5 VARIABLE LOAD TESTS

Table 15 to Table 22 shows the test data obtained according to the IEEE and IEC requirements for the tested standard and premium efficiency motors. The 15kW motors could not be loaded more than about 126% because the 15hp DC Drive together with the resistor bank were not big enough to dissipate all the power above this level. For the purpose of this report the data shown in following tables is the average of the three test done per motor however, the analysis was done on all the test individually.

Table 15: Averaged data of the 15kW standard motor

Speed [rpm]	Temp [°C]	Voltage [V]	Current [A]	Pin [W]	Freq [Hz]	Torque [Nm]	Load [%]
1429.73	109.34	379.17	39.28	22072.13	50.01	124.44	126.40
1447.93	111.58	379.87	31.06	17292.35	50.01	98.49	100.04
1463.20	110.47	381.02	24.09	12930.46	50.01	73.73	74.90
1476.86	106.64	383.15	18.13	8769.69	50.02	49.19	49.96
1488.89	103.02	384.43	13.53	4717.77	50.02	24.60	24.99

Table 16: Averaged data for the 15kW Premium Efficiency motor

Speed [rpm]	Temp [°C]	Voltage [V]	Current [A]	Pin [W]	Freq [Hz]	Torque [Nm]	Load [%]
1435.42	108.70	378.60	38.29	21461.03	49.99	122.18	124.52
1441.56	110.26	378.37	35.41	19805.21	50.01	112.41	114.57
1451.38	110.47	379.61	30.93	17217.55	50.02	97.95	99.83
1465.94	108.95	381.60	24.01	12944.38	50.04	73.52	74.93
1478.74	104.68	383.60	18.03	8809.85	50.05	49.01	49.95
1490.26	101.60	383.85	13.24	4721.73	50.06	24.47	24.94

Table 17: Averaged data for the 11kW Standard motor

Speed [rpm]	Temp [°C]	Voltage [V]	Current [A]	Pin [W]	Freq [Hz]	Torque [Nm]	Load [%]
1409.33	125.83	378.78	36.35	20234.91	50.03	108.37	150.10
1429.52	135.76	379.40	29.72	16620.91	50.02	90.25	125.00
1447.46	132.55	379.93	23.88	13171.74	50.02	72.16	99.94
1463.08	126.85	381.68	18.77	9912.65	50.03	54.15	75.00
1476.54	119.72	382.81	14.46	6786.45	50.03	36.10	50.00
1488.69	115.17	384.50	11.22	3754.67	50.03	18.04	24.99

Table 18: Averaged data for the 11kW Premium Efficiency motor

Speed [rpm]	Temp [°C]	Voltage [V]	Current [A]	Pin [W]	Freq [Hz]	Torque [Nm]	Load [%]
1429.50	98.15	380.82	34.28	19240.24	49.97	107.85	149.90
1445.99	101.24	384.55	28.17	15903.10	49.99	89.90	124.95
1459.10	101.24	385.97	22.91	12709.76	50.00	71.88	99.90
1470.61	99.29	387.35	18.23	9623.17	50.01	53.94	74.97
1481.24	96.21	388.71	14.16	6608.61	50.02	35.93	49.93
1490.87	92.33	388.71	10.97	3652.00	50.03	18.06	25.10

Table 19: Averaged data for the 7.5kW Standard motor

Speed [rpm]	Temp [°C]	Voltage [V]	Current [A]	Pin [W]	Freq [Hz]	Torque [Nm]	Load [%]
1419.31	107.93	382.60	22.94	13628.52	50.03	73.66	149.63
1436.26	112.84	383.04	18.97	11244.57	50.03	61.66	125.26
1451.93	112.82	383.75	15.23	8901.23	50.03	49.32	100.20
1465.35	110.10	382.57	11.90	6679.22	50.03	37.03	75.22
1478.06	105.74	384.29	8.96	4550.19	50.04	24.66	50.10
1489.40	101.60	385.18	6.69	2505.52	50.04	12.36	25.10

Table 20: Averaged data for the 7.5kW Premium Efficiency motor

Speed [rpm]	Temp [°C]	Voltage [V]	Current [A]	Pin [W]	Freq [Hz]	Torque [Nm]	Load [%]
1429.30	116.33	378.18	22.71	13448.82	49.99	73.64	149.60
1445.80	121.45	383.49	18.52	11067.10	50.00	61.35	124.62
1458.67	121.59	384.29	14.96	8824.46	50.02	49.08	99.71
1470.01	119.02	383.30	11.71	6663.38	50.03	36.85	74.85
1480.88	115.17	384.31	8.74	4564.02	50.04	24.56	49.89
1490.87	109.65	384.78	6.28	2513.18	50.05	12.31	25.01

Table 21: Averaged data for the 3kW Standard motor

Speed [rpm]	Temp [°C]	Voltage [V]	Current [A]	Pin [W]	Freq [Hz]	Torque [Nm]	Load [%]
1349.00	112.24	379.53	10.24	5913.87	50.05	30.92	150.00
1382.33	119.71	380.24	8.48	4829.48	50.05	25.75	124.93
1412.00	120.69	381.08	6.91	3813.20	50.05	20.62	100.03
1436.67	118.16	381.81	5.54	2863.41	50.05	15.53	75.36
1461.00	113.20	382.32	4.36	1934.21	50.05	10.28	49.89
1481.00	108.12	382.51	3.50	1075.33	50.05	5.22	25.31

Table 22: Averaged data for the 3kW Premium Efficiency motor

Speed [rpm]	Temp [°C]	Voltage [V]	Current [A]	Pin [W]	Freq [Hz]	Torque [Nm]	Load [%]
1372.33	91.42	379.90	9.57	5507.05	49.96	30.20	150.21
1398.67	93.40	380.97	7.94	4511.93	49.96	25.13	125.01
1421.67	93.17	381.86	6.53	3604.11	49.96	20.10	99.97
1442.33	91.66	382.33	5.23	2718.65	49.97	15.10	75.10
1461.67	89.46	382.95	4.10	1867.45	49.97	10.17	50.57
1480.00	86.83	383.48	3.22	1030.67	49.97	5.07	25.20

5.6 COMPARISON OF EQUIVALENT CIRCUIT PARAMETERS

The parameters of the standard and premium plus induction motors that were obtained from the Matlab code are presented in Table 23 to Table 26.

It is evident from the tables that the stator rotor resistances on the all the premium plus motors are significantly lower than the corresponding size standard motor. This can be explained by the larger copper conductors used in the high efficient motors. The stator and referred rotor leakage reactance showed no significant change between the two types of motors. The core loss resistance of the premium plus motors is about 32% higher for the 15kW and 78% higher for the 11kW motor. The 7.5kW premium plus motor has a 33% higher core resistance. The 3kW core resistance is almost 100% higher for the premium plus motor. It is evident from the results that the power loss in the core is lower on the premium plus motors since the power loss in this case is indirectly proportional to resistance i.e. = —.

Table 23: 15kW Equivalent Circuit Parameters

Standard Motor	
	0.76 Ω
	2.36 Ω
	2.36 Ω
	53.60 Ω
	1.65 Ω
	1258.50 Ω

Premium Plus motor	
	0.68 Ω
	2.44 Ω
	2.44 Ω
	57.50 Ω
	1.60 Ω
	1661.50 Ω

Table 24: 11kW Equivalent Circuit Parameters

Standard Motor	
	1.23 Ω
	3.03 Ω
	3.03 Ω
	66.60 Ω
	2.06 Ω
	1048.70 Ω

Premium Plus motor	
	0.92 Ω
	3.09 Ω
	3.09 Ω
	69.15 Ω
	1.92 Ω
	1865.60 Ω

Table 25: 7.5kW Equivalent Circuit Parameters

Standard Motor	
	2.11 Ω
	4.19 Ω
	4.19 Ω
	119.11 Ω
	2.27 Ω
	2017.50 Ω

Premium Plus motor	
	1.72 Ω
	4.06 Ω
	4.06 Ω
	131.18 Ω
	1.77 Ω
	2678.70 Ω

Table 26: 3kW Equivalent Circuit Parameters

Standard Motor	
	2.03 Ω
	3.35 Ω
	3.35 Ω
	67.40 Ω
	1.61 Ω
	3187.60 Ω

Premium Plus motor	
	1.61 Ω
	3.44 Ω
	3.44 Ω
	76.14 Ω
	1.59Ω
	6357.30 Ω

5.7 COMPARISON OF LOAD-INDEPENDENT (FIXED) LOSSES

Squirrel cage induction motors have four types of losses namely copper losses, iron loss, friction and windage loss and additional or stray load loss. These losses can be divided into two main types, i.e. load independent (or fixed) losses and load losses which are dependent on the load on the shaft. The total loss is therefore the sum of the fixed and the load losses and can be expressed as follows:

$$= + \quad (25)$$

$$= + + + \quad (26)$$

The core losses and friction and windage losses are assumed to be load independent and were obtained by no load tests at constant frequency and varied voltage. The core loss is considered constant since the voltage on the terminals of the motor is constant regardless of the load the motor is subjected to. Similarly, the friction and windage losses can be assumed fixed since the speed does not change greatly over a wide load range. The power drawn at no load is essentially the losses and comprises the sum of the stator copper loss and the fixed losses. The no load stator copper loss is calculated using equation 27:

$$_{-} = 3 \quad (27)$$

The fixed losses can be found by subtracting the no load stator copper loss from the total no load input power and can be found by equation 41:

$$= \quad - \tag{28}$$

$$= \quad + \tag{29}$$

5.7.1 Friction and Windage Losses

The friction and windage loss is obtained by calculating the fixed losses for three values below 50% of rated voltage from the no load results and plotting it against the square of the voltage. A linear regression is done on the points and the friction and windage loss is simply the intercept of the power axis when the plot is extended to zero voltage. This is done by making the assumption that no core loss exist at zero voltage.

It is evident from Table 27 and Figure 45 that the friction and windage losses are much higher on the premium plus motors compared to the same size standard motors. This can be explained by the difference in ingress protection ratings found on the two types of motors. The standard motors have an IP55 rating where as the premium plus motors have got an IP66 protection rating. This means that the latter has better, tighter seals between the shaft and the motor casing for an improved protection against the ingress of dust and water as seen from Figure 44.

Figure 44: Standard and EE motor D.E. seals

An investigation was also conducted to find out whether any changes has been brought about to the size of the motor cooling fans enable to reduce the windage loss on the premium motors. Table 28 shows the observations that were made when the fan covers of all the motors were removed. It can be seen from Table 28 that the 7.5kW EE motor was the only machine that had a smaller cooling fan than the its standard motor

equivalent. The rest of the motors had the same size fans with exactly the same number of blades.

Table 27: Comparison of the friction and windage losses

Rated Power	Standard Motor	Premium Plus motor
15 kW	98.32 W	196.52 W
11 kW	75.61 W	208.20 W
7.5 kW	51.02 W	140.58 W
3 kW	20.73 W	80.03 W

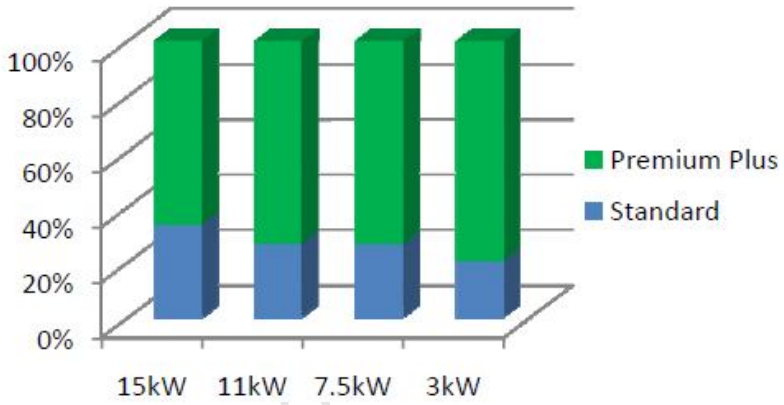

Figure 45: Friction and Windage Losses of the Range of Motors Tested

Table 28: Cooling Fan Differences between the Standard and Premium Plus Motors

Rated Power	Fan smaller?
15 kW	no
11 kW	no
7.5 kW	yes
3 kW	no

5.7.2 Core Losses

The core loss is obtained by subtracting the friction and windage loss, calculated above, from the total fixed losses at each of the voltages obtained from the no load test at varying voltages. A plot of core loss against voltage is created and is used to get the core loss at the voltages of each of the six load points. All plots in this report contain average curves of the three tests done per motor. The average curve is a polynomial of order n-1, where n is the amount of test points. The rotor core loss is neglected at since the frequency of the current in the rotor at the load slip is very small [12]. The IEEE 112-B does not compensate for the voltage drop across the stator winding resistance and the core loss can hence be extracted directly from the plot at the operating terminal voltage. The IEC 34-2-1 [13] however does compensate for the resistive voltage drop and the voltage across the core loss resistance is calculated using equation 43 below:

$$= \qquad - \sqrt{3} \times \quad \times \quad \times \qquad + \sqrt{3} \times \quad \times \quad \times \qquad (30)$$

Where:

$$= \frac{}{\sqrt{} \times \quad \times} \qquad (31)$$

$$\sin\varphi = \overline{1 - \sin \quad \varphi} \qquad (32)$$

It is clear from the equation above that the voltage across the core loss resistance is less than the terminal voltage and thus gives less core loss than the IEEE 112 standard. The variation of core loss with voltage is shown in Figure 46 to Figure 49 for the range of standard and EE motors tested. The core loss in the 15kW premium plus motor is approximately 131W or 35% less than the standard motor at rated voltage. The core loss of the 11kW premium motor is approximately 165 W less than that of the 11kW standard motor at 380V. This corresponds to a 45% reduction. The core loss in the 7.5kW EE motor is 55.5W (or 26%) lower than that of the standard motor at rated

voltage of 380V. The core loss in the 3kW EE motor is approximately 60W (50%) lower than that of the standard motor at rated supply voltage of 380V.

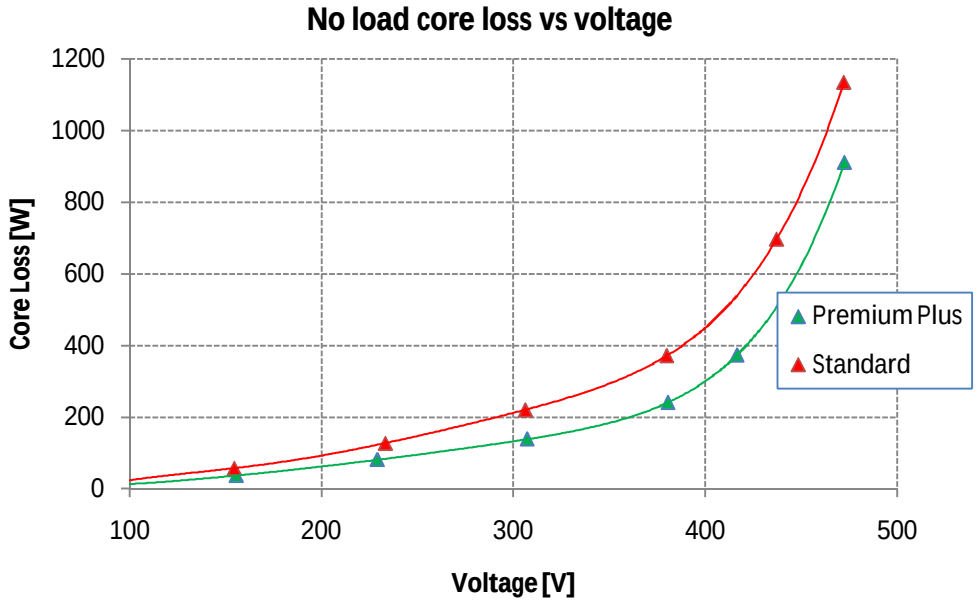

Figure 46: Variation of core loss with voltage of the 15kW standard and EE motors

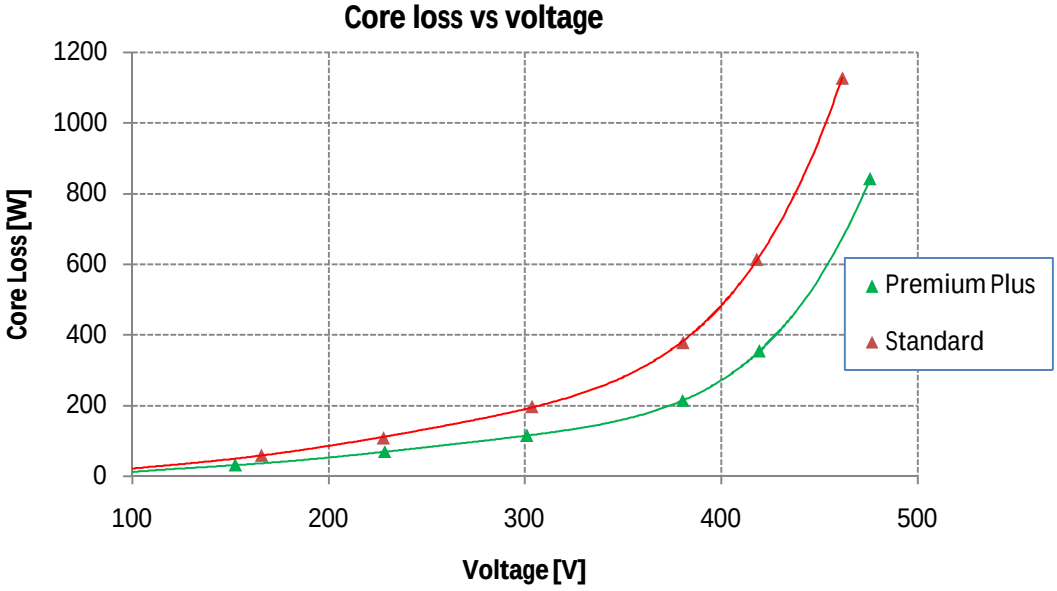

Figure 47: Variation of core loss with voltage of the 11kW standard and EE motors

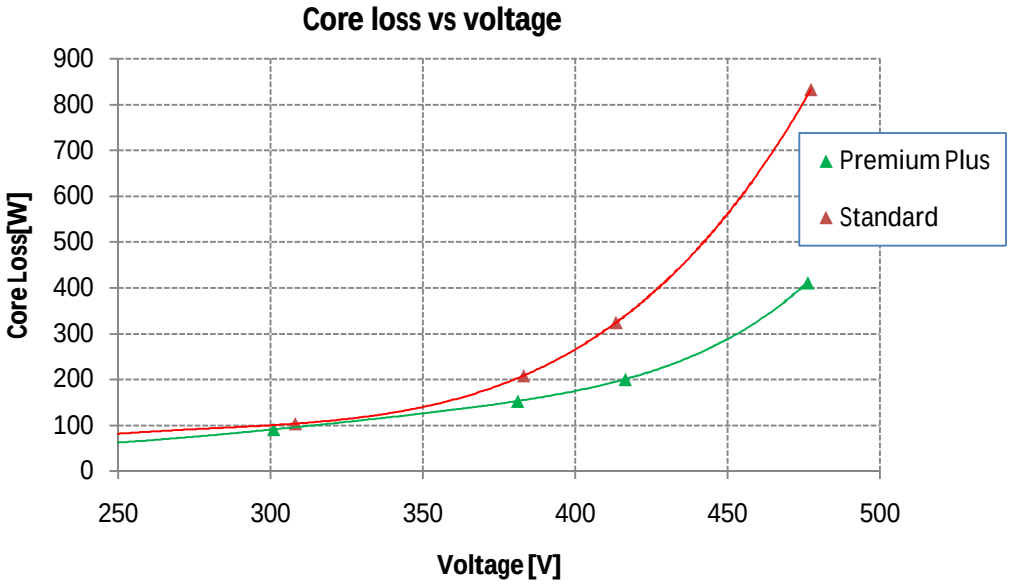

Figure 48: Variation of core loss with voltage of the 7.5kW standard and EE motors

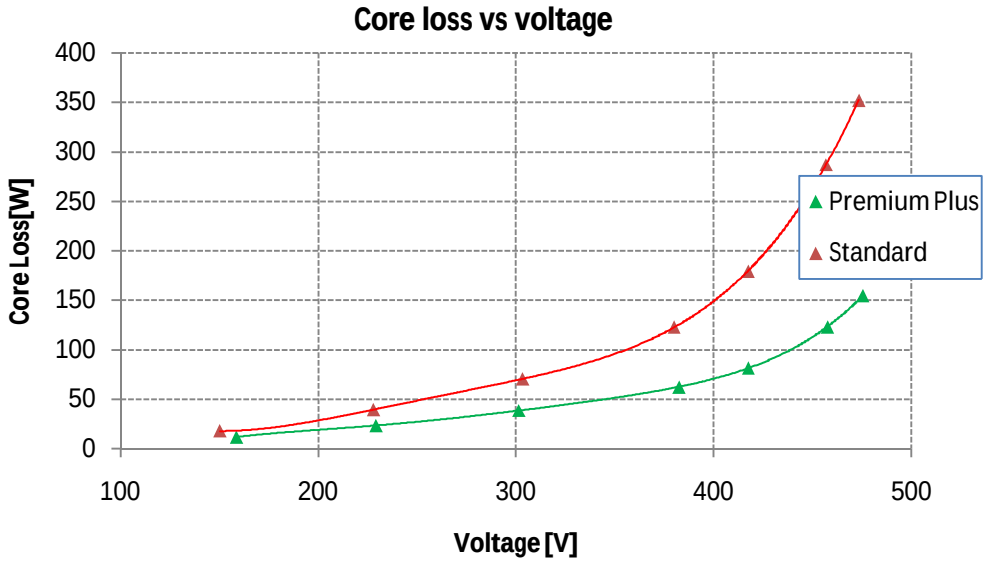

Figure 49: Variation of core loss with voltage of the 3kW standard and EE motors

The core loss in the 15kW premium plus motor is approximately 131W or 35% less than the standard motor at rated voltage. The core loss of the 11kW premium motor is approximately 165 W less than that of the 11kW standard motor at 380V. This

corresponds to a 45% reduction. The core loss in the 7.5kW EE motor is 55.5W (or 26%) lower than that of the standard motor at rated voltage of 380V. The core loss in the 3kW EE motor is approximately 60W (50%) lower than that of the standard motor at rated supply voltage of 380V.

5.8 COMPARISON OF LOAD-DEPENDENT LOSSES

The copper and stray load losses cannot be classified as load independent losses, since these losses are highly dependent on the current drawn by the motor. The current in turn is a function of the load on the motor. The stator and rotor copper losses as well as the stray load losses are calculated using the data attained from the variable load test. These losses are characterized in this section for the range of standard and EE motors tested.

5.8.1 Stator Copper losses

The stator copper loss is calculated by multiplying the square of the current at that load to the stator winding resistance corrected to a reference temperature i.e. the temperature at which the motor is operating. The variation of the stator copper losses with load is shown in Figure 50 to Figure 53 for the range of standard and EE motors tested.

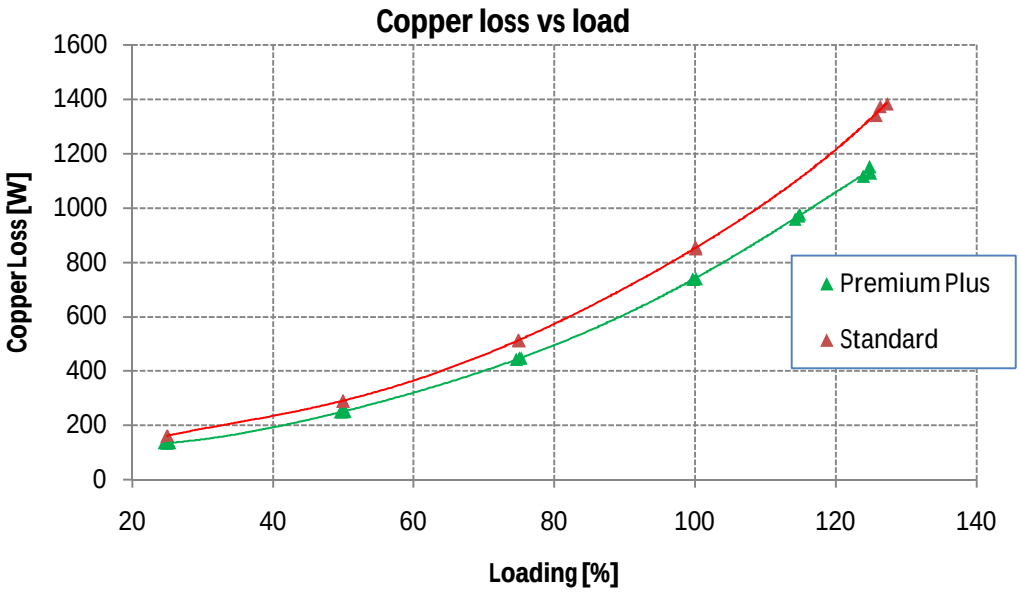

Figure 50: Stator copper loss variation with load for the 15kW motors

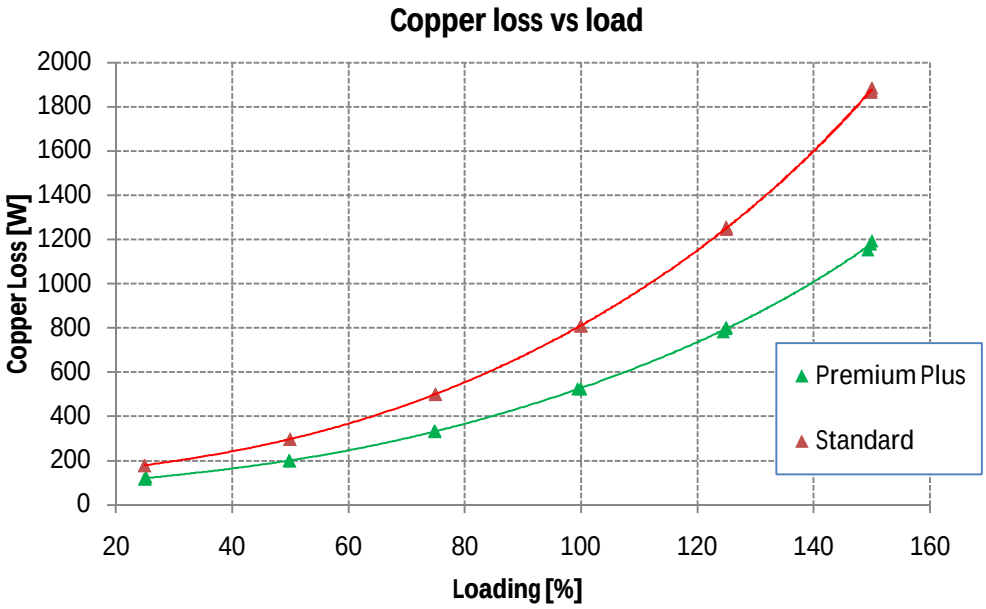

Figure 51: Stator copper loss variation with load for the 11kW motors

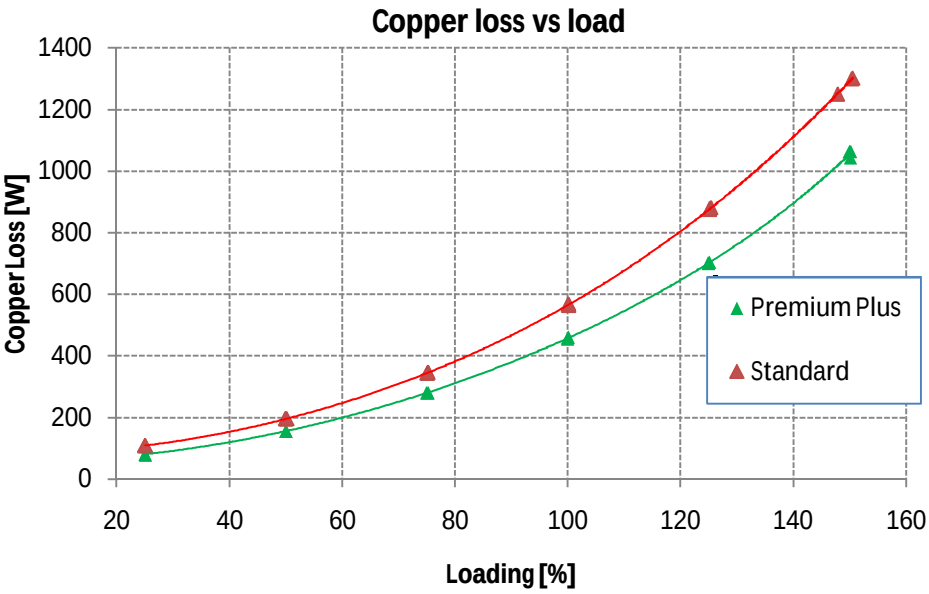

Figure 52: Stator copper loss variation with load for the 7.5kW motors

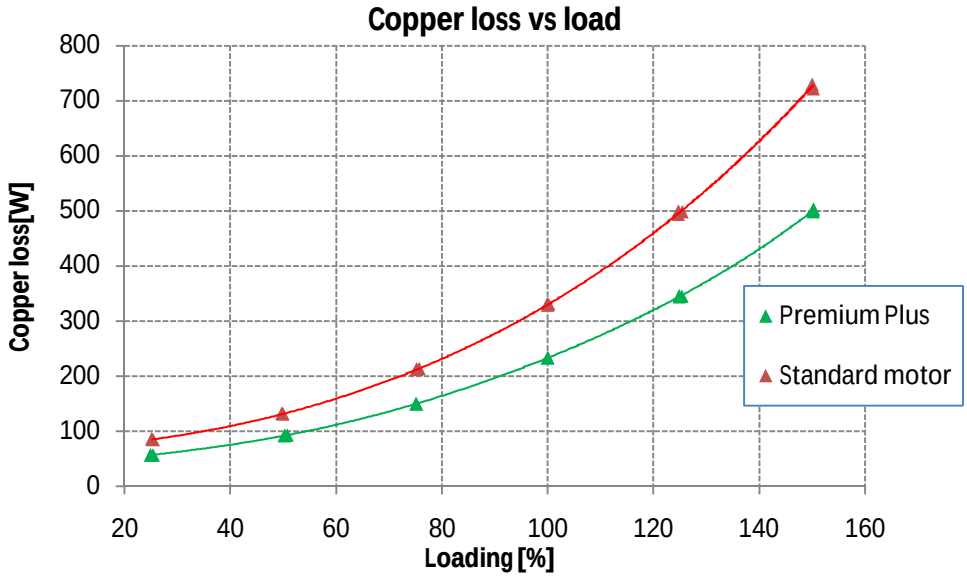

Figure 53: Stator copper loss variation with load for the 3kW motors

It can be seen from the following graphs that the power loss is not zero at zero percent load (no load). This is because the current does not vanish at no load condition. From

Figure 50 to Figure 53, it can be seen that the stator copper loss of the 15kW premium plus motor is about 114W or 13% less at full load. The copper loss of the 11kW premium plus motor is about 285 W less than the standard motor at full load i.e. a 35% reduction. At 75% and 50% load the reduction is 33.6% and 32.6% respectively. The stator copper loss in the 7.5kW premium plus motor is approximately 21% less than the equivalent standard motor. The reduction in terms of power is about 114W at rated load and about 40W at 50% load. The stator copper loss in the 3kW premium motor is approximately 30% less over the entire load range.

5.8.2 Rotor Copper losses

The power loss in the rotor winding is calculated by multiplying the slip with the power transmitted across the airgap to the rotor winding at each load using equation 48. The power transmitted to the rotor is the stator copper loss and core loss subtracted from the input power. The slip of the motor must take place at the specified temperature and were corrected the specified temperature according to [12] using equation 46 and according to [13] using equation 47, where the coolant temperature (t) is taken as the ambient temperate at the time of the test. A temperature correction is done to compensate for the effect that the ambient temperature has on the results. In other words, the same result is expected irrespective of the surrounding temperature the motor is tested in.

$$= \frac{(\quad .\ )}{(\quad .\ )} \tag{33}$$

$$= \frac{(\quad)}{(\quad)} \tag{34}$$

$$= \quad - \quad - \quad \times \tag{35}$$

The variation of the rotor copper losses with load is shown in Figure 54 to Figure 57 for the range of standard and EE motors tested. The losses shown are the average of three tests conducted on each motor.

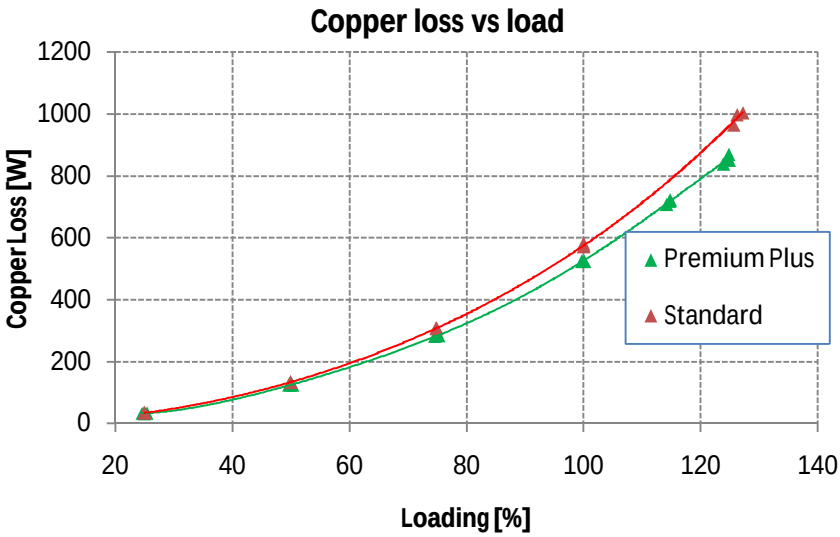

Figure 54: Rotor copper loss variation with load for the 15kW motors

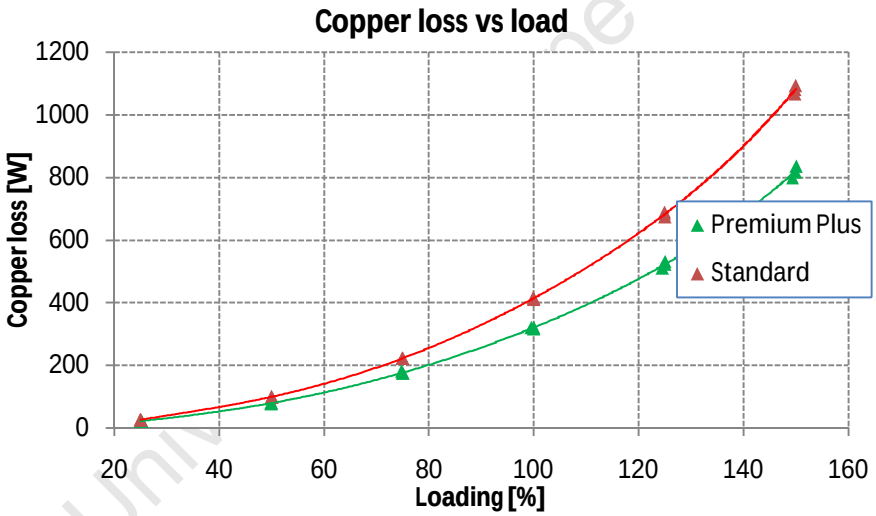

Figure 55: Rotor copper loss variation with load for the 11kW motors

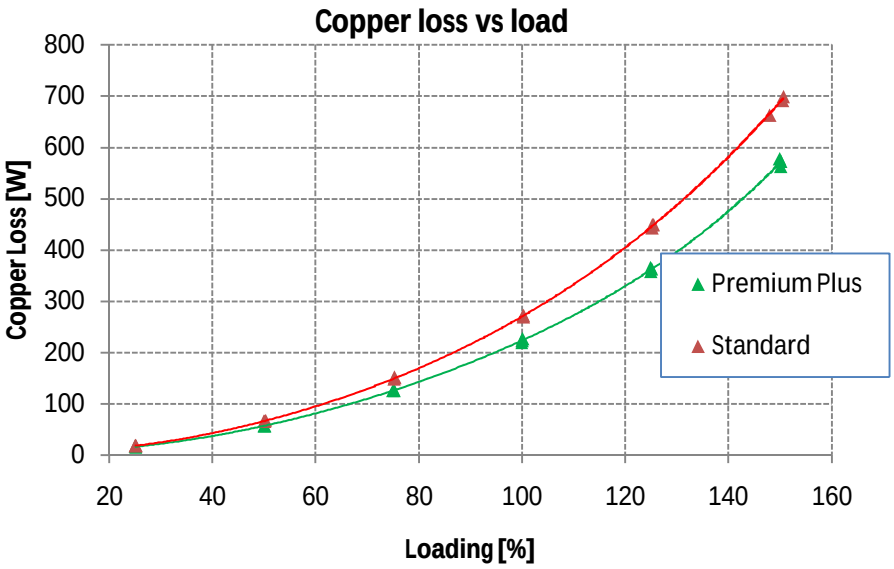

Figure 56: Rotor copper loss variation with load for the 7.5kW motors

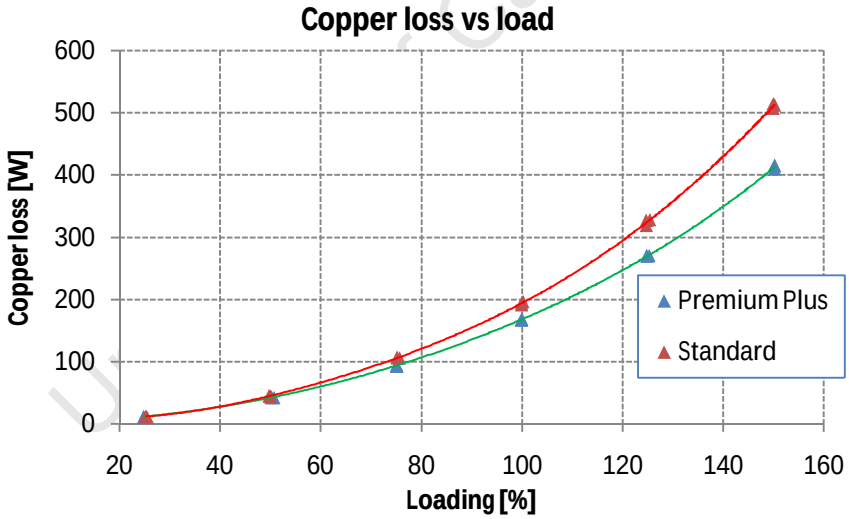

Figure 57: Rotor copper loss variation with load for the 3kW motors

The rotor copper loss in the 15kW premium plus machine is approximately 9%, 8% and 6.7% lower at 100%, 75% and 50% of full load, respectively. The reduction is about 51.8W on the premium plus motor. The reduction in rotor loss of the 11kW premium plus motor is approximately 95W at full load and about 46W at 75% load.

This translates to a reduction in rotor copper losses of 23% and 21% at 100% and 75% of full load, respectively. The rotor copper loss in the in the 7.5kW premium plus motor is about 17.5% less at rated load, 15.8% at 75% load and 14% at 50% load. The rotor copper loss in the 3kW premium plus motors is about 12-13% lower than that of the standard motor, between 75% and 100% load.

5.8.3 Stray Load Losses

The stray load loss is not covered by the above calculated losses and in [12] and [13] it is calculated by subtracting the sum of all the conventional losses i.e. copper losses, core loss, and friction and windage loss, from the total loss at each loading point. The data is then smoothed by performing a linear regression analysis on the six points and is plotted against the square of the torque. The correlation factor of IEC is 0.95 whereas the IEEE requires a minimum correlation factor of 0.9. The stray load loss is 0.5% of the input power according to the IEC34-2 standard. A comparison of the stray load loss obtained from the three standards is presented in Figure 58 to Figure 61. The green lines are the stray load loss of the premium plus motor and the red that of the standard motor.

It is evident from Figure 58 that the SLL for the 15kW motors determined from the IEC 34-2 is much less than that obtained by the other two standards. The SLL by the IEC 34-2-1 is higher than the SLL by the IEEE 112.

The SLL for the 11kW motors in Figure 59 for both machines is are significantly less than that of the other two standards. The IEC 34-2-1 gives the highest SLL for both machines.

The SLL for the 7.5kW motors (Figure 60) given by the IEC34-2 is once again significantly less than that from the the IEEE and the IEC 34-2-1. The IEC 34-2-1 gives the highest SLL of all three the standards.

The 3kW motors in Figure 61 shows the SLL obtained by the IEC34-2 is lower than that of the other two standards. The IEC 34-2-1 also gives the highest SLL in this case.

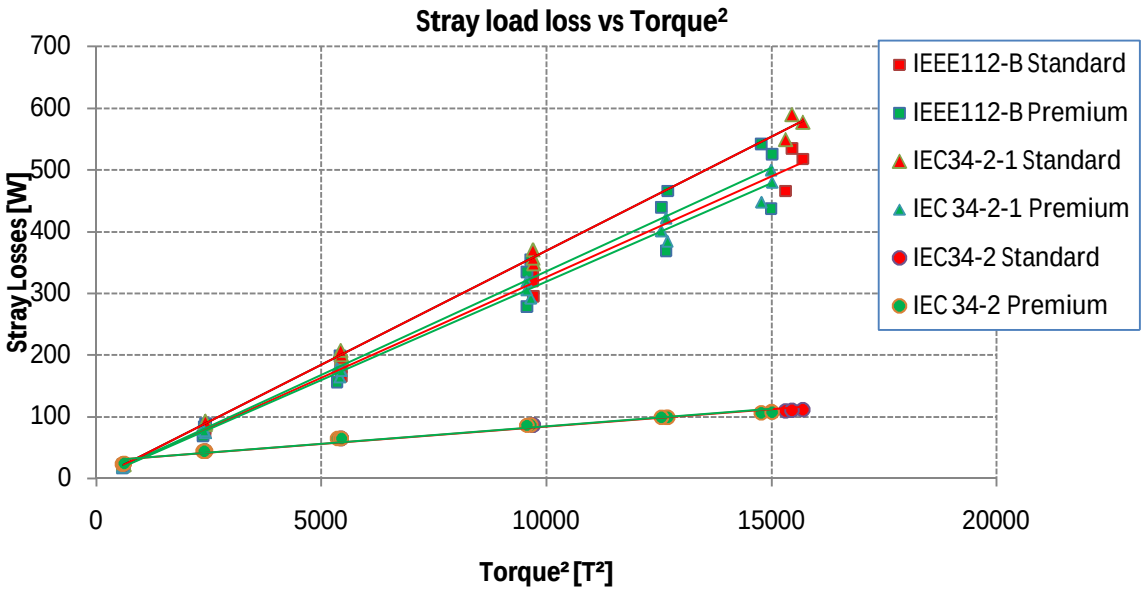

Figure 58: Stray load loss variation with torque squared for the 15kW motors

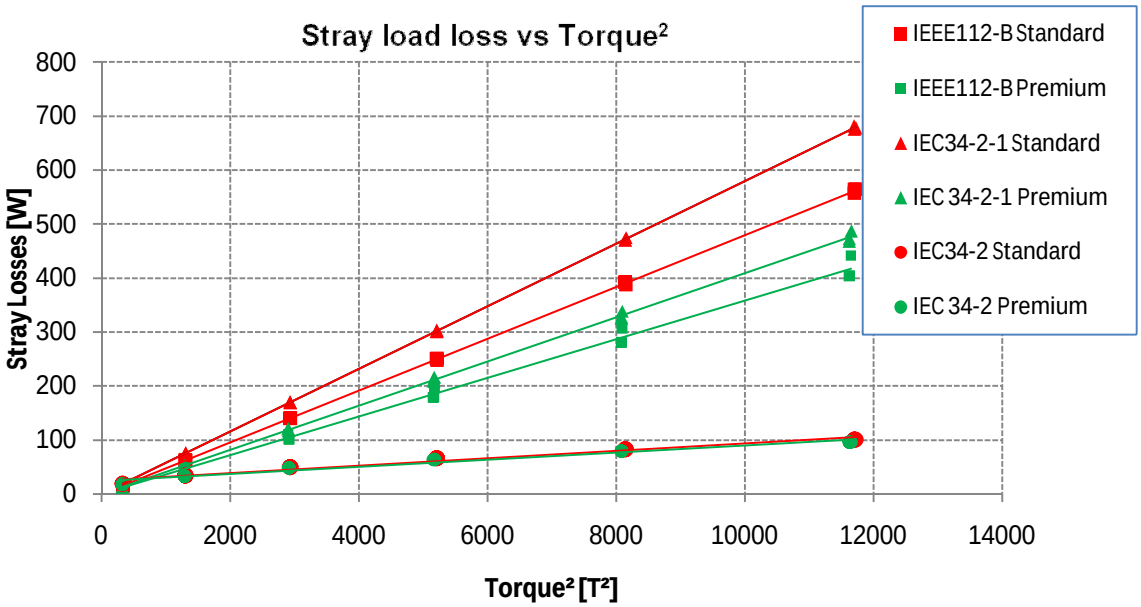

Figure 59: Stray load loss variation with torque squared for the 11kW motors

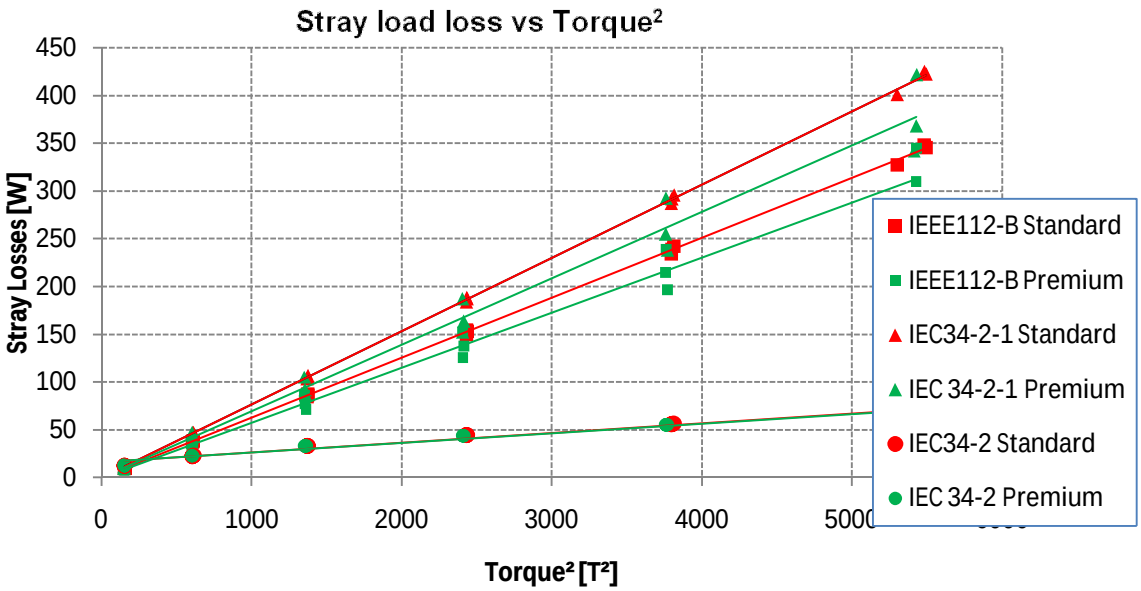

Figure 60: Stray load loss variation with torque squared for the 7.5kW motors

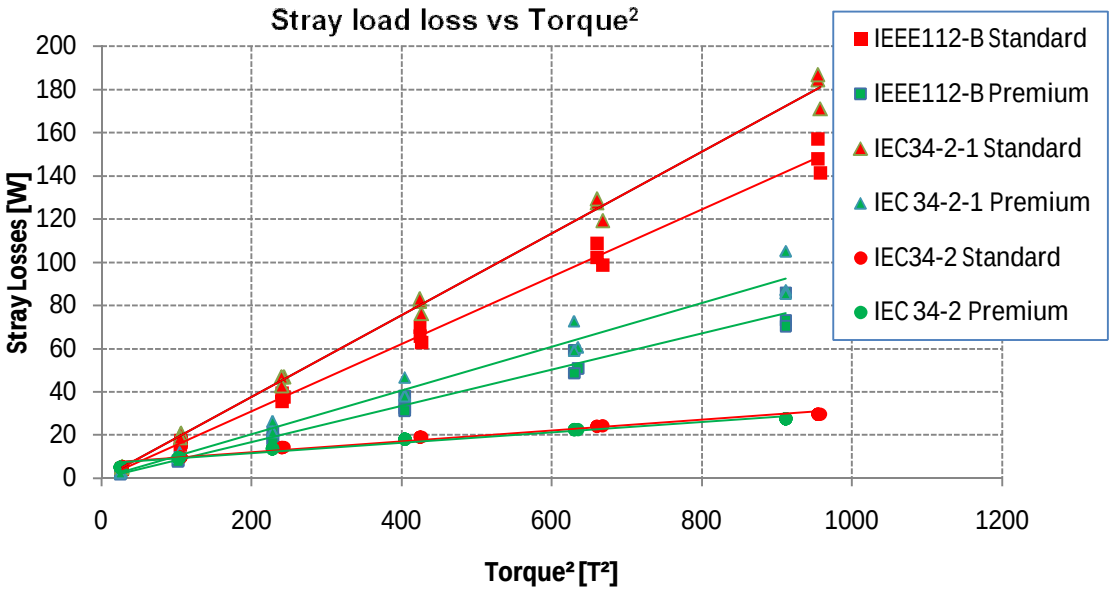

Figure 61: Stray load loss variation with torque squared for the 3kW motors

5.9 MOTOR LOSS DISTRIBUTION

The efficiency of a motor will reach its maximum value when the fixed loss equals the load loss [38]. In Figure 62 to Figure 65 the relative proportions of the individual losses at full load of each motor are represented in pie charts.

The friction and windage loss of the four standard motors that were studied contributed between 3-5% to the total loss at full load where as the premium plus motors contributed 10-14%. The contribution of the rotor copper loss to the total loss is more in the case of the premium plus motor than the standard motor except for the 7.5kW motor. The core loss contribution of premium plus motors is between 3-6% less for the eight motors that were tested.

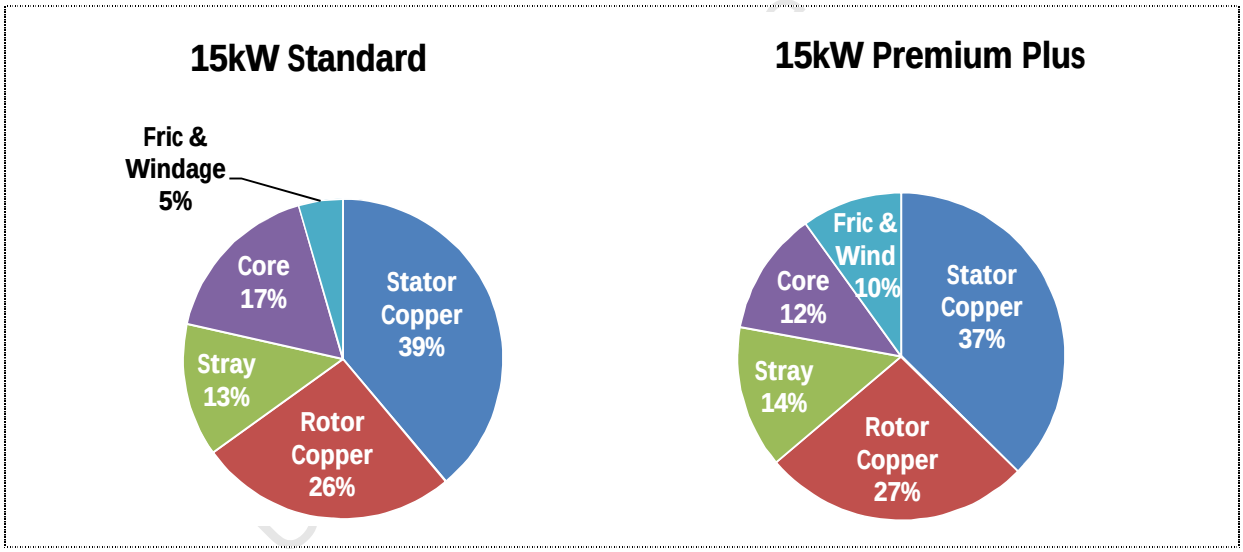

Figure 62: Loss distribution of standard and premium plus 15kW motors

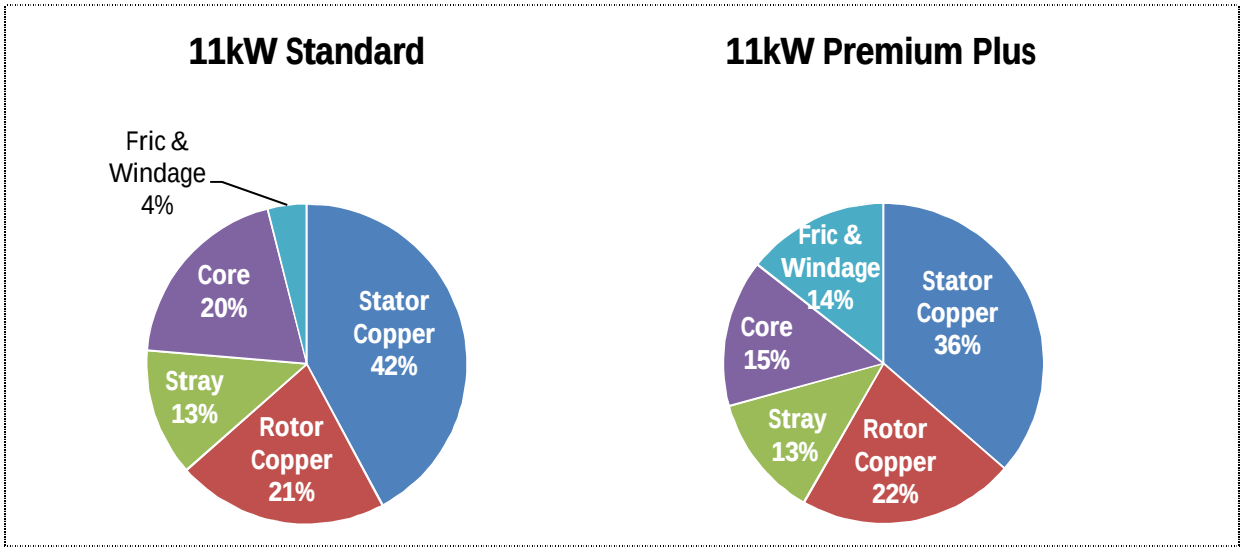

Figure 63: Loss distribution of standard and premium plus 11kW motors

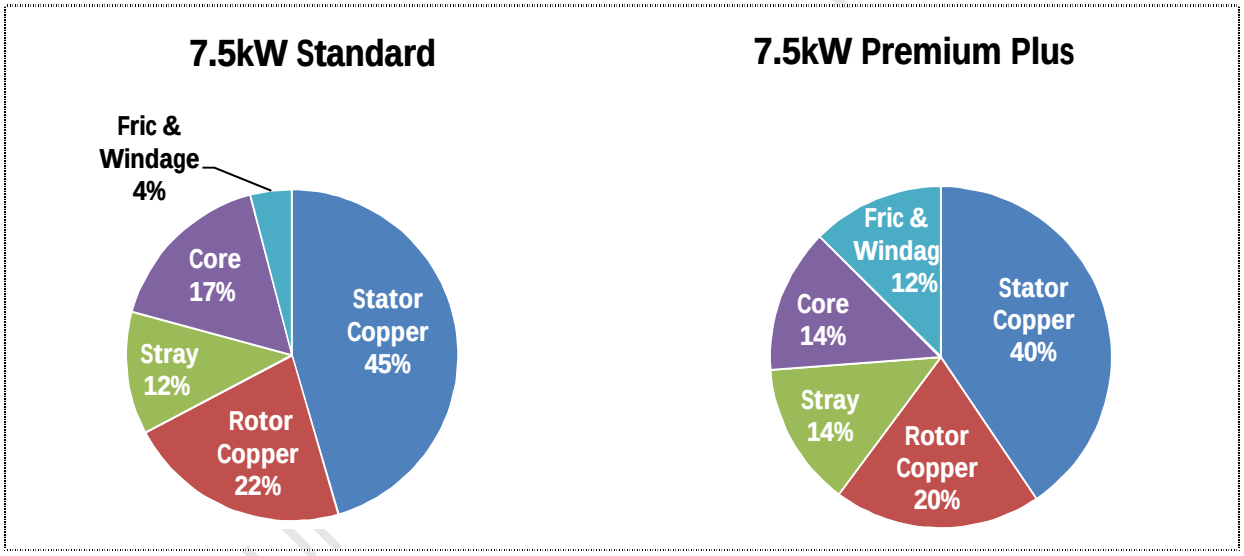

Figure 64: Loss distribution of standard and premium plus 7.5kW motors

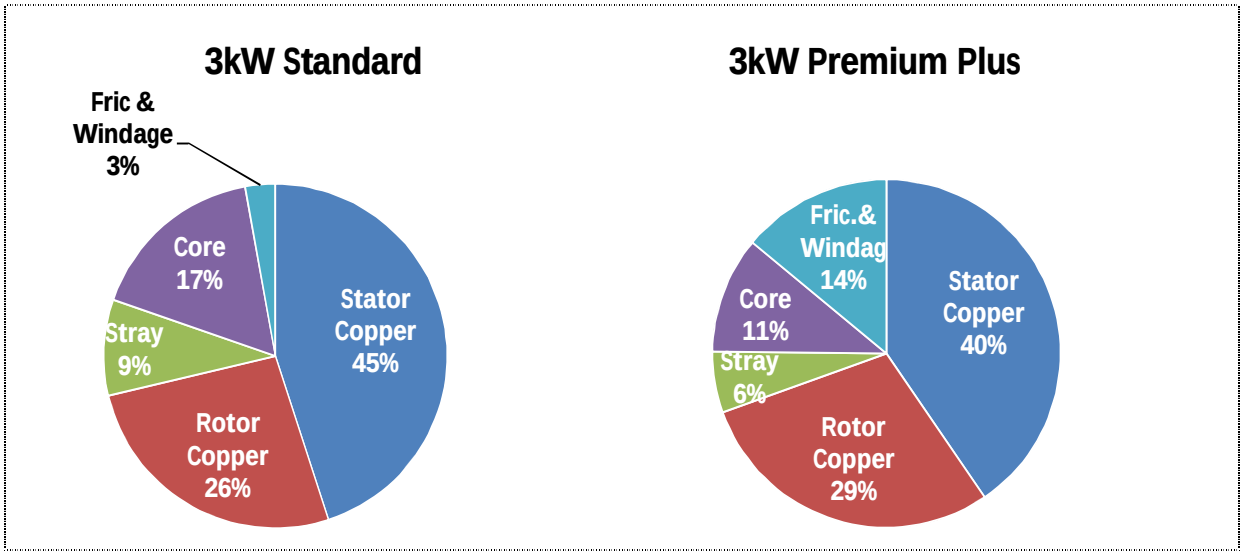

Figure 65: Loss distribution of standard and premium plus 3kW motors

5.10 STEADY-STATE OPERATIONAL PERFORMANCE DIFFERENCES

This section deals with modelling of each of the eight tested induction motors into Thevenin equivalent circuits and predicting the performance of the motors subjected to a centrifugal pump load, i.e. a load that increases exponentially with speed [39]. The pump load is configured such that it intercepts with the 75% load point of the standard motor. The torque-speed performance characteristics of the induction motors are investigated.

The theoretical performances of the standard and EE motors are compared with the performances obtained in the laboratory. The moderate correlation achieved between experimental and equivalent circuit results can be attributed to the following reasons:

- The voltages at each of the six loads are not the same as the 380V used in the theoretical model. This would change the torque curve since the torque is proportional to the square of the supply voltage i.e. $\propto$ [40].

- The stator and rotor resistances are not the same for all the six load points obtained in the laboratory because of the temperature variations. The theoretical model assumes constant parameters.

- The rotor resistance which affects the slope of the linear torque region could not be accurately corrected close enough to the operating rotor resistance of the experimental results.

5.10.1 Torque versus Speed Characteristics

The theoretical and experimental torque-speed characteristics of the motor sample are plotted on the same pair of axes in Figure 66 to Figure 69.

It is evident from Figure 66 to Figure 69 that the premium motors develop a higher torque for a given speed than the same size motor. The standard 15kW motor in Figure

66 operates at a torque of 70.6 Nm at a speed of 1431.75 rpm driving a centrifugal load. The same size premium plus motor operates at a torque of 71.6 Nm with a speed of 1435.5 rpm subjected to the same load. The premium motor thus operates at 0.6 Nm and 3.75 rpm higher than the standard motor. The output power delivered by the standard motor is 10.088 kW and the premium plus motor is 10.234kW. The input power for the standard and premium plus motor is 11.38 kW and 11.396 kW respectively. This is about 0.14% more input power drawn by the premium plus motor.

The standard 11kW motor in Figure 67 operates at a torque of 52.43 Nm at a speed of 1439.25 rpm. The premium motor is operating at 52.75 Nm and is driving the same centrifugal load at 1443.75 rpm. The latter is thus operating at 0.32 Nm higher and 4.5 rpm faster. The output power delivered by the standard and premium plus motors is 7.45kW and 7.54kW respectively and the input power is 8.61kW and 8.47kW respectively. Thus, only an improvement of 1.65% is achieved compared to the 2.5% absolute difference in efficiencies between the 2 motors, as discussed in section 5.2.2.

The standard 7.5kW motor in Figure 68 operates at 36.655 Nm at 1458 rpm. The premium plus motor is operating at 36.855 Nm at a speed of 1461.75 rpm with the same load. The standard motor delivers an output power of 5 346.96W and the premium plus motor gives an output power of 5 348.4W. The input power drawn by the standard motor is 6116.4W and 6057.76 for the premium plus motor.

The 3kW standard motor in Figure 69 is operating at 14.87 Nm at 1435.5 rpm and the premium plus one is operating at 14.93 Nm at a speed of 1438.5 rpm. The output power delivered to the pump load by the standard motor is 2 089.8W. The premium plus motor delivers 2 103.4W to the load. The latter draws 2 473.72W input power and the standard motor 2 536.2 W. The reduction in input power is about 2.52% compared to the approximately 2.7% efficiency improvement on the premium plus motor.

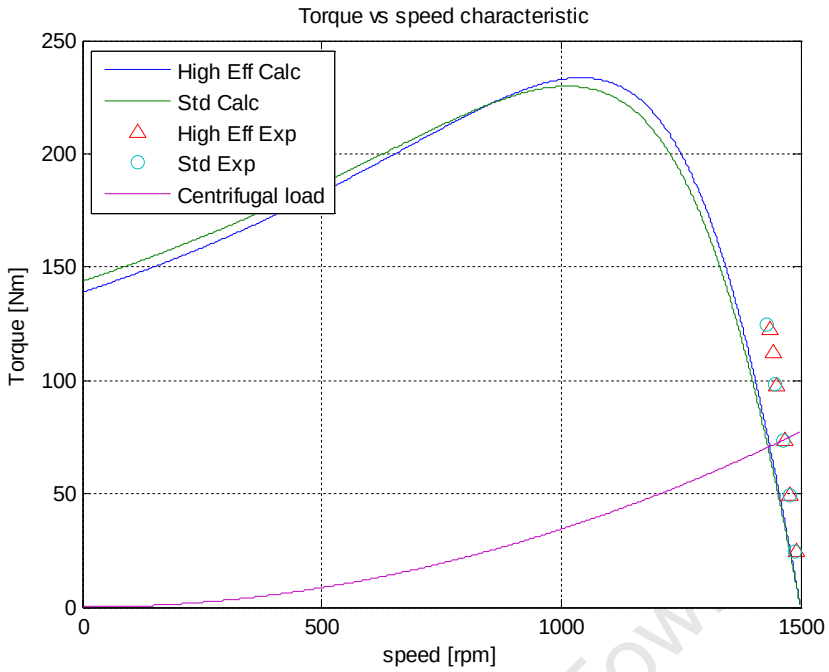

Figure 66: Torque vs speed characteristics of 15kW STD and EE motors with pump load

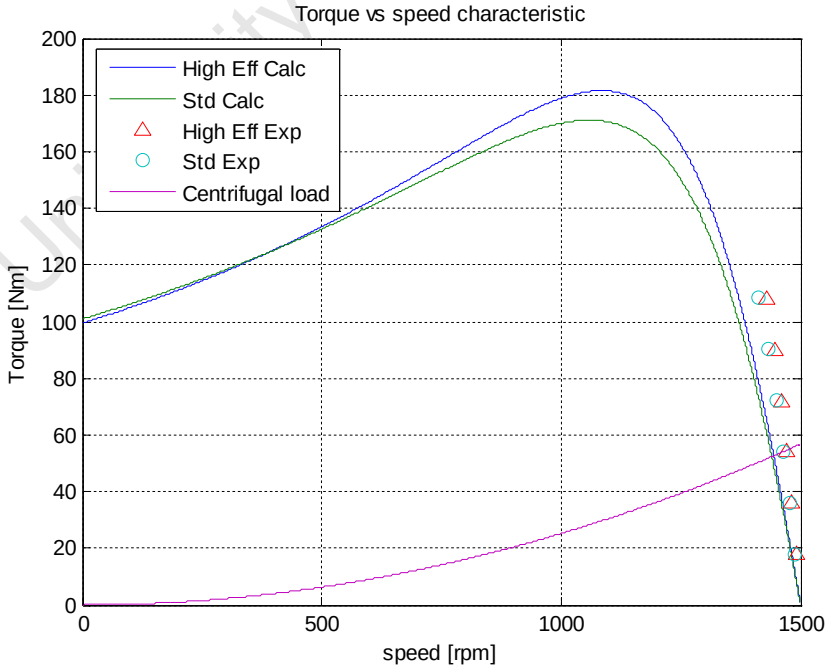

Figure 67: Torque vs speed characteristics of 11kW STD and EE motors with pump load

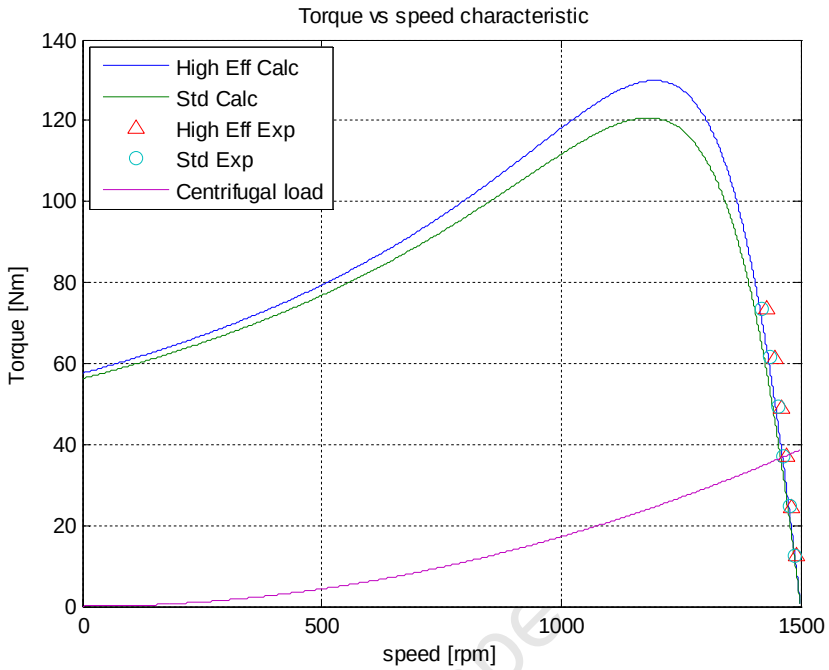

Figure 68: Torque vs speed characteristics of 7.5kW STD and EE motors with pump load

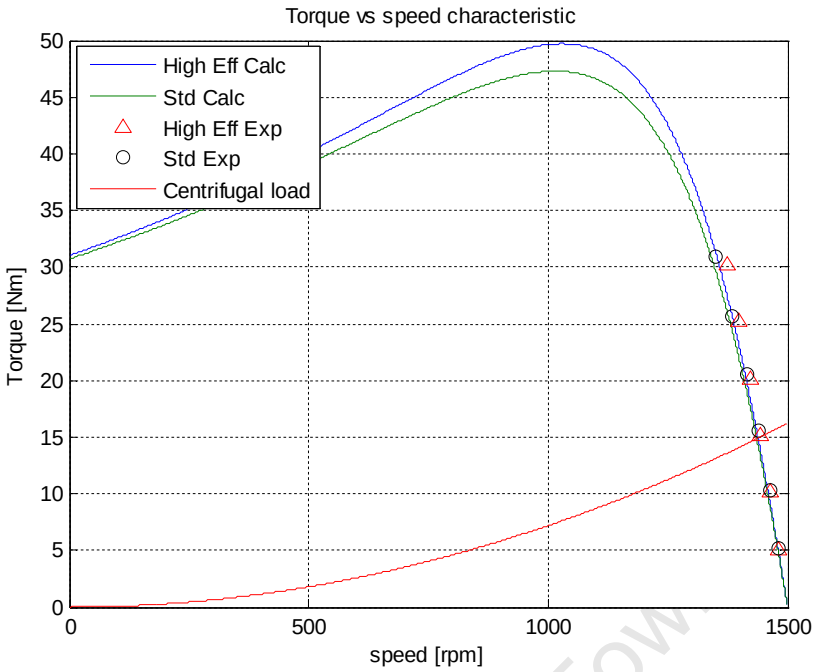

Figure 69: Torque vs speed characteristics of 3kW STD and EE motors with pump load

5.10.2 Current vs. Load Characteristics

The current vs. load characteristics were compared for the range of standard and EE motors tested. The currents were measured during load tests, whilst the load on the shaft of the motor was varied. The current were measured on stead-state with rated supply conditions applied to the motor terminals. The steady-state current vs. load characteristics are shown Figure 70 to Figure 69.

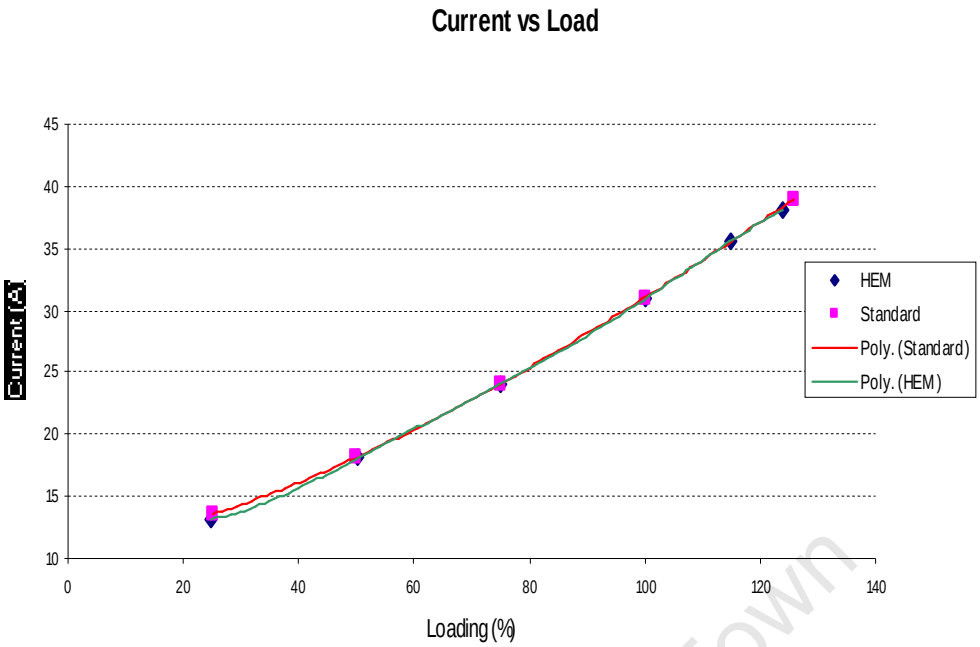

Figure 70: Current vs load characteristics for 15kW STD and EE motors

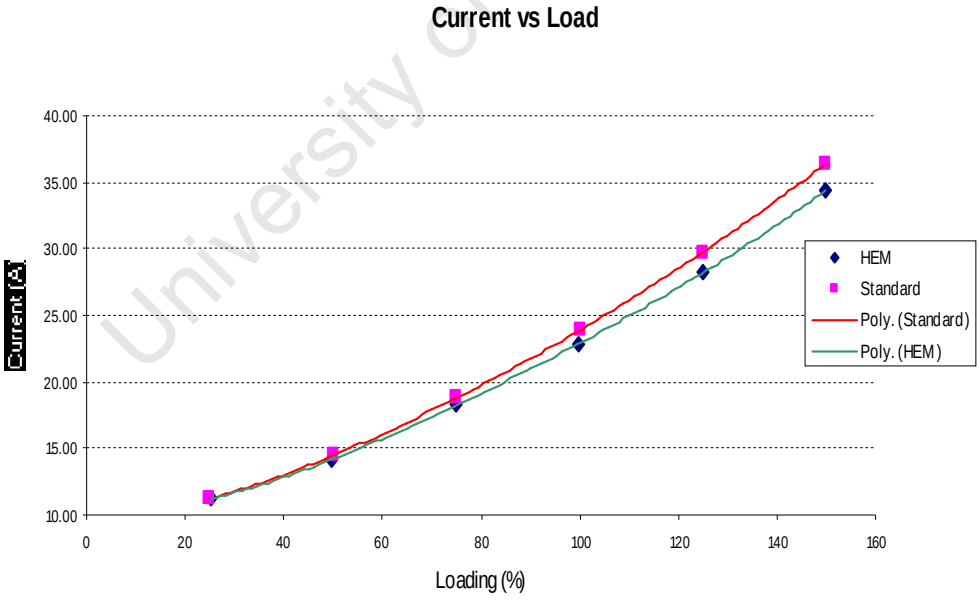

Figure 71: Current vs load characteristics for 11kW STD and EE motors

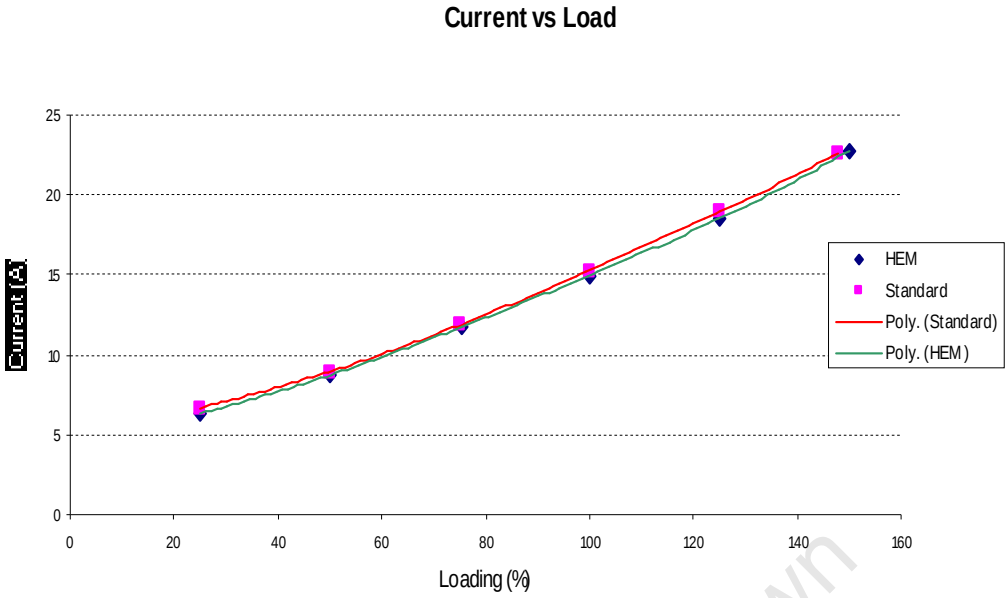

Figure 72: Current vs load characteristics for 7.5kW STD and EE motors

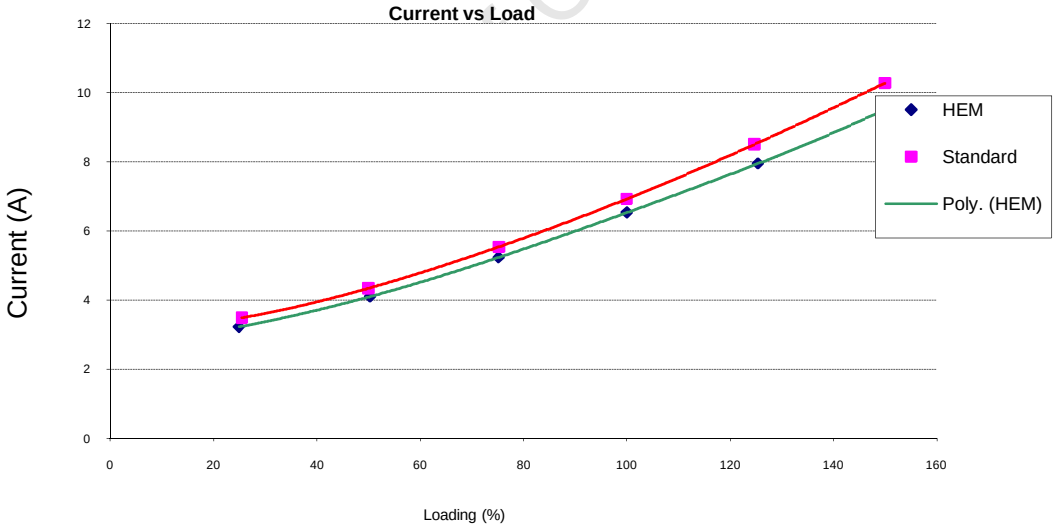

Figure 73: Current vs load characteristics for 3kW STD and EE motors

5.10.3 Operating Speed

Energy efficient motors typically have a higher full-load speed than a standard motor due to the reduced I^2R losses in the rotor. This higher full load speed may lead to higher input power to the motor depending on the type of load. Variable-torque loads e.g. fan and pump loads, follow the cube law. The extra power delivered at higher speed will be lost unless it can be used in the process. In the case of belt-driven systems t he pulley sizes can be adjusted to reduce the load [41].

5.11 TRANSIENT OPERATIONAL DIFFERENCES

The transient operational differences between standard and EE motors are discussed briefly in this section.

Upon the application of a three-phase voltage supply to the terminals of the motor, the only impedance that limits the current is the winding resistance. Because energy efficient motors have lower winding resistance than standard motors, they typically draw much higher starting current. At the instant a voltage is applied to the terminals there is no back EMF and no significant magnetic field to oppose the flow of current [42]. The first half cycle transient inrush and locked rotor current as ratios to the Full-load Amps (FLA) are higher for energy efficient motors [43]. The inrush current drawn by the motor lasts for half a cycle or so and is typically asymmetrical. As the motor accelerates, the motors back EMF opposes the applied voltage until the motor current decreases to the load current. The average locked rotor current of a standard motor is about five to six times the rated full- load current. Energy- efficient motors can draw as much as eight times its rated full-load current during startup as it can be seen from Figure 74.

The locked rotor current can last a few cycles for small motors to as long as a few seconds for large motors depending on the load inertia. The time it takes an energy efficient motor of the same size and load as a standard motor to reach steady state current is shorter as it can be seen in from Figure 74 to Figure 78. The inrush current

can be seen during the first half cycle of the transient and has a higher ratio to the FLA of the motor. The EE motor accelerates faster despite its higher rotor inertia. This is due to higher accelerating torque developed by the EE motor. The startup transient current of EE motors have direct impacts on the protection system feeding the motor. Due consideration should therefore be given to this in retrofit application in order to avoid nuisance tripping of EE motors. Obviously the first half cycle inrush current will depend on the magnitude of the mains voltage at the time and which instant on the voltage waveform it was switched on.

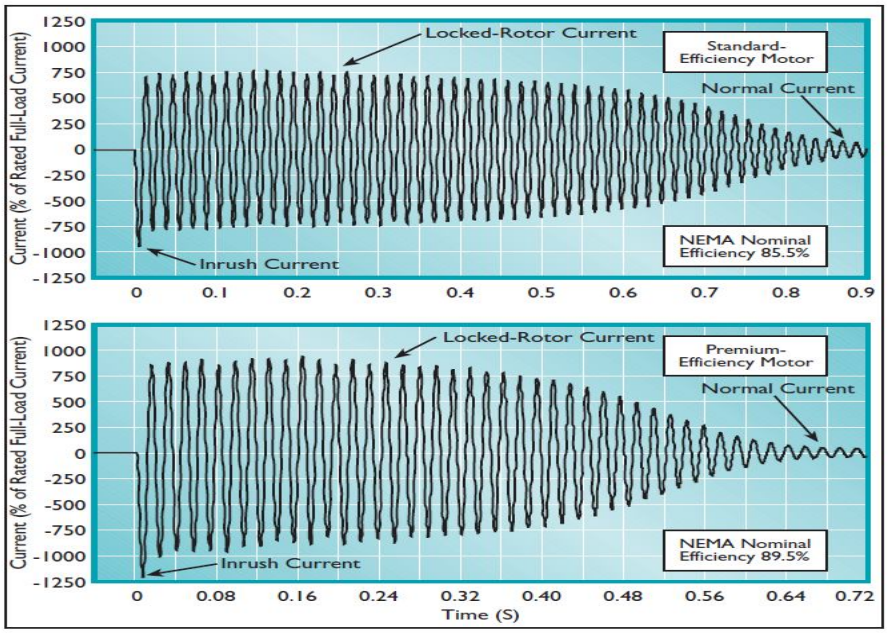

Figure 74: Inrush and locked rotor current during start-up of a 3kW STD and EE motor [12]

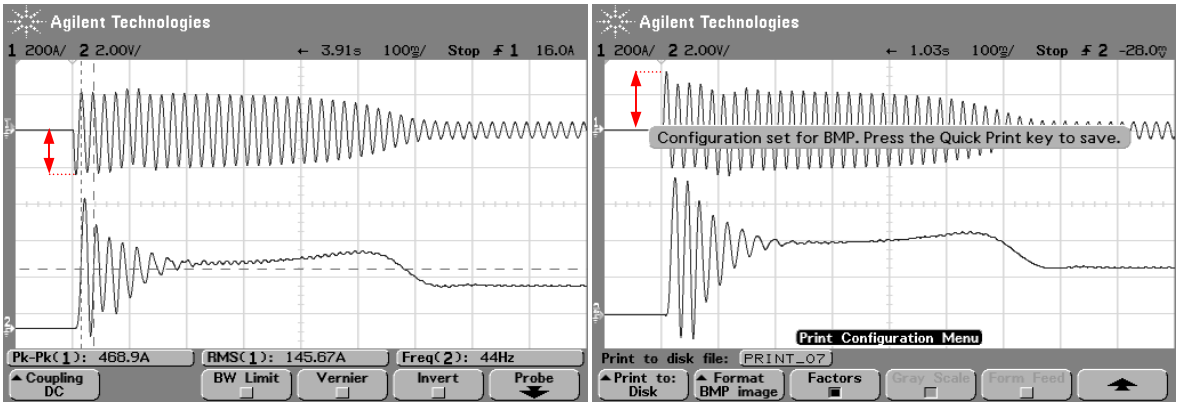

a) b)

Figure 75: Starting Current and Torque of a 15kW a) standard motor and b) EE motor

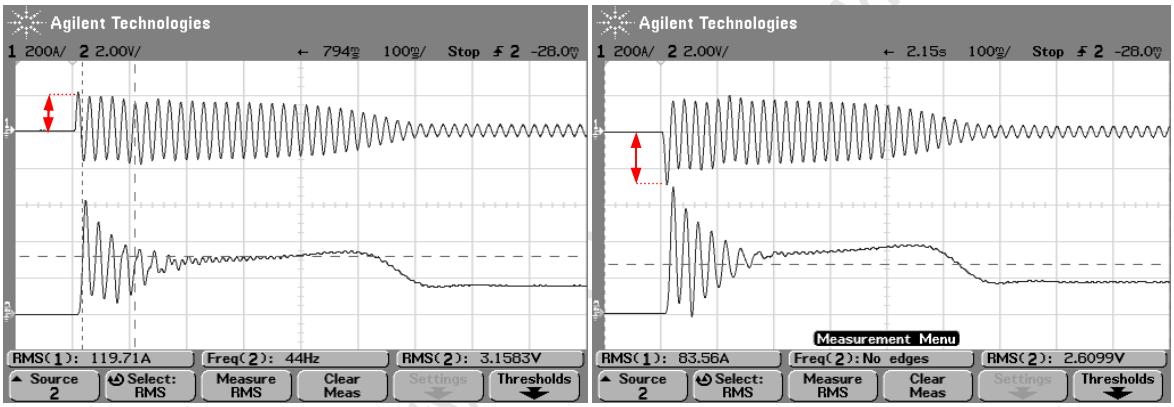

a) b)

Figure 76: Starting Current and Torque of a 11kW a) standard motor and b) EE motor

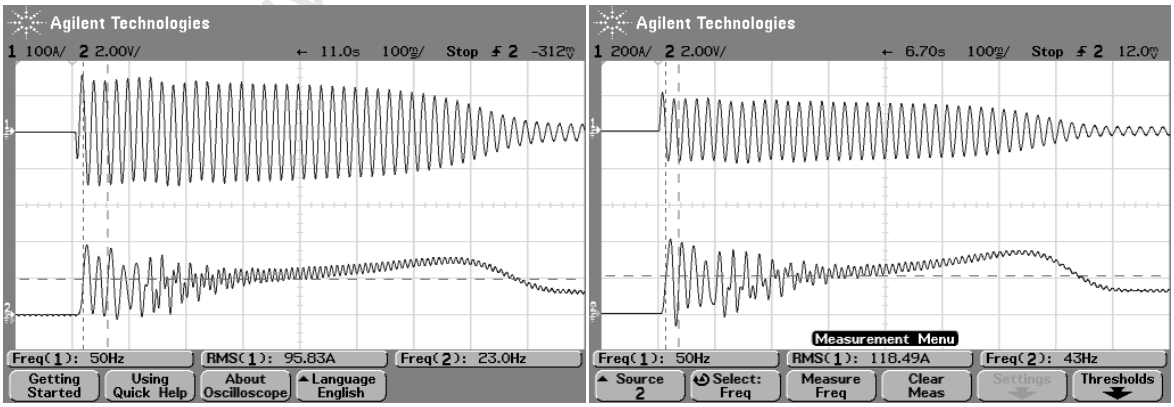

a) b)

Figure 77: Starting Current and Torque of a 7.5kW a) standard motor and b) EE motor

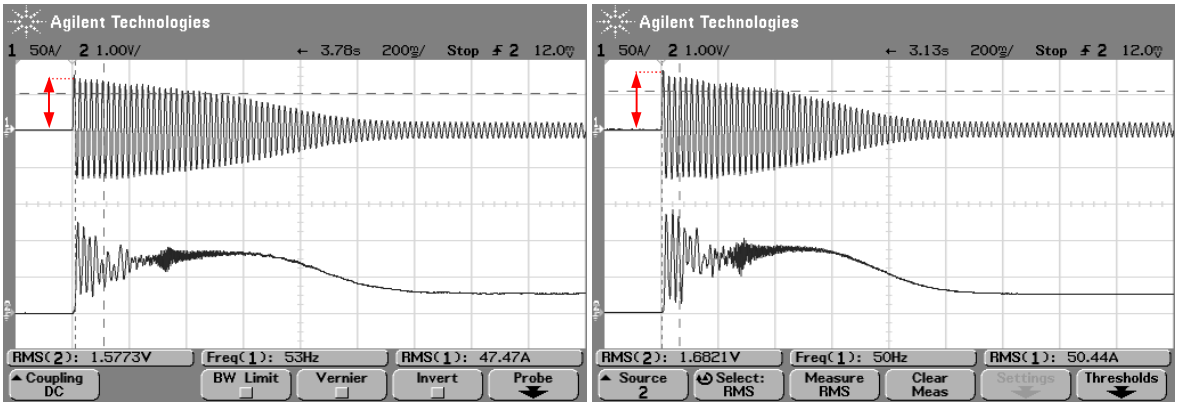

a) b)

Figure 78: Starting Current and Torque of a 3kW a) standard motor and b) EE motor

CHAPTER 6

6. IMPACT OF VOLTAGE UNBALANCE ON EE MOTORS

This chapter deals with impact of voltage unbalance on the efficiency of induction motors (IM). Firstly, comparisons of the current unbalance drawn by the two types of motors are presented before comparing the efficiencies of the motors at different supply voltage conditions. Finally, the results from the thermal model discussed in chapter 3 are given.

6.1 CURRENT UNBALANCE TEST RESULTS

Any unbalance in the supply voltage to an IM results in an associated current unbalance. In general, the % current unbalance is not necessarily the same as the % voltage unbalance. This is due the fact that the current unbalance is proportional to ratio of the negative sequence slip to the positive sequence slip. Since the negative sequence slip is equal to 2-s (two minus the positive sequence slip), the lower slip values at which EE motors operate, leads to a higher ratio. Take for example the 7.5kW motors. At 100% load, the standard motor operates at a slip of 0.034 while the EE motor operates at a slip of 0.028. Thus, using the expression in (19), for the standard motor: (2-s)/s = 57.8, and for the EE motor: (2-s)/s = 70.4. For this reason, current unbalance will be more severe in EE motors than it will be for standard motors. The same reasoning applies to why current unbalance is worse at no load than it is at full load. At full load, the slip is greater than at no load. Therefore, at full load (2-s)/s will be less than at no load and current unbalance will not be as high.

Tests were performed on several STD and EE motors to asses this. The tests were performed on 15kW, 11kW, 7.5kW, 3kW STD and EE motors to determine the effect of voltage unbalance on currents in the machines. The unbalanced stator currents drawn as a result of an unbalanced supply voltage can be defined as the ratio of negative sequence current to the positive sequence current components in the machine.

Voltage unbalances were introduced at three loading points. These load points were 25%, 50% and full load. This was found to be sufficient to show a trend in the measured results. The current unbalance measured as a function of the applied voltage unbalance is shown in Figure 79 to Figure 82.

From Figure 79 to Figure 82 it is evident that the current unbalance increases proportionally with the voltage unbalance and decreases with load. The current unbalance, which is a multiple of the voltage unbalance, is directly related to the ratio of the positive sequence impedance to the negative sequence impedance of the particular motor.

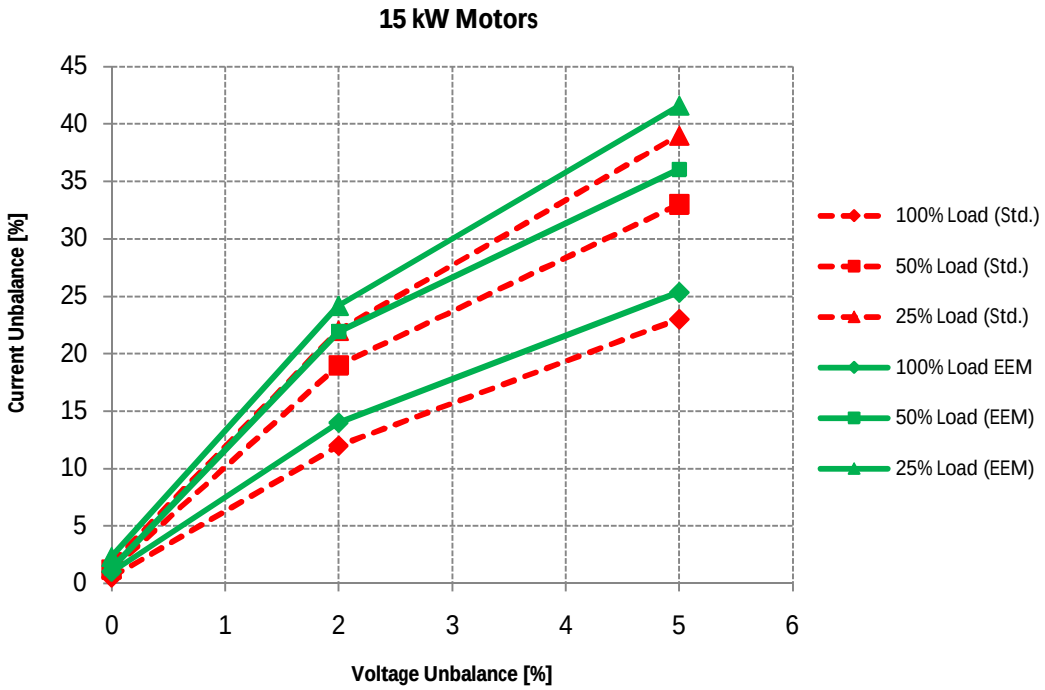

Figure 79: 15kW Standard and EE Motor current unbalance comparison as a result of voltage unbalance

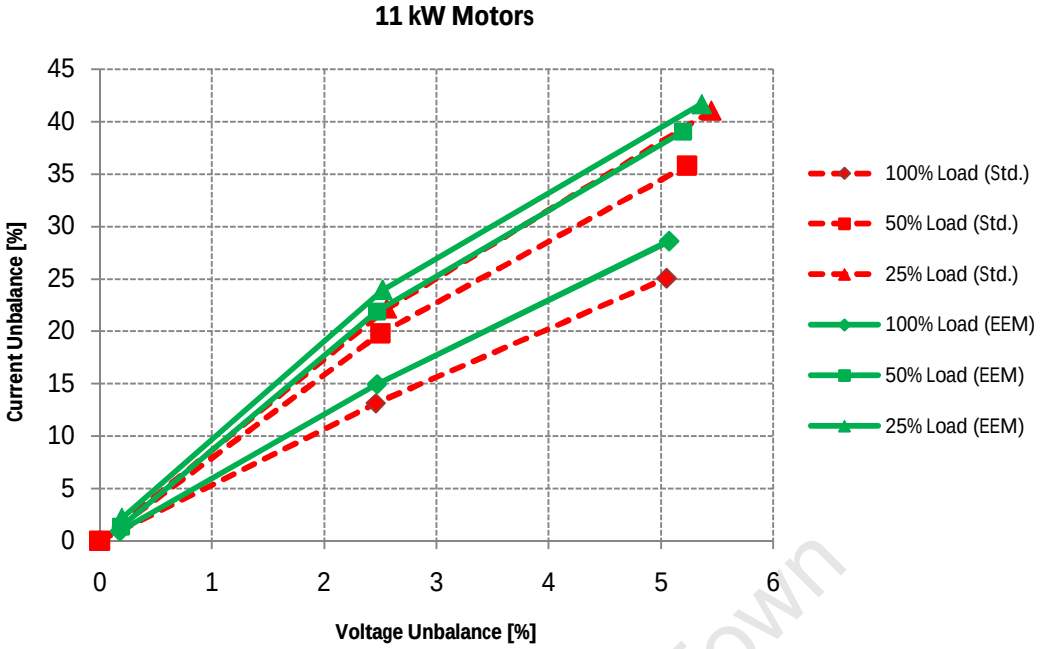

Figure 80: 11kW Standard and EE Motor current unbalance comparison as a result of voltage unbalance

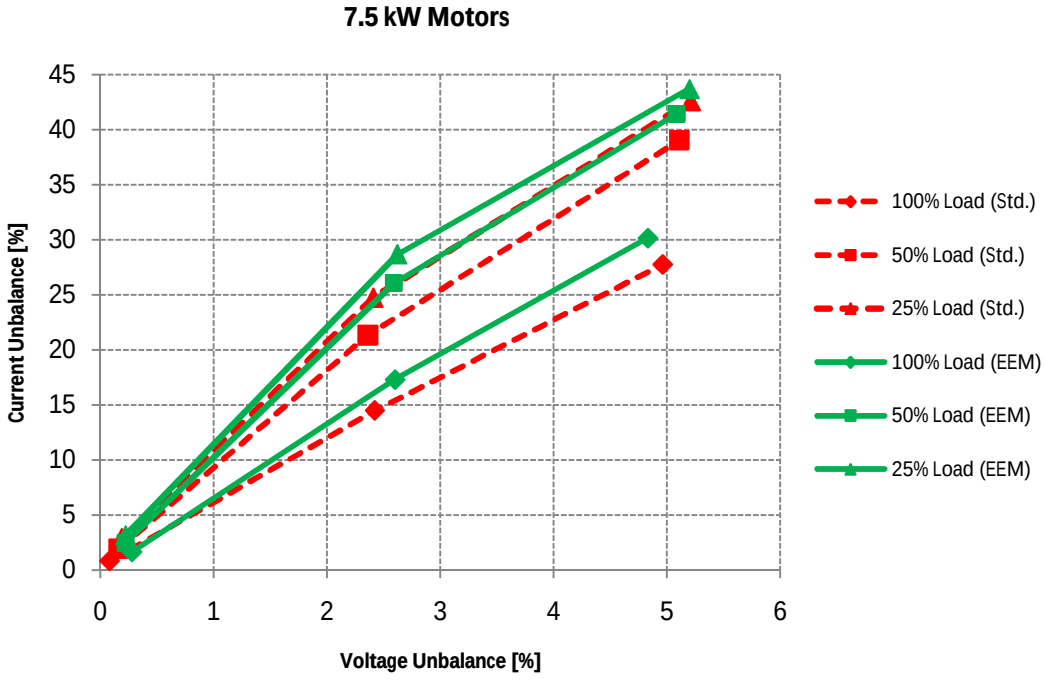

Figure 81: 7.5kW Standard and EE Motor current unbalance comparison as a result of voltage unbalance

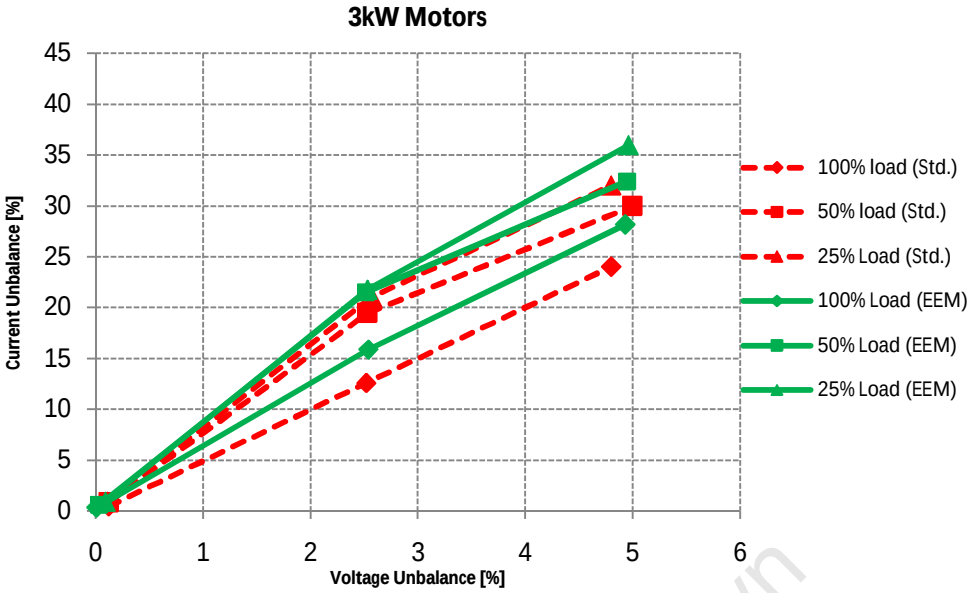

Figure 82: 15kW Standard and EE Motor current unbalance comparison as a result of voltage unbalance

Both, STD and EE motor types revealed similar trends. However, the EE motors are more susceptible to voltage unbalance. At all loading points, gradient of the trend line is steeper in the case of the EE motors which indicates that the current unbalance is greater for a given voltage unbalance. This can be explained by the fact that the EE motors operate at a lower slip when compared to the standard motors at the same loading. All four EE motors have approximately 2.5% and 3% higher current unbalance at 2.5% and 5% voltage unbalance respectively, for all motor sizes and loads.

6.2 IMPACT OF VOLTAGE UNBALANCE ON EFFICIENCY

The impact of unbalanced supply voltages on the efficiency of the STD and EE motors was assessed. Efficiency tests were performed at six loads between 150% and 25% of rated power. EE motors develop less torque than STD motors at the same shaft power due to the higher operating speed. In the light of this, the motors were tested at loads as a percentage of the motor's rated shaft power and not its rated torque, to ensure comparison of STD and EE motors under same energy delivery. The specific voltage unbalance was created by maintaining one of the phase voltages at the desired average voltage (nominal, 10%over or 10%under), and varying one phase up and the remaining

phase down until the desired voltage unbalance is achieved. The voltage unbalance was monitored in a real-time in a LABVIEW program. The unbalance cases include a 2.5% and 5% voltage unbalance measured according to the NEMA definition. The NEMA definition was adopted in this case because of its simplicity to implement in the laboratory. Besides the voltage unbalances at nominal voltage conditions, tests were also performed at a 10% over voltage (418V) and 10% under voltage (342V). Voltage unbalances of 2.5% and 5% were at the 10% over-voltage condition and at the 10% under voltage conditions.

The effects of voltage unbalance on the efficiency of the eight motors tested are shown in Figure 83 to Figure 106. The input-output method in accordance with the IEEE112 method A was used here, since no specification currently exists for the efficiency testing of IM's under the influence of voltage unbalance supplies. The IEEE112 method B and IEC34-2-1 only allows a voltage unbalance up to 0.5%. Also, The IEEE112 method B and IEC34-2-1 use an average phase voltage and current in calculation of power. This was considered to potentially lead to greater errors than the direct method, which uses actual phase voltages and currents in the power calculations. Furthermore, the absolute efficiency values of the motors were considered as less important and were merely used to compare trends.

Each efficiency graph includes the efficiency characteristic of the motor under balanced and nominal (380V) supply conditions. This is used as the basis for comparison of the various unbalanced supply conditions, over/under voltage conditions.

To reduce the testing time and to avoid permanent damage to the motors due to thermal overload, the tests were performed at the motor's rated temperature rise as recorded under rated supply and load conditions.

Directly below each motor's efficiency characteristic graph at a specific supply voltage condition, the actual voltage unbalance during the test is indicated. For practical reasons it was not possible to maintain the unbalanced condition at exactly the value indicated on the efficiency vs load graphs. This was due to the variations in the supply voltage

during variations in load and asymmetrical volt drops in the variacs and supply cables. The actual unbalance in supply voltage was however carefully tracked and reported as mentioned above.

6.2.1 Impact of Voltage Unbalance on Efficiency of 15kW STD and EE Motors

15kW Motors: Rated Voltage with Unbalance

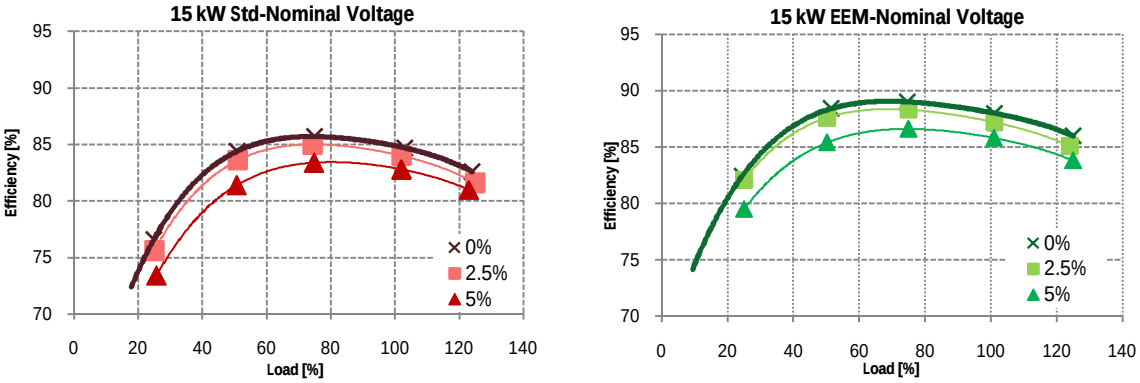

Figure 83: Efficiency characteristic according to the IEEE112-A for the standard and energy efficient motors at various supply unbalance cases

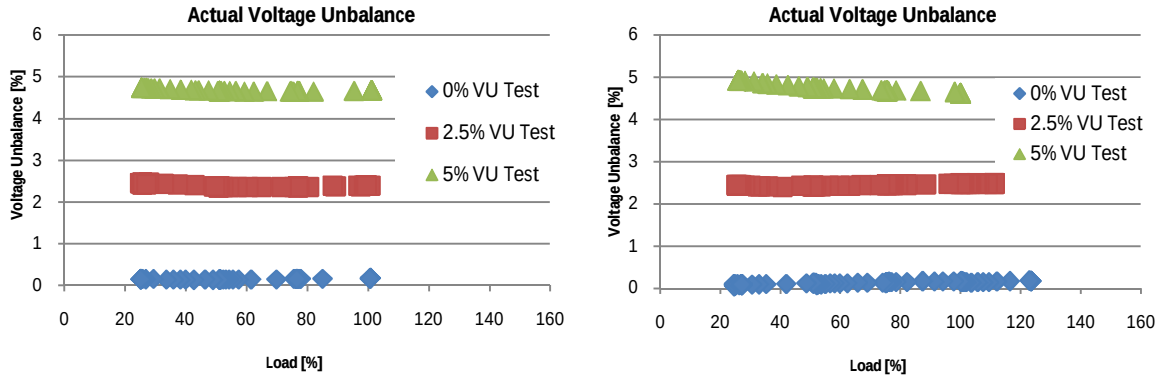

Figure 84: The actual voltage unbalance recorded for the directly above efficiency characteristic

15kW Motors: 10% Under voltage with Unbalance

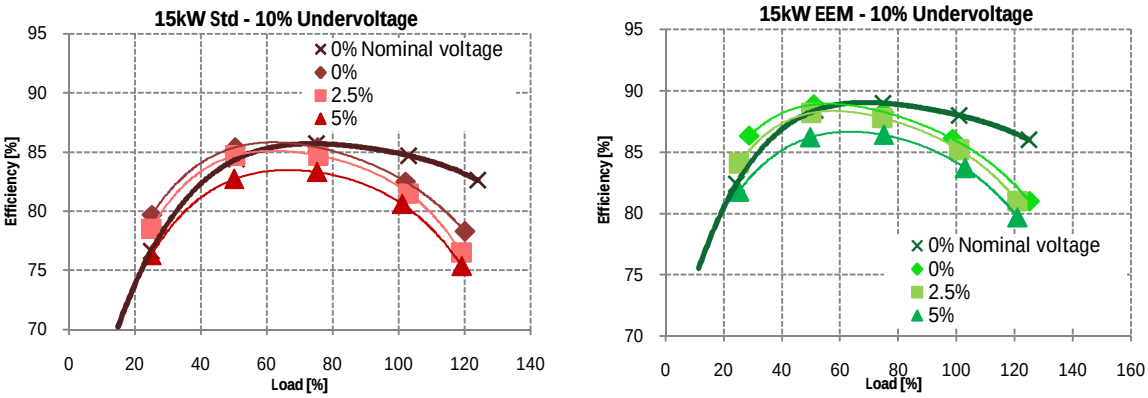

Figure 85: Efficiency characteristic according to the IEEE112-A for the standard and energy efficient motors at various supply unbalance cases

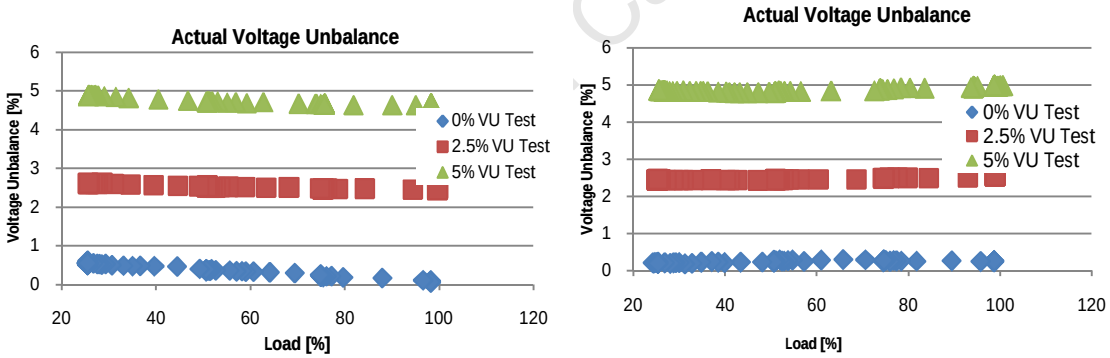

Figure 86: The actual voltage unbalance recorded for the directly above efficiency characteristic

15kW Motors: 10% Overvoltage with Unbalance

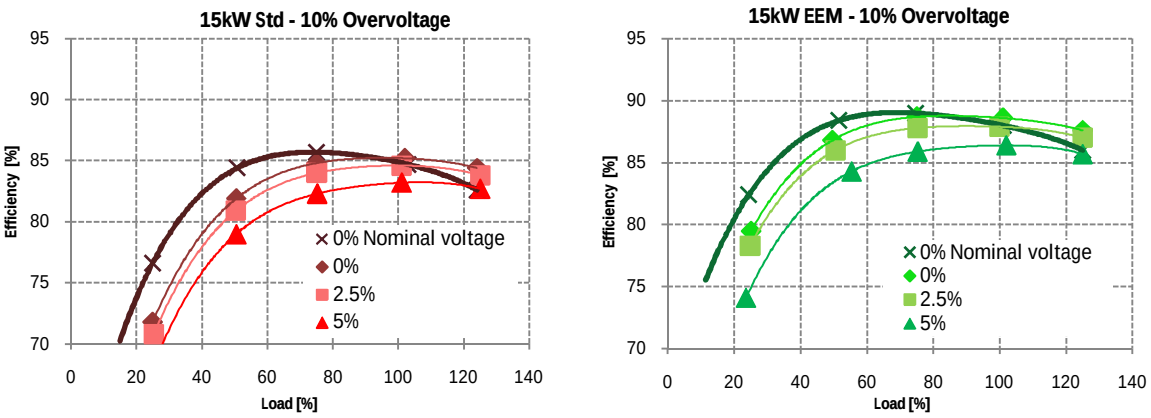

Figure 87: Efficiency characteristic according to the IEEE112-A for the standard and energy efficient motors at various supply unbalance cases

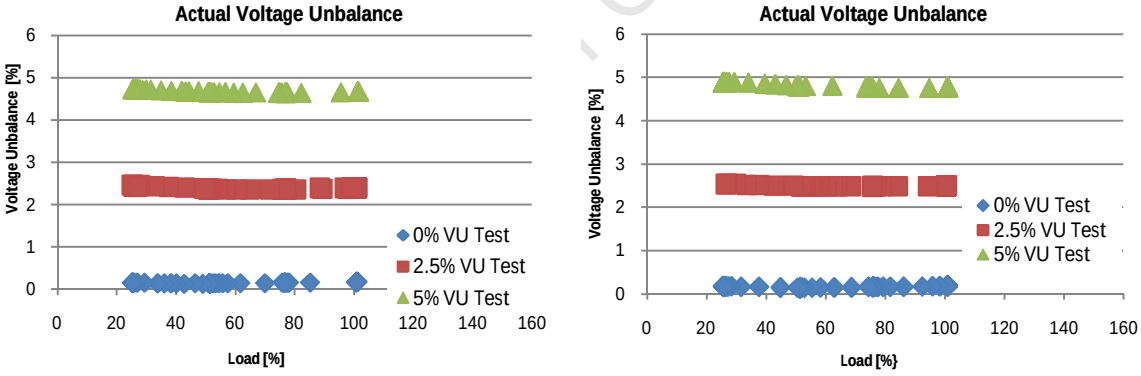

Figure 88: The actual voltage unbalance recorded for the directly above efficiency characteristic

6.2.2 Impact of Voltage Unbalance on 11kW STD and EE Motors

11kW Motors: Rated Voltage with Unbalance

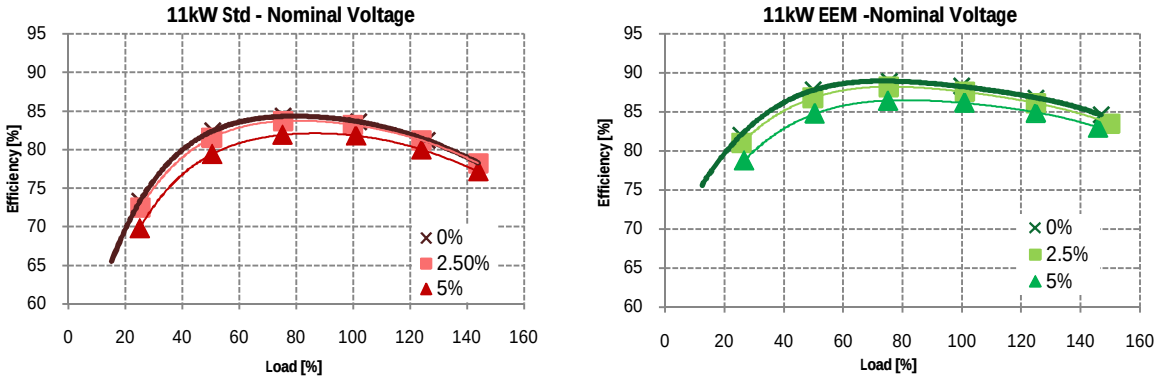

Figure 89: Efficiency characteristic according to the IEEE112-A for the standard and energy efficient motors at various supply unbalance cases

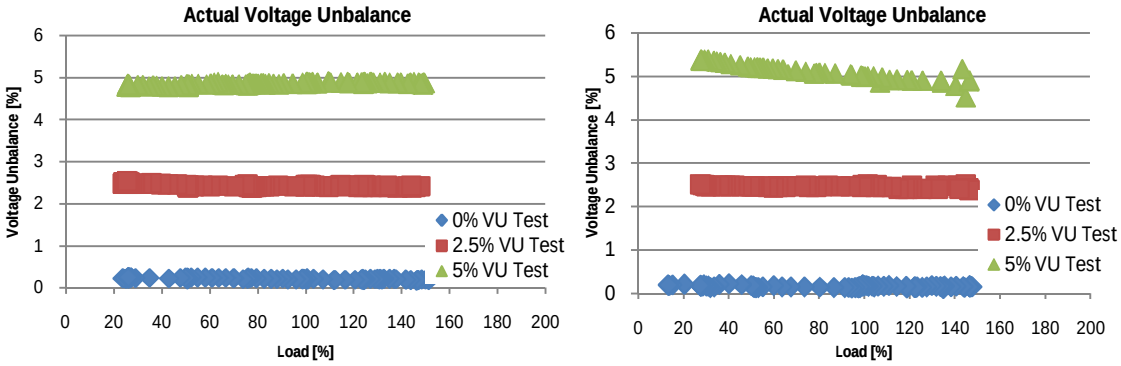

Figure 90: The actual voltage unbalance recorded for the directly above efficiency characteristic

11kW Motors: 10% Undervoltage with Unbalance

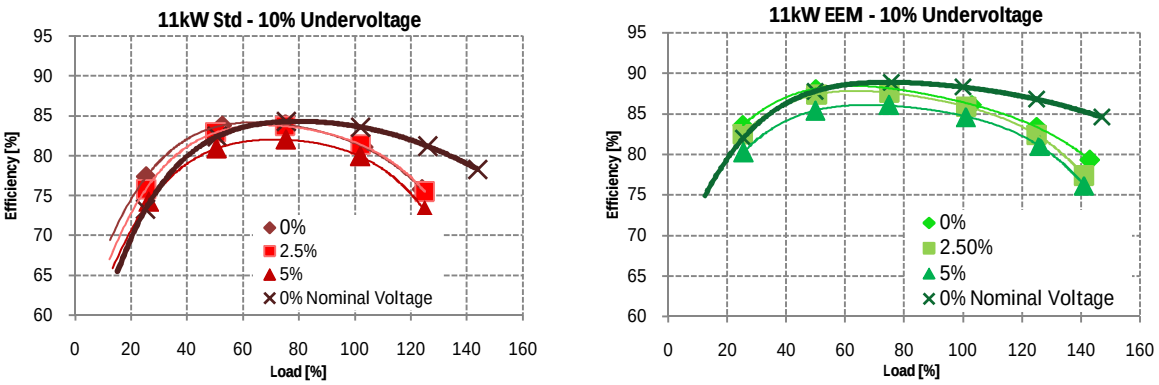

Figure 91: Efficiency characteristic according to the IEEE112-A for the standard and energy efficient motors at various supply unbalance cases

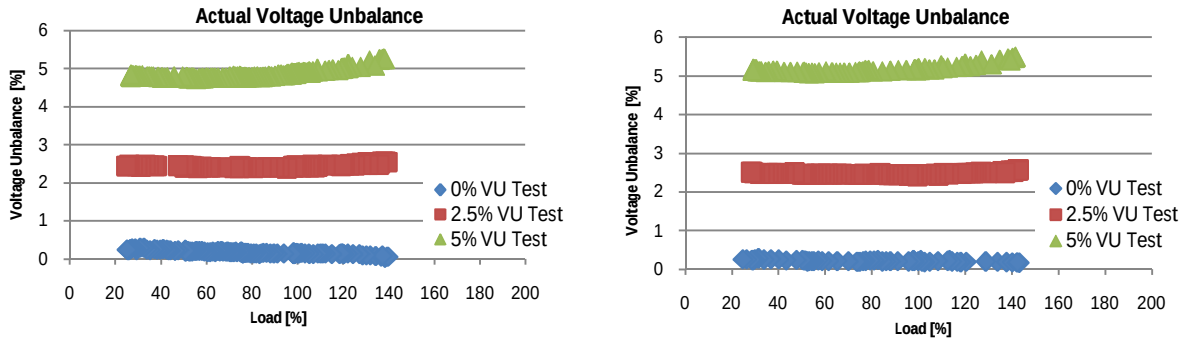

Figure 92: The actual voltage unbalance recorded for the directly above efficiency characteristic

11kW Motors: 10% Overvoltage with Unbalance

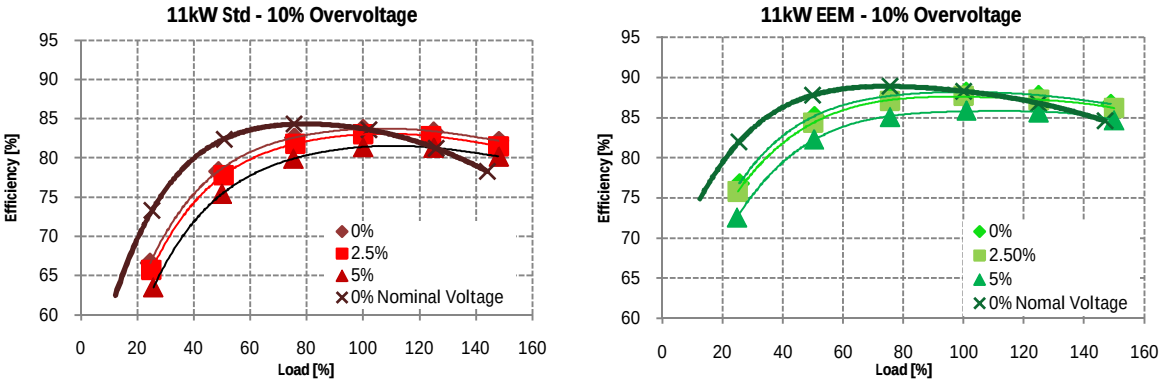

Figure 93: Efficiency characteristic according to the IEEE112-A for the standard and energy efficient motors at various supply unbalance cases

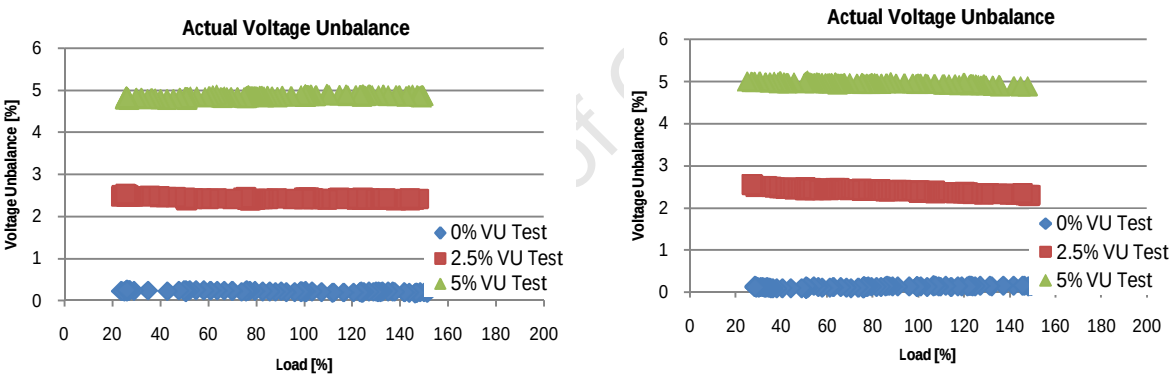

Figure 94: The actual voltage unbalance recorded for the directly above efficiency characteristic

6.2.3 Impact of Voltage Unbalance on 7.5kW STD and EE Motors

7.5kW Motors: Rated Voltage with Unbalance

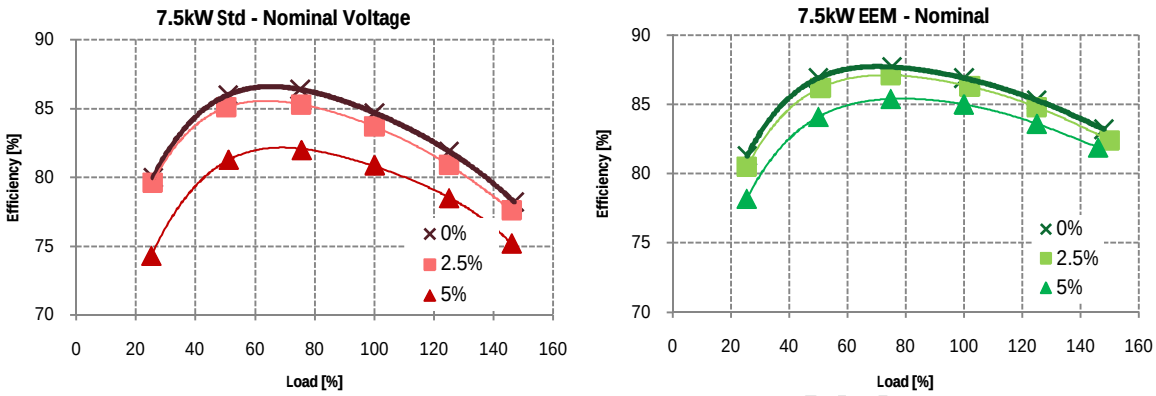

Figure 95: Efficiency characteristic according to the IEEE112-A for the standard and energy efficient motors at various supply unbalance cases

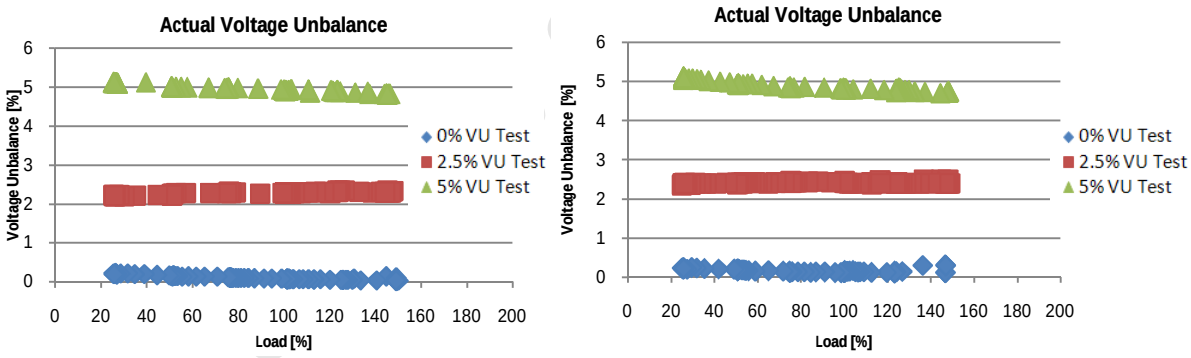

Figure 96: The actual voltage unbalance recorded for the directly above efficiency characteristic

7.5kW Motors: 10% Undervoltage with Unbalance

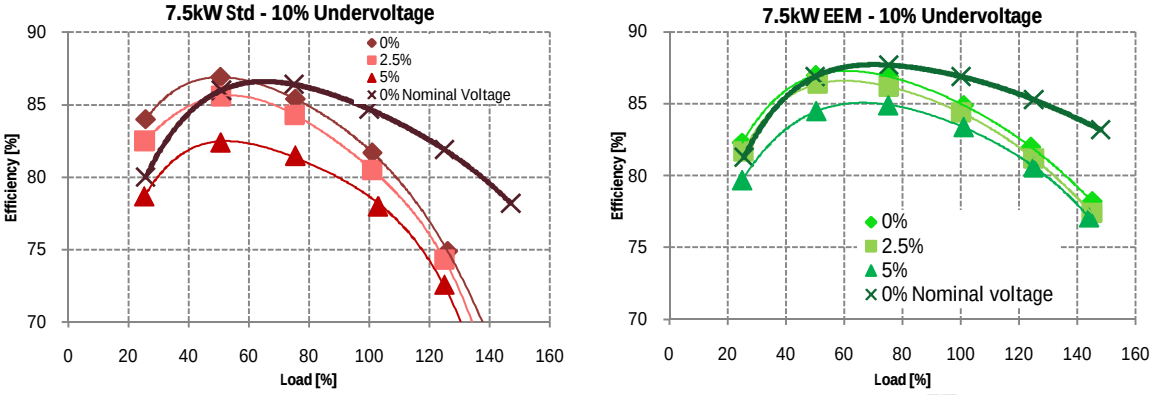

Figure 97: Efficiency characteristic according to the IEEE112-A for the standard and energy efficient motors at various supply unbalance cases

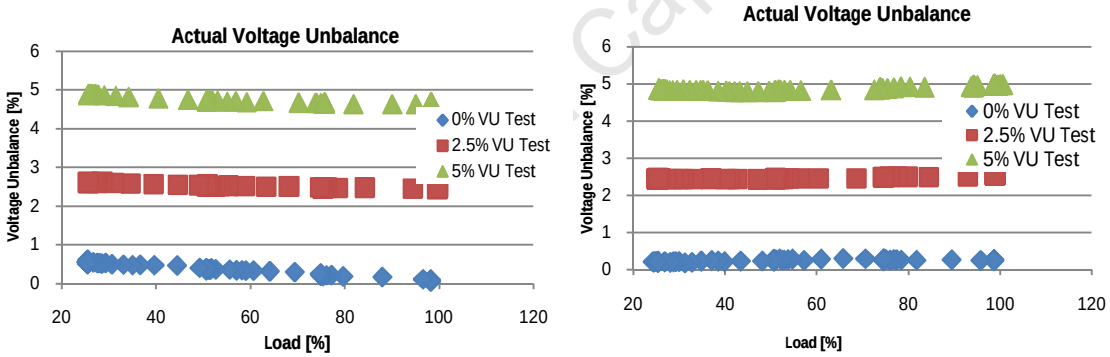

Figure 98: The actual voltage unbalance recorded for the directly above efficiency characteristic

7.5kW Motors: 10% Overvoltage with Unbalance

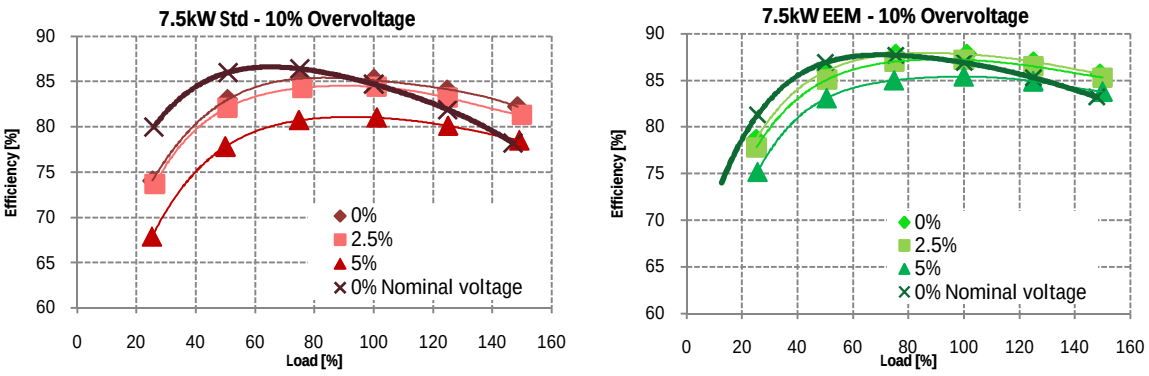

Figure 99: Efficiency characteristic according to the IEEE112-A for the standard and energy efficient motors at various supply unbalance cases

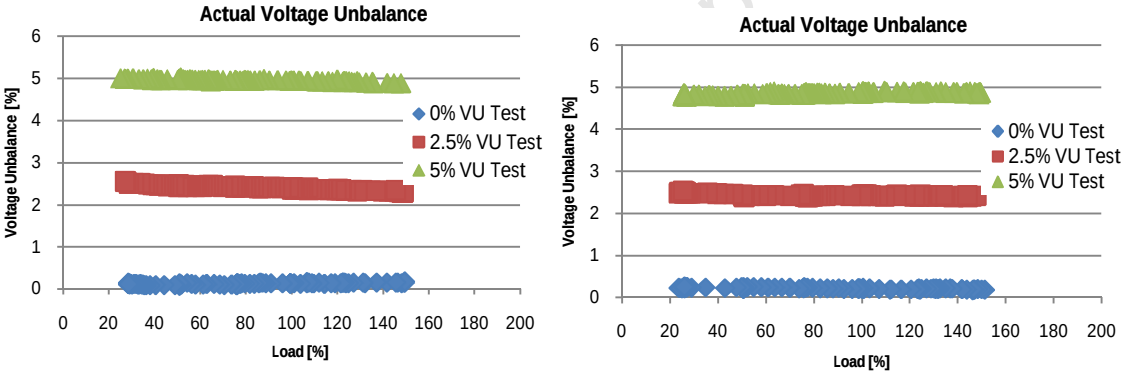

Figure 100: The actual voltage unbalance recorded for the directly above efficiency characteristic

6.2.4 Impact of Voltage Unbalance on 3kW STD and EE Motors

3kW Motors: Rated Voltage with Unbalance

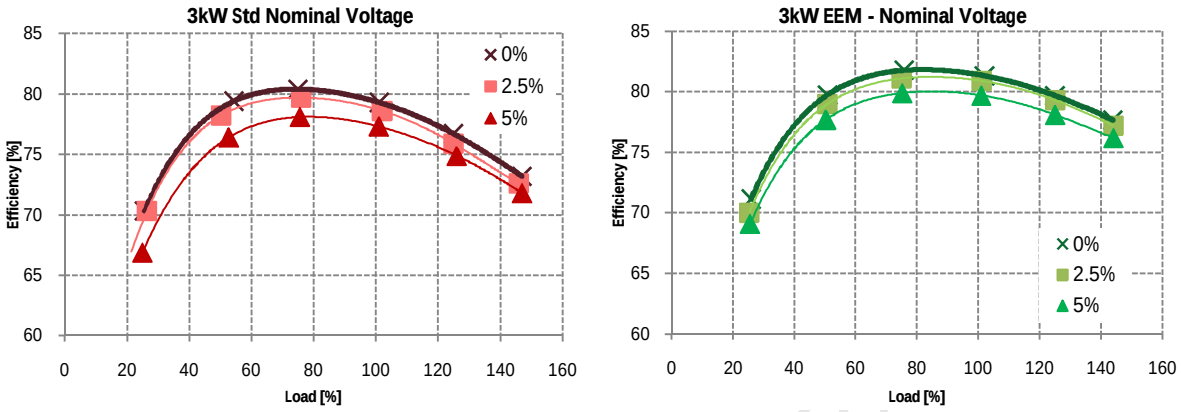

Figure 101: Efficiency characteristic according to the IEEE112-A for the standard and energy efficient motors at various supply unbalance cases

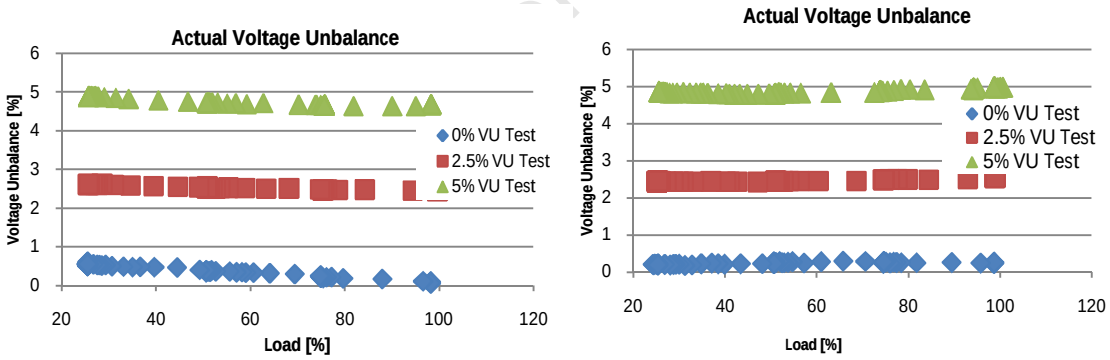

Figure 102: The actual voltage unbalance recorded for the directly above efficiency characteristic

3kW Motors: 10% Under voltage with Unbalance

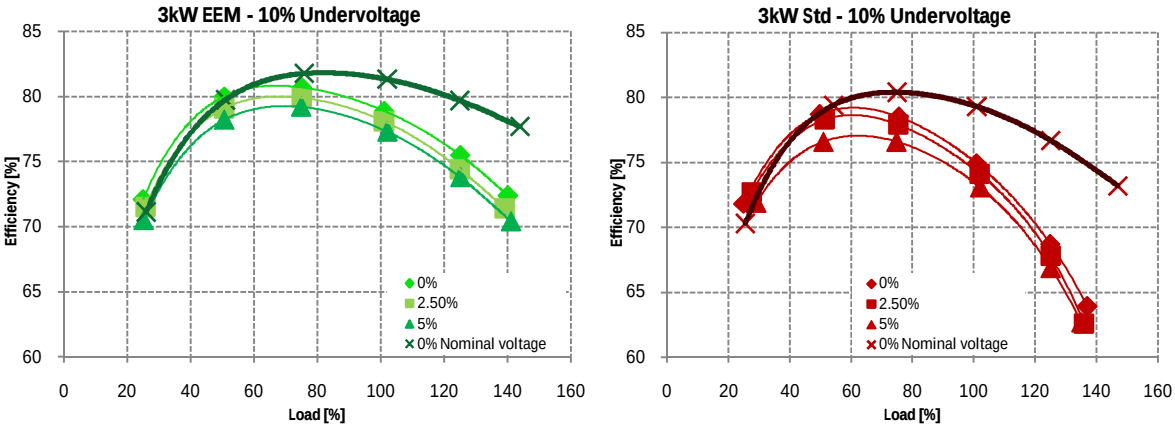

Figure 103: Efficiency characteristic according to the IEEE112-A for the standard and energy efficient motors at various supply unbalance cases

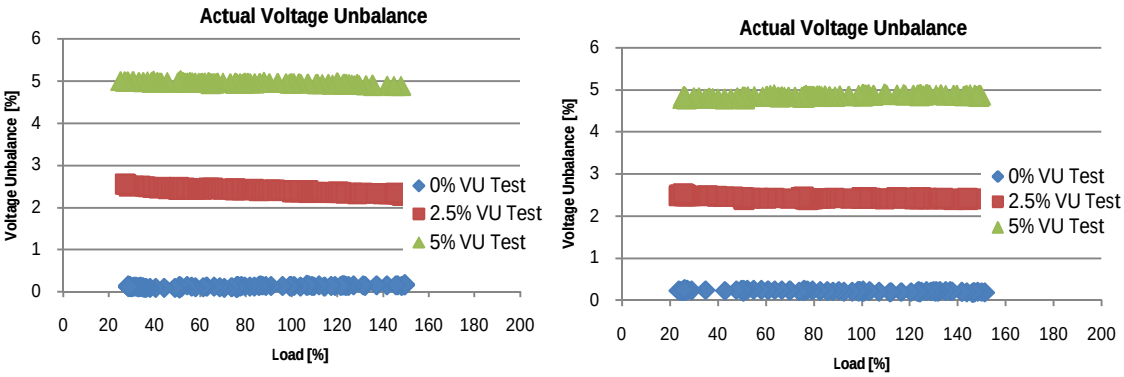

Figure 104: The actual voltage unbalance recorded for the directly above efficiency characteristic

3kW Motors: 10% Overvoltage with Unbalance

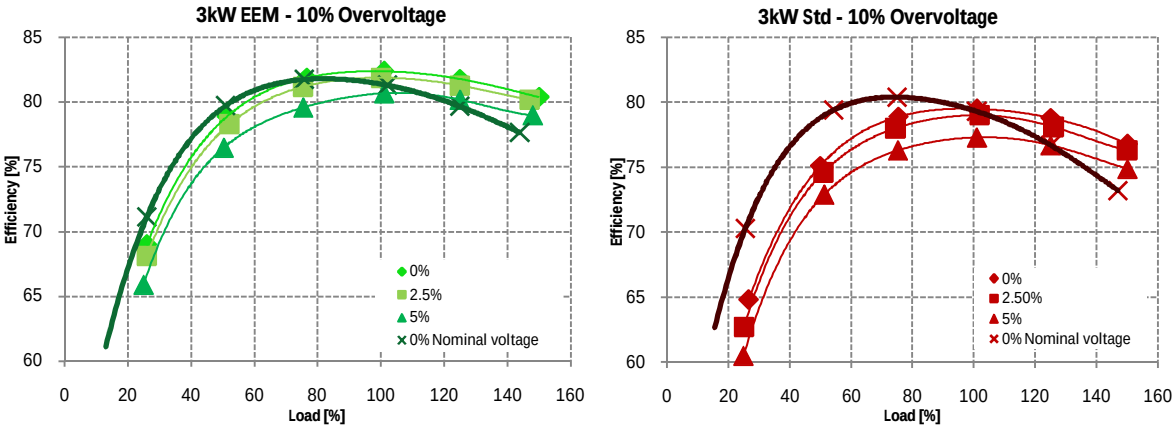

Figure 105: Efficiency characteristic according to the IEEE112-A for the standard and energy efficient motors at various supply unbalance cases

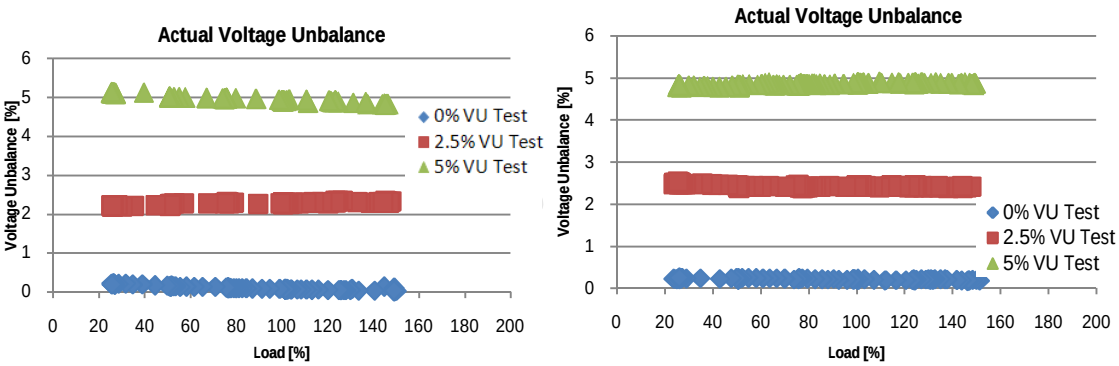

Figure 106: Actual voltage unbalance for the overvoltage tests on the 3kW motors

6.2.5 Interpretation and discussion of Voltage Unbalance results

As depicted in Figure 83 to Figure 106, the efficiency of both standard and EE motors decrease with unbalance in the supply voltages. This decrease is expected since the core, stator and rotor losses are directly influenced by the unsymmetrical voltage supplied. In Figure 107 it is graphically illustrated how the torque vs speed curve is reduced as the supply voltage increases. The reduction in the resultant torque is due to the reverse air gap field (MMF) caused by the negative sequence currents. It also shows how the slip incrementally increases with supply unbalance although the shaft torque is maintained at full load.

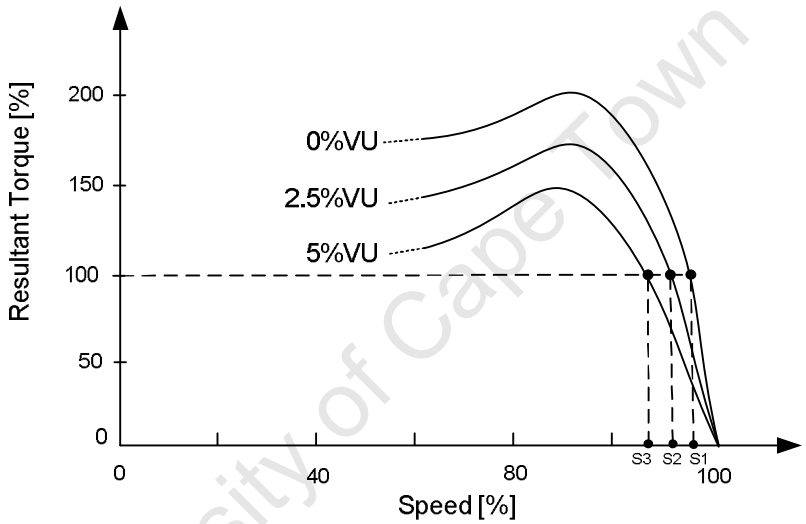

Figure 107: Change in Torque vs load speed and resulting slip values with variation in voltage unbalance

The increase in slip results in additional losses in the rotor as well as the stator winding. It was found in section 7.1 that the current unbalance drawn by EE motors are between 2 and 5% higher than that of standard motors. This results in larger negative sequence currents in EE motors and hence a larger reverse airgap torque. The resultant shaft torque of the EE motors are lower, thereby resulting in operation at a larger slip for the same load condition. The increase in slip results in increased stator and rotor losses in EE motors. Slip is proportional to temperature rise and is inversely proportional to efficiency; hence the decrease in the efficiencies of all the motor results shown in Figure 83 to Figure 106. The constant loss, and more importantly the core loss, also increases

with an increase in voltage unbalance. As mentioned above the supply voltage unbalances were achieved varying two phase voltages equally but in opposite directions and maintaining the third phase voltage at the desired average voltage; 342V, 380V or 418V. Additional core loss arises from the one phase voltage that is above the rated voltage since the core loss increases exponentially as a function of voltage squared at approximately rated voltage. This additional core loss is partly offset by the on phase voltage that is set below rated voltage. However, the net core loss is higher than the core loss at nominal supply conditions. The increase in core loss under unbalance supply voltage conditions is less significant in EE motor than STD motors due to lower saturation effect of the core material as was shown by the balanced supply core loss results in section 5.7.2. Figure 108 below show a graphical illustration of the change in load losses, constant losses and resultant efficiencies for a change in supply voltage conditions.

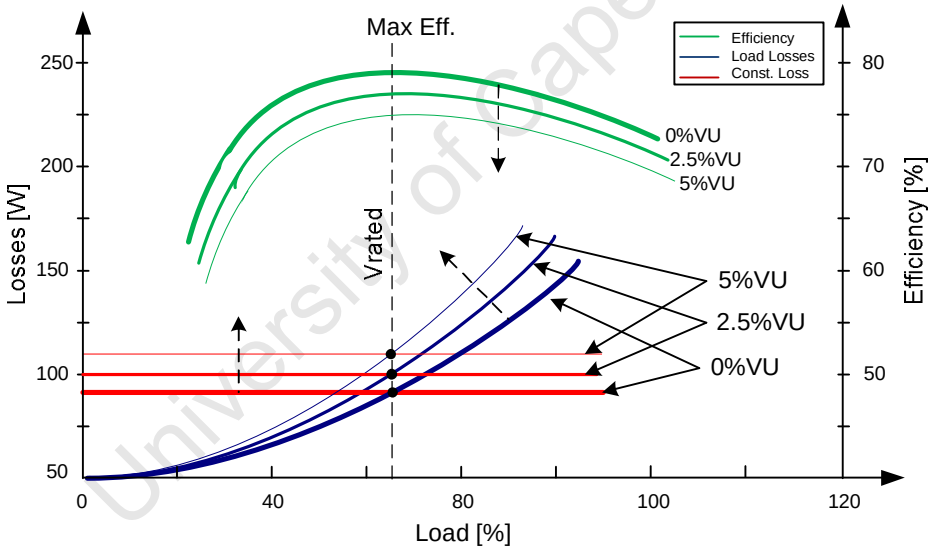

Figure 108 Efficiency and loss curves for 0%, 2.5% and 5% voltage unbalance cases

From the graphs it is clear that the maximum efficiency occurs at the loading where the ratio of the load losses to the constant losses is one. It also shows that the losses increases with an increase in voltage unbalance as mentioned above. It can be seen that the maximum efficiency occurs at approximately the same load position regardless of the extent of the supply voltage unbalance provided the average supply voltage remain

unchanged. This is confirmed by the experimental voltage unbalance results in Figure 83 to Figure 106. The extent by which the efficiency decreases with voltage unbalance is comparable for the two motor types. However, the temperature of the motors had not been allowed to stabilize whilst operating under the specific unbalance supply condition, to prevent permanent damage of the motor and due to time limitations as mentioned above. Figure 109 illustrates the influence of the motor temperature on its losses and efficiency.

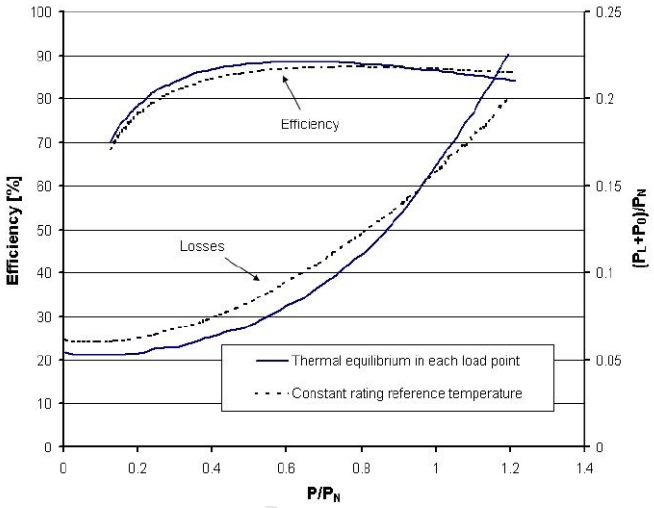

Figure 109: Influence of operating temperature on motor efficiency and losses [11].

From the above graph it is shown that losses are over estimated at partial loads if the efficiency test is performed within 5°C of the motor's rated temperature as prescribed by the standards. The motor's efficiency therefore, is under estimated at partial loads. The opposite is true at loads above the rated power. This is because the motor's actual operating temperature at partial loads will be lower than the rated temperature, if allowed to stabilize. It can therefore be concluded from this that motor's efficiency is slightly over estimated if it is not stabilized at the specific voltage unbalance and load. However, the trends in efficiencies of the STD and EE motors are of more importance in this case rather than the absolute values of the efficiencies.

6.2.6 Interpretation and discussion of Over and Under Voltage Unbalance results

As discussed above, the effects of over and under voltage supplies were also investigated. When the motors are subjected to an under supply voltage condition, the core and friction & windage losses decreases but in order to deliver the same power to the load, a higher line current is drawn to compensate for the reduced magnetisation of the core. This will therefore affect the loading position at which the peak of efficiency of the motor is reached. For the under-voltage supply conditions, the efficiency peak shifts towards the left to a lower load region, thereby deviating from the original or nominal peak efficiency position. In contrast, for the overvoltage conditions, the peak of the efficiency vs load curve is shifted towards higher loading. This is due to an increase in the core magnetization and consequently the lower currents that are drawn from the supply to develop the required load torque. The core loss increases exponentially with an increase in average voltage squared due to saturation of the lamination core material. With a higher supply voltage and thus higher magnetization, less current is required to develop the required torque. This results in lower stator and rotor losses in the motors.

In general, the load dependent losses are inversely proportional to the square of the supply voltage. In contrast, the constant losses are directly proportional to the supply voltage, in the absence of core saturation. However, it increases at a higher rate as soon as saturation occurs. It was found that saturation occurs at lower voltages in STD motors than in EE motors. This is mainly due to the low quality steel and core design used in STD motors. A motor's maximum efficiency occurs when its load dependant losses are equal to its constant losses, as illustrated in Figure 110.

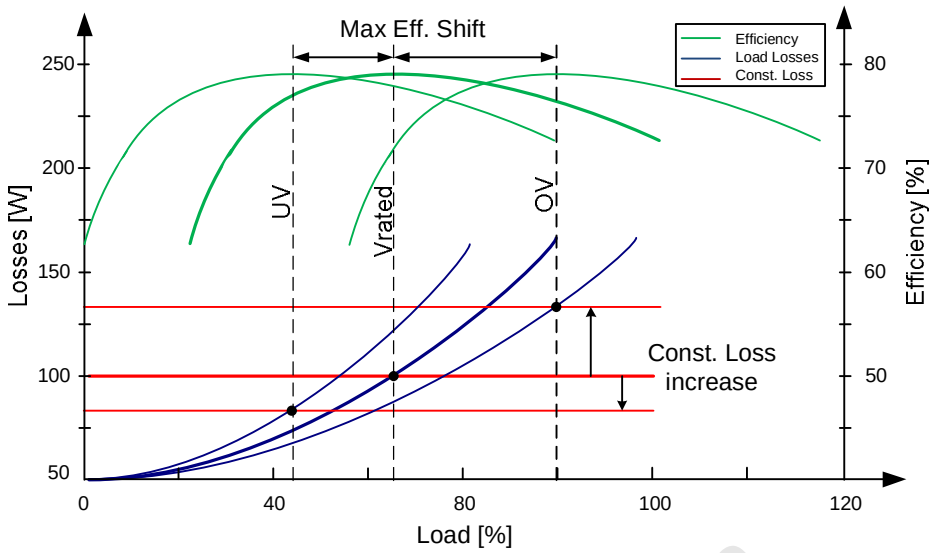

Figure 110: Efficiency and loss curves for rated voltage, under voltage and over voltage cases

The above figure clearly show the load dependent losses, constant losses and efficiency curves for rated, over and under voltage conditions in the absence of voltage unbalance. It shows how the efficiency peak shifts to a lower load as the supply voltage decreases and towards a higher load as it increases. Saturation causes the constant losses to increase more with voltage compared to the same decrease in voltage. The effect of this is a bigger shift in the peak of the efficiency vs load to the right (higher load) then to the left (lower load). This is confirmed further with the laboratory results presented in Figure 83 to Figure 105. With a 10% reduction in average voltage, the efficiency peaks at approximately 10% lower load with respect to rated voltage condition. This was found to be the case for all the motors investigated. However, a 10% increase in voltage resulted in approximate 20% percent shift in the efficiency curve to the right in all the EE motors and an approximate 30% percent shift in the case of the standard motors. This confirmed the theoretical expectation illustrated Figure 110.

6.2.7 Interpretation and discussion of the combination Voltage Unbalance and variation results

The combined effects of over or under voltage and unbalance voltage are found in Figure 83 to Figure 106. In the cases where the voltage supply is unbalanced at an under voltage supply condition, the efficiency curves shift toward the left but decreases at the same time. Under over voltage conditions the curves shift to a higher loading and decrease if an unbalance supply is present. The higher the unbalance the more the efficiency decreases.

The load losses are more prominent during under voltage conditions. This is due to lower magnetization of the core and hence more line current is required to sustain the shaft power. Since, developed torque is proportional to voltage squared, the average voltage is 10% lower than rated voltage, and the motors developed torque would drop to approximately 81% of the nominal torque. On top of this reduction in torque, the voltage unbalance will also cause the develop torque to decrease as was shown in Figure 107. At higher loads, the torque vs speed curve becomes highly non-linear which result in a non-linear increase in slip and hence, load losses. This explains the sharp decrease in efficiency at higher loads at under voltage supply conditions. The efficiencies under over voltage conditions however, appear relatively flatter than the latter. This is because the motor is magnetized more and so the constant losses are predominant less current is required to drive the load. Less variation on losses results in a flatter efficiency curve.

6.3 TEMPERATURE RISE COMPARISON

The thermal model in section 3.4 is used to predict the steady state winding temperature of motors supplied with an average voltage of 342V, 380V and 418V and a combination of voltage unbalances. The parameters obtained through the parameters test described in [19] initially lead to a large error in the temperature results when compared with the experimental results. The parameters were then calibrated to the experimental temperature rises. The electrical models in section 3.3 are used to obtain the motor stator winding loss and core loss, which are the heat sources in the thermal model. The

advantage of using these models is that temperature rises of each of the motors could be obtained at any supply condition in a much shorter time than doing it experimentally. Losses from the positive and negative sequence circuits are added and fed into the thermal model. The 15kW and 3kW standard and energy efficient motors were modelled. These motors were selected since they represent high and low end of the range of motors under investigation. A comparison of the stator winding losses, core losses and temperature rises of the standard and EE motors is presented in Table 29 and Table 30. The temperatures in the tables represent the highest calculated stator winding temperature. An ambient temperature of 25°C is used in the model.

From Table 29 and Table 30 it can be seen that the winding temperature of both EE motors are less than that of the standard motors regardless of the supply condition implemented. However, the EE motors show greater temperature increase with increase in voltage unbalance. This is illustrated in Figure 111 and Figure 112 for the winding temperature of the motors at 0%, 2.5% and 5% voltage unbalance and at its rated value of 380V. Under balanced conditions the temperature rise is caused by only the positive sequence circuits since the negative sequence loss contribution is zero. From Figure 111 and Figure 112 it can be seen that the temperature difference for the 15kW and 3kW STD and EE motors are 12.1°C and 24.7°C respectively at 0% un balance and 380V. As the voltage unbalance increases from 0% to 5%, the temperature difference between 15kW and 3kW STD and EE motors decreases to 4°C and 13.1°C respectively. This indicates that the temp rise for the EE motors increases more with unbalance than it does for STD motors subjected to the same degree of unbalance. This is due to the higher negative sequence currents that EE motors draw and hence higher negative sequence losses (heat sources).

Table 29: Thermal model predicted winding temperatures with under, balanced and over voltage in combination with voltage unbalances

		15kW					
		Standard Motor			EE Motor		
Average voltage [V]	**Unbalance [%]**	**Stator winding loss [W]**	**Core loss [W]**	**Calculated temperature [˚C]**	**Stator winding loss [W]**	**Core loss [W]**	**Calculated temperature [˚C]**
342	0	1010	280	126.5	909	180	112.3
	2.5	1026	300	137.7	9.38	197	129.6
	5	1042	318	148.4	960	222	143.2
380	0	815	320	115.2	735	239	103.1
	2.5	829	339	127.4	758	260	121.5
	5	846	360	139.1	779	270	135.1
418	0	690	550	105.9	520	395	91.2
	2.5	719	580	117.2	542	425	109.4
	5	730	604	129.1	563	449	122.7

Table 30: Thermal model predicted winding temperatures with under, balanced and over voltage in combination with voltage unbalances

		3kW					
		Standard Motor			EE Motor		
Average voltage [V]	**Unbalance [%]**	**Stator winding loss [W]**	**Core loss [W]**	**Calculated temperature [˚C]**	**Stator winding loss [W]**	**Core loss [W]**	**Calculated temperature [˚C]**
342	0	470	76	120.4	326	49	109.3
	2.5	482	90	126.1	341	64	119.2
	5	495	105	132.4	356	79	130.1
380	0	325	125	111.9	221	61	87.2
	2.5	336	141	117.1	237	76	98.6
	5	349	156	123.9	252	81	110.8
418	0	222	175	101.4	162	82	80.5
	2.5	235	182	108	177	99	94.7
	5	246	202	119	192	111	117.4

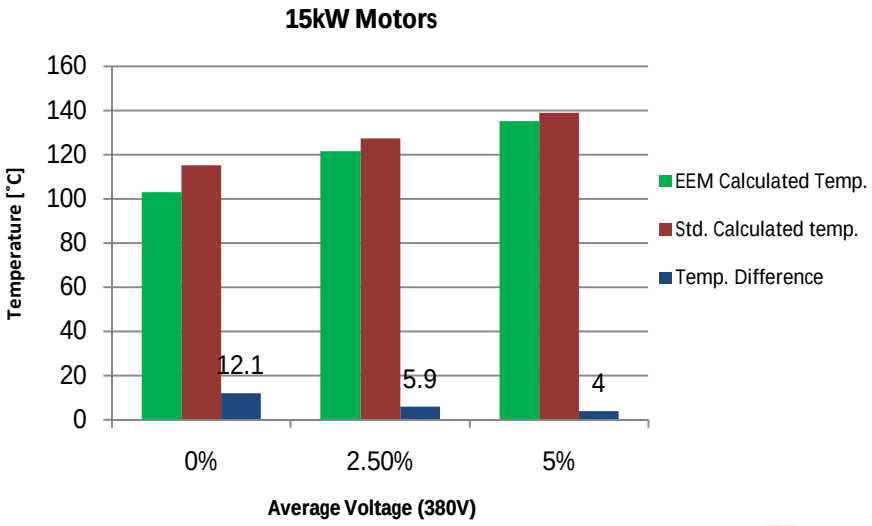

Figure 111: Comparison of calculated temperature rise for 15kW motors with average voltage of 380V

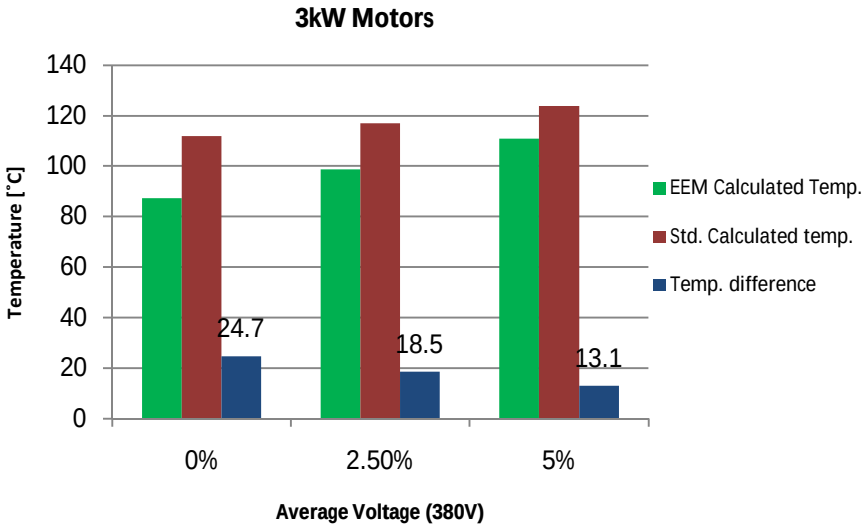

Figure 112: Comparison of calculated temperature rise for 3kW motors with average voltage of 380V

CHAPTER 7

7. MEASUREMENT UNCERTAINTY ANALYSIS

7.1 BACKGROUND

The previous chapters presented methodologies and results of induction motor (IM) testing. It was shown that the operating efficiency of an IM is dependent to the following factors: motor design (EE vs STD motor design), power quality and load. The accuracy of the efficiency estimate of an IM is of course dependent on uncertainties in the measurement procedure.

This chapter will focus on the measurement uncertainty and analyse its effect on estimated efficiency of IM's. This section continuous by giving the background of this chapter, before the three sources of measurement errors is described. The method of calculating uncertainty is then explained and finally the uncertainty results for the 11kW and 3kW STD and EE motors are given. The uncertainty results of three efficiency measuring methods are presented. These methods are the IEEE112-B, IEC60034-2-1 and the direct method.

There are few publications which thoroughly discuss the different aspects of uncertainties associated with efficiency estimates of IM's. Bonnett points out in [45] that with the use of existing technologies it is unreasonable to expect a higher accuracy than ±0.5 % in the efficiency estimated. In 1999, Auinger investigates further and shows that if the efficiency is determined directly (Direct method), the measurement errors, which are unavoidable, will influence the accuracy of the result negatively [11]. He also illustrates that the uncertainty of the efficiency estimate can be as much as ±2%, if the measurement accuracy for the determination of the electric input and the mechanical output powers are not better than 1%. It is reported by [11] that the indirect methods (standards) for efficiency estimation, that are based on the separation of losses, are more appropriate in order to achieve higher accuracies in the estimation of efficiency of an IM.

The aim of this chapter is to quantify the uncertainty associated with the instruments used in the newly constructed 22kW test rig discussed in this thesis. The individual uncertainties are then combined to form the uncertainty band associated with the efficiencies of the tested motors.

All measurements in practise have to some degree of uncertainty. A quoted measurement result is only complete when accompanied by its associated uncertainty. Good practice, which includes: calibration of all instruments used, careful calculation and interpretation of methodology, and confirming of measurements, can greatly reduce measurement uncertainties. However, it can never be totally eliminated.

Uncertainty is defined as the doubt associated with the measured or estimated result, result and where as the measurement error is defined as the difference between the measured value and the 'true value' of the quantity being measured [46]. However, the 'true value' of the measured quantity can never be established, which can therefore not be used in motor efficiency estimation.

A measurement process as outlined by the induction motor testing standards involves a number of sources of uncertainty, which can collectively yield the combined uncertainty in an efficiency estimate. The measurement process always results in a value, which is the best estimate of the measurand (i.e. efficiency) and the associated uncertainty gives the range within which the analyst (test operator) is confident that the 'true value' of the measurand lies within.

True values are seldom known because experiments have errors due to instruments, data acquisition, data reduction, and environmental effects.

The following steps may be taken to calculate the uncertainty associated with the measurement:

1. Identify the sources of uncertainty in a measurement
2. Estimate the size of the uncertainty of each source
3. Combine the uncertainties from each source to give the overall result

7.2 SOURCES OF MEASUREMENT ERRORS AND UNCERTAINTIES

A typical experiment normally consists of three main types of error components, which can be expressed as follows [28]:

$$\zeta = \zeta_h + \zeta_m + \zeta_i \quad (36)$$

Where ζ is the total absolute measurement error, ζ_i is the instrumentation error, ζ_m is the error due to the method used and process followed, and ζ_h is the operator error.

7.2.1 Test Operator Error

The operator error arises when the method (in this case the motor testing standard) is interpreted differently by the person conducting the test. It is highly unlikely that everyone will follow a particular method exactly as the author(s) of the methodology intended it. More experienced operators will probably deviate less from the method than someone conducting the test for the first time. This will ultimately also result in an error in the final efficiency value. The uncertainty due to operator error is extremely difficult to quantify and will not be taken into account in this thesis. Errors could also be incurred when incorrect readings are recorded from instruments. The measurement process is greatly automated at the machines lab, which prevents gross mistakes when capturing readings.

7.2.2 Methodological Error

The methodological error associated with IM efficiency testing could be considered as a consequence of the error associated with the model used to represent the losses in an

induction motor. There are four conventional types of losses and a residual loss component. The conventional losses are stator and rotor winding losses, core losses and friction and windage losses. The stator and rotor winding losses are a function of resistance, which cannot be measured directly during a test. The measured temperature in turn varies depending on where in the machine a thermocouple is placed. Errors therefore, are likely to occur. There are many motor testing standards worldwide, which include the IEEE 112 and the IEC 60034-2-1. The standards are all based on the equivalent circuit of an induction motor. There are certain assumptions made by these standards which could reduce the accuracy of the end result.

7.2.3 Instrumentation Error

The instrumentation error, as the name implies, arises from instruments used to determine the measurement. The instruments include torque transducers, voltmeters, ammeters, current transformers etc. This type of error is probably the most significant amongst the afore mentioned error sources and can be quantified relatively easy since the errors of all the instruments are normally known. In this chapter, emphasis is placed on quantifying the total instrumentation error in order to incorporate mitigation measures to improve the accuracy of the test bench.

7.3 UNCERTAINTY MEASUREMENT CALCULATION

This section deals with quantifying the uncertainty of efficiency measurements due to the errors associated with the instrumentations used. According to the "Guide to expression of Uncertainty in Measurements" (GUM) [46], the uncertainties of all input measurements i.e. voltage, current, torque etc. can be estimated by either a 'Type A' or 'Type B' evaluations and in most situations a combination of both are used. These categories will be discussed in detail below.

7.3.1 Type A:

In this category, the uncertainty of a measurement source is estimated using statistical analysis. This is achieved through repeatedly executing the tests at least 30 times, with

the mean and the standard deviation taken to calculate the standard uncertainty [47]. The data collected will under most circumstances have a normal distribution as shown in Figure 113. A probability density function is plotted of a number of data points taken under the same conditions.

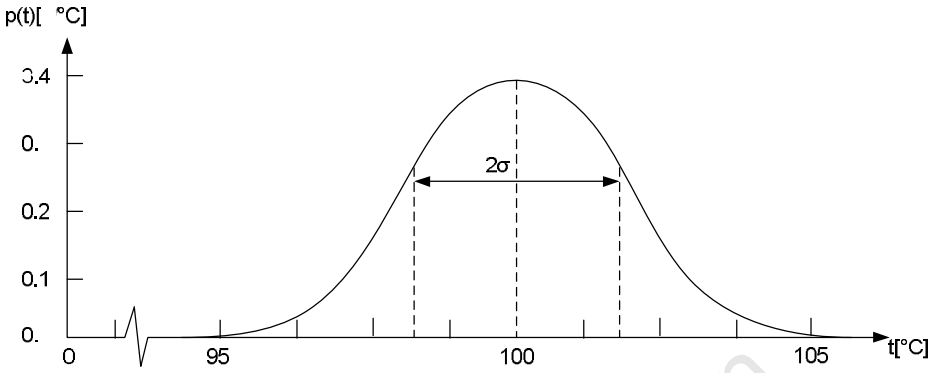

Figure 113: Graphical illustration of evaluating the standard uncertainty of an input variable (temperature)from repeated observations

An example of this is the winding temperature recorded during an efficiency test. The mean in this case is 100°C and the standard deviation is ±1.5°C.

The following equation is used to calculate the standard deviation [46]:

$$= \sqrt{\frac{(\quad)}{\quad}} \qquad (37)$$

Where σ is the standard deviation (STD)

x_i is the measured variable,

μ is the mean

N is the number of measured data points

If there are any outliers, they should be removed and replaced with additional data points. The standard uncertainty is calculated by dividing the standard deviation by the square root of the number of data points as follow [47]:

$$( ) = \quad = \frac{}{\sqrt{}} \qquad (38)$$

Where: ( ) is the standard uncertainty

is the standard error

is the standard deviation

7.3.2 Type B:

These types of uncertainties are evaluated using available information. This could include uncertainty information quoted on a calibration certificate.

The worst case estimation (WCE) [28] has been used for the assessment of measurement uncertainty. This method essentially treats all the measurement uncertainties in input variables equally, despite their distinctly different influence on the output variable. This technique will of course overestimate the magnitude of measurement uncertainty, but it provides a simplistic approach to determine the uncertainty. The relative worst case error for the output variable can be expressed as [28]:

$$= \frac{\Delta}{} = \quad \frac{\Delta}{} + \frac{1}{} \quad \frac{}{} \qquad (38)$$

Where y is the output,

x_i are the measurement uncertainties in the input variables (where $i = 1,\ldots,n$)

z_i is the additive noise from the instruments

is the sensitivity factor of the measurement associated with input variable i

In order to improve this technique, a realistic perturbation based estimation (RPBE) was proposed by Cao et al [28] for assessing the error in losses and efficiency of IM's.

The RPBE takes into account the "weight" of the input variable as it relates to its sensitivity on the output variable. It assumes that all instrument errors are random and will not occur at the same time. Small errors are propagated through the efficiency transfer function ("black box") illustrated in Figure 114.

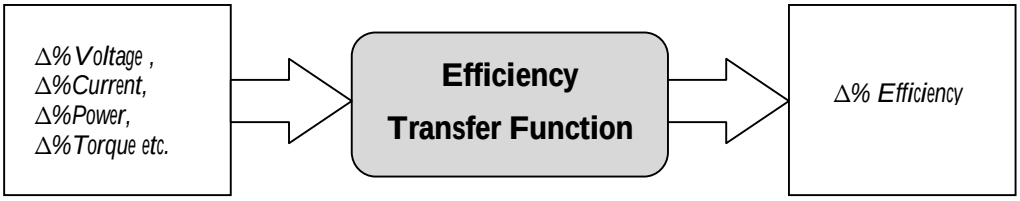

Figure 114: Schematic of efficiency estimation by motor testing [28]

This gives the change in the efficiency as a function of the change in the instrument measurement, and in turn, results in that measurement's influence on the efficiency. This influence is further in this chapter referred to as the sensitivity factor. The perturbation Δx in the instrument measurement x will lead to a change Δy in y. The sensitivity factor of the variable x is defined as [28]:

$$= \frac{\Delta\ /}{\Delta\ /} = \text{——} \tag{39}$$

The error contribution of this instrument measurement to total efficiency error is given by multiplying its sensitivity factor by the measurement accuracy. In so doing, all the measured parameters become comparable. The error contributions are added up of quadrature addition, and an overall realistic error in the efficiency is given. This can be expressed as [28]:

$$= \frac{\Delta}{\text{——}} = \sum \frac{\Delta}{\text{——}} + \text{—}\sum \text{——} \tag{**Error! Bookmark not defined.**}$$

Perturbations of 2% were injected into the motor efficiency estimation model. The input variables to the efficiency estimation model were; voltage, current, input power,

torque, speed, winding resistance and temperature. The respective change in efficiency is then recorded and plotted as shown in Figure 115 to Figure 118.

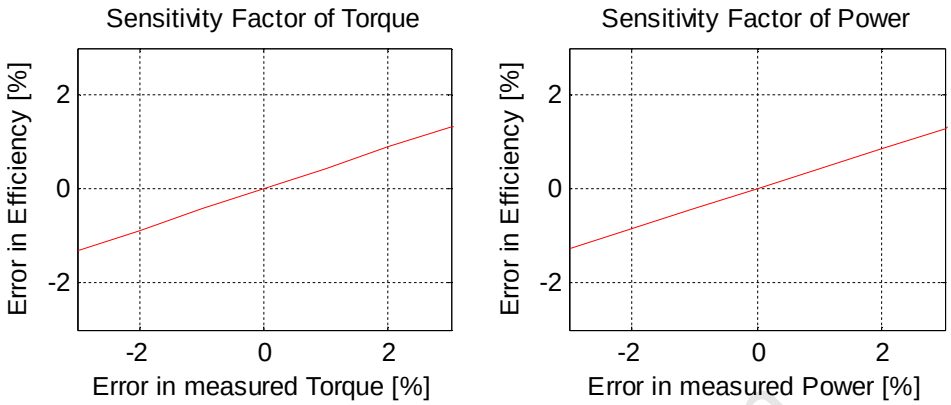

Figure 115: Significance factors of torque and input power on efficiency

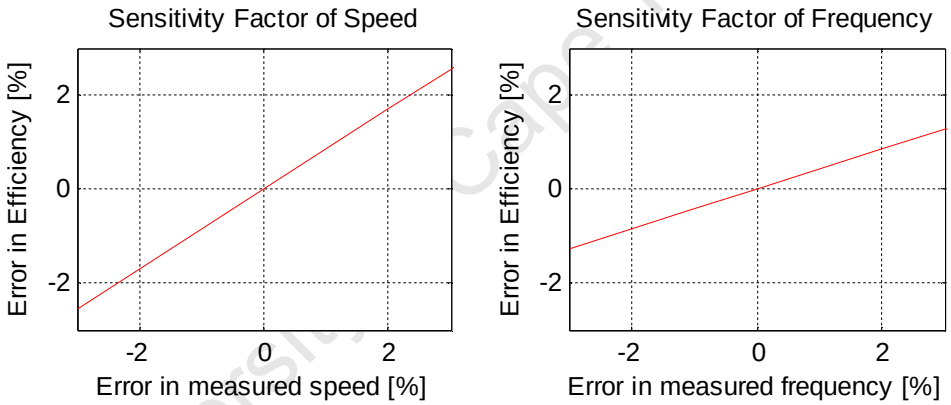

Figure 116: Significance factors of speed and frequency on efficiency

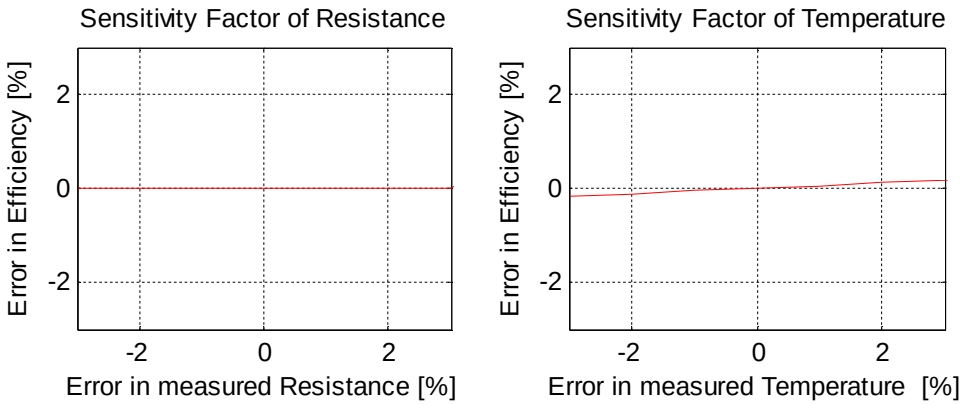

Figure 117: Significance factors of resistance and temperature on efficiency

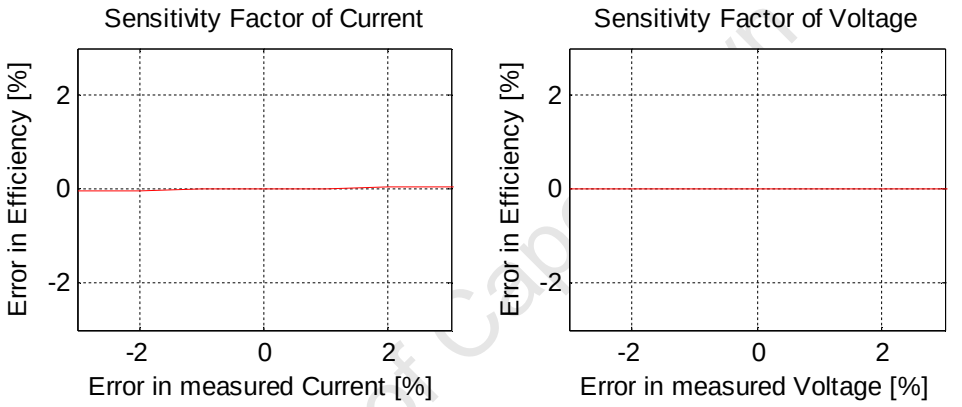

Figure 118: Significance factors of current and voltage on efficiency

The figures above show the influence or the sensitivity that each of the input variables have individually on the efficiency result. It can be seen that efficiency is most sensitive to load torque, input power and speed. This is expected since these variables influence the losses of the motor directly.

7.4 Instrument Accuracy

As discussed in the previous section, the accuracy of the instruments are multiplied by its sensitivity factor. The contribution of each instrument is then summed up in quadrature terms to form the RPBE. In [28], Cao uses the minimum instrumentation accuracies specified by the IEEE112 and IEC34-2-1 standards to calculate the RPBE.

The minimum instrumentation accuracies required by the four most prominent induction machine efficiency standards are illustrated in Table 31.

Table 31: Minimum instrumentation accuracy in % (or specified) required by the four most prominent induction motor efficiency testing standards [11]

Variable	IEEE 112	IEC 34-2 ('96) (*)	IEC 34-2 ('07)	IEC 61972
Voltage	0.2	0.5	0.2	0.2
Current	0.2	0.5	0.2	0.2
Power	0.2	1	0.2	0.2
Resistance	0.2	0.5	0.2	0.2
Frequency	0.1	0.5	0.1	0.1
Temperature	1°C	2°C	1°C	1°C
Torque	0.2	0.5	0.2	0.2
Speed	1 rpm	2 rpm (*)	1 rpm	0.5-1 rpm (*)
Instrument transformers	0.5 (general) 0.3/0.2 (**)	0.5	0.5 (general) 0.3 (***)	0.2

The efficiency estimated in this manner with the minimum values prescribed by the standards does not represent the "real" value associated with the instruments used in the actual test rig. It does however provide an indication of the worst case error if and only if the actual instrument accuracy is better than that specified by the standards.

All instruments used in this thesis for motor testing were sent off for calibration except for the DMM used for winding resistance measurement and the thermocouples. The Yokogawa WT1600 Power Meter is a 0.1% accuracy class instrument, and was used for measuring Voltage, Current, Power and frequency. From the calibration certificate of the power meter the error associated with voltage, current and power, measurements are: 0.03%, 0.51% and 0.51% respectively. The error problem of the power analyser should be assessed in more detail. A possible solution is to apply a correction factor to the current reading in order to improve the current and power accuracies to acceptable limits. Another possibility is to replace the current shunts or the input modules on the power. The frequency error was not given on the calibration certificate and was therefore assumed to be the same as the voltage error since the frequency of the voltage waveform is measured. A new torque transducer with speed sensing was acquired and came with its calibration certificate. The error noted for the torque measurement was a maximum of 0.058%. The accuracy of the speed measurement was not indicated on the

calibration certificate. However, since speed was measured within the transducer, the minimum accuracy of speed measurement as specified by the standard was assumed. The same assumption was made for the winding resistance and temperature measurement, and the min error values of the standard were used. The power analyser is used for the no-load and load tests and it is assumed that the same voltage, current and power errors are present for both these tests.

7.5 SENSITIVITY AND SIGNIFICANCE OF MEASUREMENTS ON EFFICIENCY

As discussed previously, the perturbation of errors in the measurements of the input variables was processed through the efficiency determination model and shown to result in the gradient or sensitivity of the efficiency to each of the input measurements in turn. This is an alternative to deriving the actual transfer function for efficiency which could be a very complex exercise. The sensitivity factor is an indication of the change in efficiency caused by every 1% change in the particular measurement. The sensitivity and error contribution of all the instruments at full load is given in Table 32.

Table 32: Sensitivity factor and Instrumentation errors for efficiency measurement at full load associated with the 11kW STD motor

Measurement	Sensitivity Factor	Realistic Error [%]	Ranking	Minimum Instrument Accuracy [%]	Actual Instrument Error [%]
Torque	0.438	0.02539	3nd	0.2	0.058
Power	0.432	0.22051	1nd	0.2	0.51
Speed	0.855	0.04276	2nd	0.05	0.05
Freq	0.428	0.01710	4nd	0.1	0.04
Temp	0.0003	0.00006	6nd	0.2	0.2
Current	0.0001	0.00008	5nd	0.2	0.51
Resistance	0.0032	0.00003	7nd	0.2	0.01
Voltage	0.000004	0.0000001	8nd	0.2	0.03

From Table 32, it can be seen that power, speed and torque are the most significant measurements in terms of contribution to the total error in the estimated efficiency.

Although, efficiency is the most sensitive to speed, realistically it only causes a 0.04276% error at full load. This is because speed can generally be measured very accurately by the transducer and the error is seldom more than 1rpm.

7.6 THE IEEE112-B REALISTIC AND WORST CASE ERROR RESULTS

This section deals with the sensitivity of efficiency with a change in the input variables and shows the calculated error in efficiency using the IEEE minimum accuracy requirements and the actual errors of the test rig instruments. The sensitivities of the input measurements and the uncertainty are shown at six loads. The 11kW and 3kW STD and EE motors were analysed as these give a good representation of all the motors investigated in this thesis. Three uncertainty bands are depicted at each load. The first is the RPBE, calculated according to the procedure as described in section 7.3.2, using the minimum error for instruments required by the IEEE. The second uncertainty being the RPBE(Test Rig) using the actual instrument errors noted on their respective calibration certificates. The last column gives the WCE(Test Rig), which is the error in efficiency should all the instrument errors on the calibration certificates occur at the same time. Table 33 to Table 36 gives the sensitivity factors and the error estimations for the 11kW STD and EE motors when the IEEE112 method is used for efficiency determination.

7.6.1 The Sensitivity factors and Errors of the 11kW motors – IEEE method

Table 33: Sensitivity on Efficiency of IEEE 112-B on the 11kW STD Motor

11kW STD Motor Sensitivity Factors								
Load[%]	**Torque**	**Power**	**Speed**	**Freq.**	**Temp**	**Current**	**Resist.**	**Voltage**
150	0.642	0.628	0.821	0.410	0.0006	0.0003	0.0017	0.000002
125	0.544	0.536	0.831	0.416	0.0008	0.0004	0.0023	0.000003
100	0.438	0.432	0.855	0.428	0.0003	0.0001	0.0032	0.000004
75	0.327	0.323	0.880	0.440	0.0004	0.0002	0.0024	0.000005
50	0.213	0.208	0.899	0.450	0.0013	0.0006	0.0003	0.000007
25	0.096	0.089	0.869	0.435	0.0027	0.0013	0.0050	0.000008

Table 34: Estimated Errors of 11kW STD Motor (method used is IEEE 112-B)

Load [%]	RPBE (IEEE)	RPBE (Test Rig)	WCE (Test Rig)
150	±0.19	±0.33	±0.42
125	±0.16	±0.28	±0.36
100	±0.14	±0.23	±0.31
75	±0.11	±0.17	±0.25
50	±0.09	±0.12	±0.18
25	±0.07	±0.07	±0.11

Table 35: Sensitivity on Efficiency of IEEE 112-B on 11kW EE Motor

11kW EE motor Sensitivity Factors								
Load[%]	**Torque**	**Power**	**Speed**	**Freq.**	**Temp**	**Current**	**Resist.**	**Voltage**
150	0.681	0.667	0.849	0.165	0.0015	0.0016	0.0054	0.00007
125	0.572	0.563	0.862	0.285	0.0014	0.0037	0.0037	0.00009
100	0.458	0.451	0.879	0.414	0.0010	0.0048	0.0046	0.00013
75	0.340	0.336	0.897	0.546	0.0006	0.0034	0.0075	0.00019
50	0.219	0.216	0.906	0.674	0.0003	0.0006	0.0132	0.00025
25	0.099	0.096	0.897	0.782	0.0000	0.0038	0.0261	0.00031

Table 36: Estimated Errors of 11kW EE Motor (method used is IEEE 112-B)

Load [%]	RPBE (IEEE)	RPBE (Test Rig)	WCE (Test Rig)
150	±0.20	±0.34	±0.43
125	±0.17	±0.29	±0.38
100	±0.14	±0.24	±0.32
75	±0.12	±0.18	±0.26
50	±0.10	±0.12	±0.20
25	±0.10	±0.07	±0.13

7.6.2 The Sensitivity factors and Errors of the 3kW motors – IEEE method

Table 37: Sensitivity on Efficiency of IEEE 112-B on 3kW Standard Motor

3kW STD motor Sensitivity Factors								
Load[%]	**Torque**	**Power**	**Speed**	**Freq.**	**Temp**	**Current**	**Resist.**	**Voltage**
150	0.592	0.578	0.743	0.148	0.0014	0.0049	0.0024	0.00004
125	0.503	0.494	0.764	0.257	0.0020	0.0020	0.0010	0.00005
100	0.409	0.403	0.792	0.376	0.0016	0.0044	0.0022	0.00007
75	0.311	0.307	0.820	0.499	0.0010	0.0034	0.0017	0.00009
50	0.200	0.195	0.833	0.620	0.0006	0.0024	0.0011	0.00013
25	0.092	0.086	0.795	0.689	0.0005	0.0102	0.0049	0.00024

Table 38: Estimated Errors of 3kW Standard Motor (method used is IEEE 112-B)

Load [%]	**RPBE (IEEE)**	**RPBE (Test Rig)**	**WCE (Test Rig)**
150	±0.17	±0.30	±0.37
125	±0.15	±0.26	±0.33
100	±0.13	±0.21	±0.29
75	±0.11	±0.16	±0.24
50	±0.09	±0.11	±0.18
25	±0.08	±0.07	±0.12

Table 39: Sensitivity on Efficiency of IEEE 112-B on 3kW EE Motor

3kW EE motor Sensitivity Factors								
Load[%]	**Torque**	**Power**	**Speed**	**Freq.**	**Temp**	**Current**	**Resist.**	**Voltage**
150	0.631	0.607	0.795	0.161	0.0120	0.0150	0.0126	0.0139
125	0.532	0.509	0.820	0.282	0.0140	0.0222	0.0172	0.0169
100	0.427	0.404	0.846	0.410	0.0170	0.0281	0.0219	0.0215
75	0.319	0.292	0.870	0.539	0.0211	0.0344	0.0274	0.0280
50	0.212	0.176	0.888	0.663	0.0297	0.0476	0.0386	0.0405
25	0.096	0.034	0.873	0.762	0.0542	0.0856	0.0701	0.0746

Table 40: Estimated Errors of 3kW EE Motor (method used is IEEE 112-B)

Load[%]	**RPBE (IEEE)**	**RPBE (Test Rig)**	**WCE (Test Rig)**
150	±0.18	±0.31	±0.40
125	±0.16	±0.27	±0.36
100	±0.13	±0.21	±0.31
75	±0.11	±0.16	±0.26
50	±0.10	±0.11	±0.20
25	±0.10	±0.07	±0.15

From the tables above it can be seen that the sensitivity factors of the torque and power increases with load for the results of all the four motors presented. However, the sensitivity of frequency decreases with an increase in load. The rest do not show a consistent upward or downward trend. The actual errors of the instruments were also used to determine for the 11kW and 3kW STD motor and EE motors. The uncertainties at six loads are tabulated. For example at full load, the RPBE(Test Rig) for the 11kW STD and EE motors are ±0.23% and ±0.24% respectively. The WCE(Test Rig) is ±0.31% and ±0.32% for STD and EE motors respectively at full load. The estimated errors in efficiency for the 3kW STD and EE motors are slightly lower than that of the 11kW motors.

7.7 THE IEC60034-2-1 REALISTIC AND WORST CASE ERROR RESULTS

Although the IEEE and the new IEC standards for IM efficiency estimation have a lot of similarities, they do not give the same efficiency results. This is mainly due to the manner in which the core and stator winding losses are calculated. Due to this, the sensitivity of the input measurements on the efficiency will be different. This section looks at the ssensitivity factors and the error estimations for the 11kW STD and EE motors when the IEC60034-2-1 standard is used for efficiency estimation. The RPBEs and WCEs are obtained in the same manner as was done in the previous section. The only difference being the sensitivity factors of input measurements as this was found by using the IEC60034-2-1 model for efficiency estimation. Table 41 to Table 48 shows the results found.

7.7.1 The Sensitivity factors and Errors of the 11kW motors – IEC method

Table 41: Sensitivity on Efficiency of IEC60034-2-1 on 11kW STD Motor

11kW STD motor Sensitivity Factors								
Load[%]	**Torque**	**Power**	**Speed**	**Freq.**	**Temp**	**Current**	**Resist.**	**Voltage**
150	0.642	0.624	0.824	0.178	0.0006	0.0060	0.0003	0.0052
125	0.544	0.529	0.852	0.303	0.0005	0.0018	0.0024	0.0066
100	0.438	0.424	0.877	0.431	0.0006	0.0005	0.0043	0.0091
75	0.327	0.313	0.895	0.556	0.0005	0.0022	0.0054	0.0130
50	0.213	0.196	0.899	0.673	0.0006	0.0076	0.0052	0.0178
25	0.096	0.074	0.862	0.751	0.0017	0.0177	0.0030	0.0233

Table 42: Estimated Errors of 11kW STD Motor (method used is IEC60034-2-1)

Load [%]	RPBE (IEC)	RPBE (Test Rig)	WCE (Test Rig)
150	±0.18	±0.32	±0.41
125	±0.16	±0.28	±0.36
100	±0.14	±0.22	±0.30
75	±0.12	±0.17	±0.25
50	±0.10	±0.11	±0.19
25	±0.09	±0.07	±0.13

Table 43: Sensitivity on Efficiency of IEC60034-2-1 on 11kW EE Motor

11kW EE motor Sensitivity Factors								
Load[%]	**Torque**	**Power**	**Speed**	**Frequency**	**Temp**	**Current**	**Resistance**	**Voltage**
150	0.681	0.672	0.883	0.198	0.0007	0.0166	0.0050	0.0007
125	0.572	0.569	0.905	0.326	0.0003	0.0145	0.0032	0.0012
100	0.458	0.458	0.923	0.456	0.0003	0.0169	0.0032	0.0021
75	0.340	0.345	0.935	0.583	0.0003	0.0239	0.0049	0.0031
50	0.219	0.232	0.939	0.705	0.0003	0.0386	0.0092	0.0036
25	0.099	0.131	0.917	0.801	0.0003	0.0727	0.0204	0.0011

Table 44: Estimated Errors of 11kW EE Motor (method used is IEC60034-2-1)

Load [%]	RPBE (IEC)	RPBE (Test Rig)	WCE (Test Rig)
150	±0.20	±0.35	±0.44
125	±0.17	±0.30	±0.39
100	±0.14	±0.24	±0.33
75	±0.12	±0.19	±0.28
50	±0.11	±0.13	±0.23
25	±0.10	±0.09	±0.19

7.7.2 The Sensitivity factors and Errors of the 3kW motors– IEC method

Table 45: Sensitivity on Efficiency of IEC60034-2-1 on 3kW STD Motor

3kW STD motor Sensitivity Factors								
Load[%]	**Torque**	**Power**	**Speed**	**Freq.**	**Temp**	**Current**	**Resist.**	**Voltage**
150	0.592	0.582	0.761	0.165	0.0024	0.0106	0.0074	0.00492
125	0.503	0.496	0.797	0.289	0.0044	0.0091	0.0065	0.00704
100	0.409	0.406	0.828	0.411	0.0056	0.0089	0.0065	0.00938
75	0.311	0.312	0.850	0.528	0.0071	0.0111	0.0084	0.01239
50	0.200	0.207	0.856	0.642	0.0108	0.0201	0.0152	0.01690
25	0.092	0.114	0.808	0.702	0.0205	0.0361	0.0310	0.02542

Table 46: Estimated Errors of 3kW STD Motor (method used is IEC60034-2-1)

Load [%]	RPBE (IEC)	RPBE (Test Rig)	WCE (Test Rig)
150	±0.17	±0.30	±0.38
125	±0.15	±0.26	±0.34
100	±0.13	±0.21	±0.29
75	±0.11	±0.17	±0.25
50	±0.10	±0.12	±0.20
25	±0.09	±0.08	±0.16

Table 47: Sensitivity on Efficiency of IEC60034-2-1 on 3kW EE Motor

3kW EE motor Sensitivity Factors								
Load[%]	**Torque**	**Power**	**Speed**	**Freq.**	**Temp**	**Current**	**Resist.**	**Voltage**
150	0.631	0.608	0.820	0.186	0.0032	0.0083	0.0080	0.03300
125	0.532	0.511	0.850	0.312	0.0032	0.0132	0.0113	0.03944
100	0.427	0.406	0.875	0.439	0.0039	0.0173	0.0146	0.04914
75	0.319	0.295	0.895	0.564	0.0050	0.0219	0.0189	0.06497
50	0.212	0.182	0.906	0.680	0.0072	0.0322	0.0275	0.09567
25	0.096	0.046	0.886	0.775	0.0129	0.0604	0.0504	0.17768

Table 48: Estimated Errors of 3kW EE Motor (method used is IEC60034-2-1)

Load [%]	RPBE (IEC)	RPBE (Test Rig)	WCE (Test Rig)
150	±0.18	±0.32	±0.40
125	±0.16	±0.27	±0.35
100	±0.13	±0.21	±0.30
75	±0.11	±0.16	±0.25
50	±0.10	±0.11	±0.20
25	±0.10	±0.07	±0.14

The results from Table 42 Table 44 show that the RPBE(Test Rig) at full load is ±0.22% and ±0.24% for the 11kW STD and EE motors respectively. The worst case error for the STD motor is ±0.3% and ±0.33% for the EE motor.

In Table 46Table 48 it is shown that the realistic uncertainty associated with the efficiency estimate, when performed on the new test rig, was found to be ±0.21% for both the 3kW STD and EE motors at full load. The WCE at full is ±0.29% and ±0.30% for the STD and EE motors respectively.

From the above error estimations it can be seen that in most cases there is a bigger uncertainty associated with the efficiency of the EE motors. This is due to the higher efficiency values of these types of motors. Thus, the more efficient a motor the more accurate the measuring instruments need to be.

7.8 DIRECT EFFICIENCY METHOD REALISTIC AND WORST CASE ERROR RESULTS

The third and final method for determining efficiency that was dealt with in this chapter is the input-output or direct method. The uncertainty associated with the direct method differs significantly with the IEEE112-B and IEC60034-2-1 standards.
The efficiency of an induction motor can directly be estimated as follows:

$$= \frac{}{} = \frac{\times}{} \qquad (37)$$

From the equation above it can be seen that the efficiency is only a function of input power, torque and speed and so will only be influenced by these three parameters. Power could also be considered a function of voltages and currents, but since it was captured directly by the power analyser, there is no need for investigating voltage and current.

The output and input values of induction motors are generally very large and don't differ much due to its efficient design. Small errors in either of these values can lead to a large error in the efficiency result [48].

Furthermore, the uncertainty associated with efficiency of the direct method when motors operate with unbalance supplies was investigated. Eight standard and energy-efficient motors were subjected to three voltage unbalances (VU) in combination with over and under supply voltage conditions. However, only the voltage unbalances at rated (380V) supply voltage was dealt with in this chapter. These voltage unbalances are 0%, 2.5% and 5% according to the NEMA definition. The estimated efficiencies of the motors under these supply conditions were obtained by the direct method and the results are presented in chapter 6. The RPBE and WCE methods were used to determine the uncertainties associated with the estimated efficiency results. The 11kW and 3kW STD and EE motors were analysed and the associated sensitivity factors and uncertainties are presented in Table 49 to Table 60.

7.8.1 The Sensitivity factors and Errors of the 11kW STD motor– Direct method

Table 49: Sensitivity factors and Uncertainty bands for efficiency 11kW STD motor based on the Direct Method with **0% VU**

	Load [%]	Sensitivity on Efficiency			RPBE (IEEE)	RPBE (Test Rig)	WCE (Test Rig)
		Torque	Power	Speed			
380V@ 0% Voltage Unbalance	**150**	0.793	0.777	0.793	±0.23	±0.40	±0.48
	125	0.824	0.808	0.824	±0.23	±0.42	±0.50
	100	0.841	0.824	0.841	±0.24	±0.43	±0.51
	75	0.844	0.827	0.844	±0.24	±0.43	±0.51
	50	0.823	0.807	0.823	±0.23	±0.42	±0.50
	25	0.738	0.723	0.738	±0.21	±0.37	±0.45

Table 50: Sensitivity factors and Uncertainty bands for efficiency 11kW STD motor based on the Direct Method with **2.5% VU**

	Load [%]	Sensitivity on Efficiency			RPBE (IEEE)	RPBE (Test Rig)	WCE (Test Rig)
		Torque	Power	Speed			
380V@ 2.5% Voltage Unbalance	**150**	0.782	0.766	0.782	±0.22	±0.40	±0.48
	125	0.819	0.803	0.819	±0.23	±0.41	±0.50
	100	0.832	0.816	0.832	±0.24	±0.42	±0.51
	75	0.837	0.820	0.837	±0.24	±0.42	±0.51
	50	0.815	0.799	0.815	±0.23	±0.41	±0.50
	25	0.726	0.712	0.726	±0.21	±0.37	±0.44

Table 51: Sensitivity factors and Uncertainty bands for efficiency 11kW STD motor based on the Direct Method with **5% VU**

	Load [%]	Sensitivity on Efficiency			RPBE (IEEE)	RPBE (Test Rig)	WCE (Test Rig)
		Torque	Power	Speed			
380V@ 5% Voltage Unbalance	**150**	0.771	0.756	0.771	±0.22	±0.39	±0.47
	125	0.804	0.788	0.804	±0.23	±0.41	±0.49
	100	0.819	0.803	0.819	±0.23	±0.41	±0.50
	75	0.820	0.804	0.820	±0.23	±0.41	±0.50
	50	0.794	0.779	0.794	±0.23	±0.40	±0.48
	25	0.698	0.684	0.698	±0.20	±0.35	±0.42

From the above tables it can be seen that all three measurements have approximately the same influence on the efficiency when determined directly. This is not surprising since efficiency is directly related to the product of the torque and the speed and inversely proportional to the input power.

The sensitivity of these three measurements on the efficiency is the highest at 75% load and decreases slightly as the load changes from this point. This occurs in the region where the efficiency of the motor is at its highest. The calculated RPBE, using the minimum accuracy required by the IEEE and IEC for instruments varies between ±0.23% and ±0.24% for the three unbalance supply conditions at full load. The calculated RPBE, using the errors on the calibration certificates varies between ±0.41 and ±0.43 respectively at full load for the three supply conditions. Figure 119 illustrates the uncertainty band in which the "true efficiency" value lies with a 95% confidence factor.

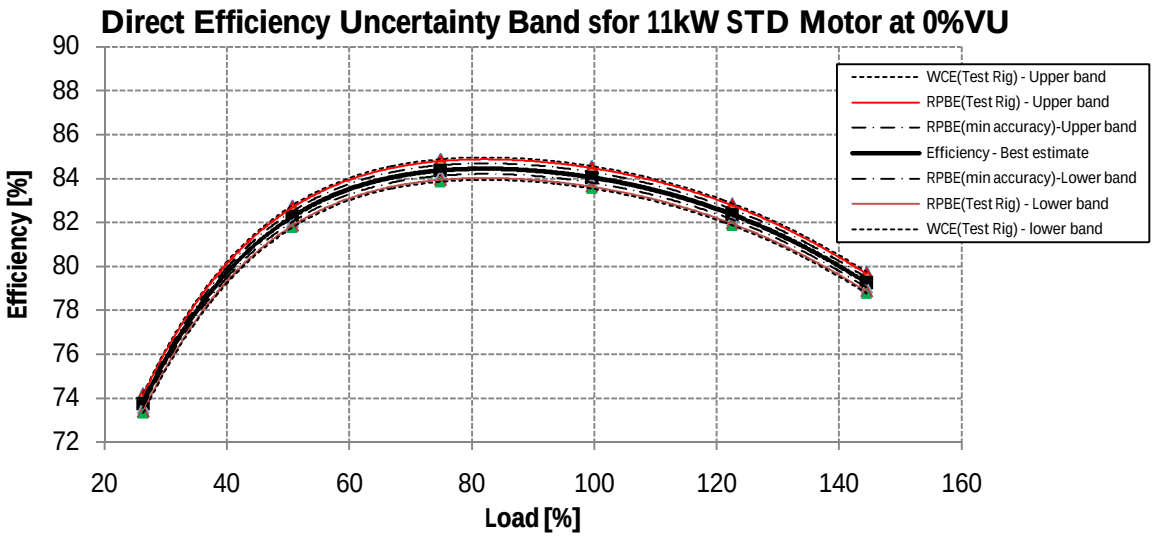

Figure 119: RPBE and WCE Uncertainty bands for efficiency based on the Direct Method

Figure 119 shows how the RPBE and WCE uncertainty bands widens as the load increases from 25% to about 75% where after it narrows down towards the 150% load.

7.8.2 The Sensitivity factors and Errors of the 11kW EE motor– Direct method

Table 52 to Table 54 summarises the results of the 11kW EE motor at 0%, 2.5% and 5% voltage unbalance. The sensitivity factors and RPBE and WCE at loads 25% to 150% are given at each supply condition.

Table 52: Sensitivity factors and Uncertainty bands for efficiency 11kW EE motor based on the Direct Method with **0% VU**

	Load [%]	Sensitivity on Efficiency			RPBE (IEEE)	RPBE (Test Rig)	WCE (Test Rig)
		Torque	Power	Speed			
380V@ 0% Voltage Unbalance	**150**	0.846	0.830	0.846	±0.24	±0.43	±0.51
	125	0.868	0.851	0.868	±0.25	±0.44	±0.53
	100	0.883	0.866	0.883	±0.25	±0.45	±0.54
	75	0.889	0.871	0.889	±0.25	±0.45	±0.54
	50	0.878	0.861	0.878	±0.25	±0.44	±0.53
	25	0.820	0.804	0.820	±0.23	±0.41	±0.50

Table 53: Sensitivity factors and Uncertainty bands for efficiency 11kW EE motor based on the Direct Method with **2.5% VU**

	Load [%]	Sensitivity on Efficiency			RPBE (IEEE)	RPBE (Test Rig)	WCE (Test Rig)
		Torque	Power	Speed			
380V@ 2.5% Voltage Unbalance	**150**	0.834	0.817	0.834	±0.24	±0.42	±0.51
	125	0.863	0.846	0.863	±0.25	±0.44	±0.52
	100	0.877	0.860	0.877	±0.25	±0.44	±0.53
	75	0.882	0.864	0.882	±0.25	±0.45	±0.54
	50	0.868	0.851	0.868	±0.25	±0.44	±0.53
	25	0.810	0.794	0.810	±0.23	±0.41	±0.49

Table 54: Sensitivity factors and Uncertainty bands for efficiency 11kW EE motor based on the Direct Method with **5% VU**

	Load [%]	Sensitivity on Efficiency			RPBE (IEEE)	RPBE (Test Rig)	WCE (Test Rig)
		Torque	Power	Speed			
380V@ 5% Voltage Unbalance	**150**	0.830	0.814	0.830	±0.24	±0.42	±0.50
	125	0.848	0.832	0.848	±0.24	±0.43	±0.52
	100	0.863	0.846	0.863	±0.25	±0.44	±0.52
	75	0.864	0.847	0.864	±0.25	±0.44	±0.53
	50	0.848	0.831	0.848	±0.24	±0.43	±0.52
	25	0.788	0.773	0.788	±0.22	±0.40	±0.48

The calculated errors increase slightly as the voltage unbalance improves for both motors investigated. This can also be explained by the fact that the efficiency increases as voltages unbalance improves. Therefore, the ratio between the numerator and denominator approaches one. A small error in the numerator or denominator will result in a larger efficiency error.

The calculated RPBE is ± 0.25%, using the minimum accuracy required by the IEEE and IEC for instruments. The calculated RPBE and WCE, using the errors on the calibration certificates is ±0.45 and ±0.54 respectively at full load with a voltage unbalance of 0%. Figure 120 shows the uncertainty bands in efficiency for the 11kW EE motor when determined by the direct method.

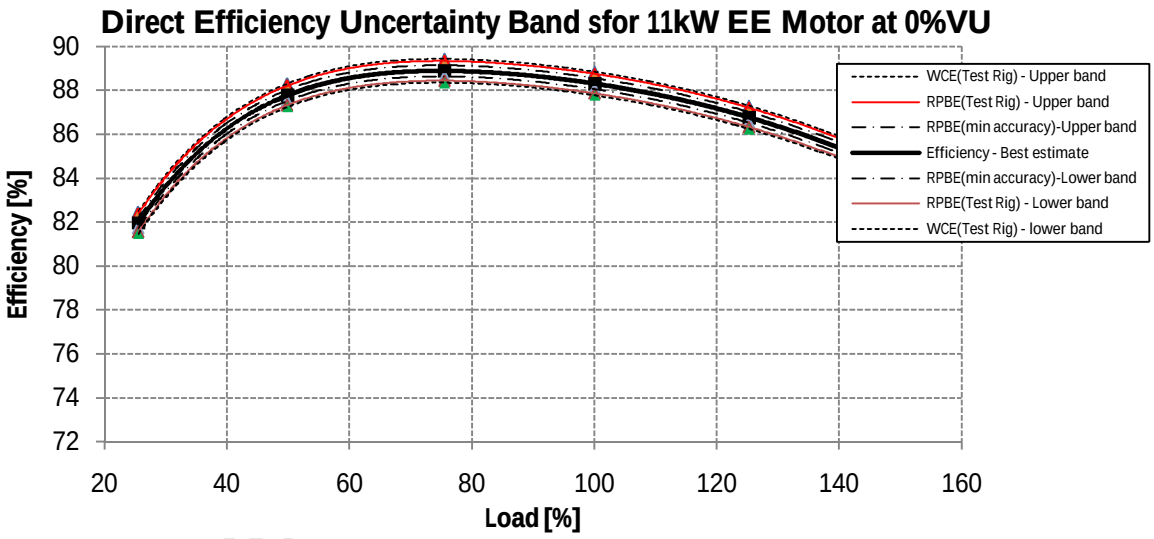

Figure 120: RPBE and WCE Uncertainty bands for efficiency based on the Direct Method

7.8.3 The Sensitivity factors and Errors of the 3kW STD motor– Direct method

Table 55 to Table 57summarises the results of the 3kW STD motor at 0%, 2.5% and 5% voltage unbalance. The sensitivity factors and RPBE and WCE at loads 25% to 150% are given at each supply condition.

Table 55: Sensitivity factors and Uncertainty bands for efficiency 3kW STD motor based on the Direct Method with **0% VU**

	Load [%]	Sensitivity on Efficiency			RPBE (IEEE)	RPBE (Test Rig)	WCE (Test Rig
		Torque	Power	Speed			
380V@ 0% Voltage Unbalance	**150**	0.729	0.715	0.729	±0.21	±0.37	±0.44
	125	0.766	0.751	0.766	±0.22	±0.39	±0.47
	100	0.791	0.775	0.791	±0.22	±0.40	±0.48
	75	0.803	0.788	0.803	±0.23	±0.41	±0.49
	50	0.793	0.777	0.793	±0.23	±0.40	±0.48
	25	0.712	0.698	0.712	±0.20	±0.36	±0.43

Table 56: Sensitivity factors and Uncertainty bands for efficiency 3kW STD motor based on the Direct Method with **2.5% VU**

	Load [%]	Sensitivity on Efficiency			RPBE (IEEE)	RPBE (Test Rig)	WCE (Test Rig)
		Torque	Power	Speed			
380V@ 2.5% Voltage Unbalance	**150**	0.727	0.713	0.727	±0.21	±0.37	±0.44
	125	0.762	0.747	0.762	±0.22	±0.39	±0.46
	100	0.786	0.770	0.786	±0.22	±0.40	±0.48
	75	0.798	0.782	0.798	±0.23	±0.40	±0.48
	50	0.786	0.770	0.786	±0.22	±0.40	±0.48
	25	0.703	0.689	0.703	±0.20	±0.36	±0.43

Table 57: Sensitivity factors and Uncertainty bands for efficiency 3kW STD motor based on the Direct Method with **5% VU**

	Load [%]	Sensitivity on Efficiency			RPBE (IEEE)	RPBE (Test Rig)	WCE (Test Rig)
		Torque	Power	Speed			
380V@ 5% Voltage Unbalance	**150**	0.718	0.704	0.718	±0.20	±0.36	±0.44
	125	0.754	0.739	0.754	±0.21	±0.38	±0.46
	100	0.774	0.758	0.774	±0.22	±0.39	±0.47
	75	0.764	0.749	0.764	±0.22	±0.39	±0.46
	50	0.780	0.765	0.780	±0.22	±0.39	±0.47
	25	0.694	0.681	0.694	±0.20	±0.35	±0.42

7.8.4 The Sensitivity factors and Errors of the 3kW EE motor– Direct method

Table 58 to Table 60 summarises the results of the 3kW EE motor at 0%, 2.5% and 5% voltage unbalance. The sensitivity factors and RPBE and WCE at loads 25% to 150% are given at each supply condition.

Table 58: Sensitivity factors and Uncertainty bands for efficiency 3kW EE motor based on the Direct Method with **0% VU**

	Load [%]	Sensitivity on Efficiency			RPBE (IEEE)	RPBE (Test Rig)	WCE (Test Rig)
		Torque	Power	Speed			
380V@ 0% Voltage Unbalance	**150**	0.772	0.757	0.772	±0.22	±0.39	±0.47
	125	0.796	0.780	0.796	±0.23	±0.40	±0.48
	100	0.809	0.793	0.809	±0.23	±0.41	±0.49
	75	0.812	0.796	0.812	±0.23	±0.41	±0.49
	50	0.791	0.775	0.791	±0.22	±0.40	±0.48
	25	0.700	0.686	0.700	±0.20	±0.35	±0.43

Table 59: Sensitivity factors and Uncertainty bands for efficiency 3kW EE motor based on the Direct Method with **2.5% VU**

	Load [%]	Sensitivity on Efficiency			RPBE (IEEE)	RPBE (Test Rig)	WCE (Test Rig)
		Torque	Power	Speed			
380V@ 2.5% Voltage Unbalance	**150**	0.772	0.757	0.772	±0.22	±0.39	±0.47
	125	0.795	0.779	0.795	±0.23	±0.40	±0.48
	100	0.809	0.794	0.809	±0.23	±0.41	±0.49
	75	0.812	0.796	0.812	±0.23	±0.41	±0.49
	50	0.790	0.775	0.790	±0.22	±0.40	±0.48
	25	0.700	0.686	0.700	±0.20	±0.35	±0.43

Table 60: Sensitivity factors and Uncertainty bands for efficiency 3kW EE motor based on the Direct Method with **5% VU**

	Load [%]	Sensitivity on Efficiency			RPBE (IEEE)	RPBE (Test Rig)	WCE (Test Rig)
		Torque	Power	Speed			
380V@ 5% Voltage Unbalance	**150**	0.762	0.747	0.762	±0.22	±0.39	±0.46
	125	0.782	0.766	0.782	±0.22	±0.40	±0.48
	100	0.797	0.782	0.797	±0.23	±0.40	±0.48
	75	0.799	0.784	0.799	±0.23	±0.40	±0.49
	50	0.777	0.762	0.777	±0.22	±0.39	±0.47
	25	0.692	0.678	0.692	±0.20	±0.35	±0.42

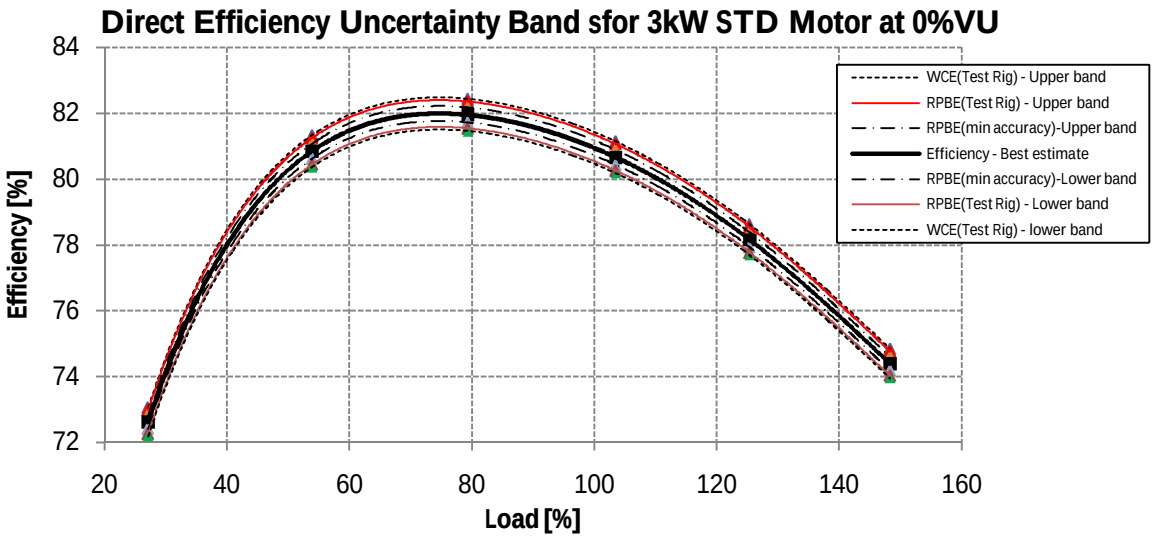

Figure 121: RPBE and WCE Uncertainty bands for efficiency based on the Direct Method

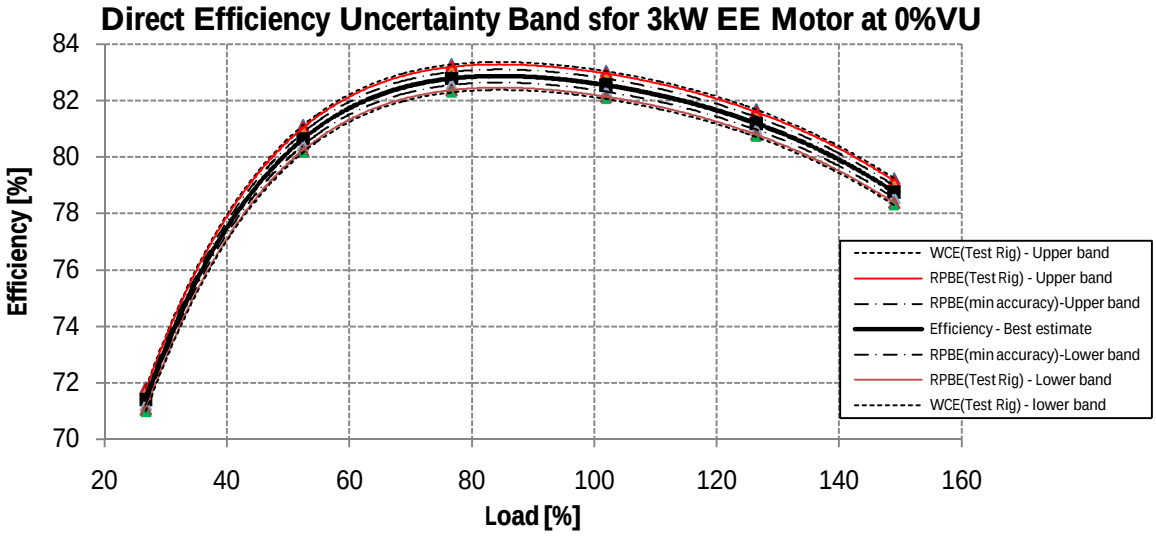

Figure 122: RPBE and WCE Uncertainty bands for efficiency based on the Direct Method

The direct method proved to be very sensitive to instrument errors with a realistic error in efficiency of approximately 0.45% and 0.4% for the 11kW and 3kW motors respectively.

CHAPTER 8

8. CONCLUSIONS AND RECOMMENDATIONS

8.1 CONCLUSIONS

Based on the findings presented in this thesis the following conclusions can be drawn:

- Improvements in motor efficiency can yield significant energy savings and therefore delay the need for additional generating capacity. Most electric motors imported into and used in South Africa are still of the standard efficiency type. A better understanding of the steady-state behaviour of EE motors is essential, as this will support Eskom DSM's EE motor program. There are several significant power quality and performance issues with EE motors. The power quality problems which were investigated in this thesis are voltage unbalanced supplies and over/under voltages and a combination there off. These issues need to be thoroughly investigated in order to achieve the overall energy saving objectives of the program.

- Voltage unbalance is not uniquely defined and depends on the definition used. In this thesis the voltage unbalance definitions developed by NEMA, IEEE and IEC have been studied. The NEMA and IEEE calculate the unbalance in a similar way, except that the IEEE uses phase voltages and the NEMA uses line voltages. No phase angle information is required for these two definitions. The IEC definition or the "true definition" does contain phase angles and phase or line voltages can be used. A formula that approximates the IEC definition was also looked at in this thesis. The NEMA definition was used throughout this thesis due to its ease of implementation in a laboratory.

- It was shown in the results presented in this thesis that the efficiency value estimated for a motor is not indisputable, but depends on a particular standard used. When compared to the IEEE 112-B, the IEC34-2 gave the highest efficiencies in all cases.

The IEEE 112-B and the IEC34-2-1 gave similar results. The IEEE 112-A was adopted to test and investigate the effects of voltage unbalance on standard and energy efficient motors. This method, also known as the direct method, was used since the separation of losses methods assumes balanced supply voltages to the motor and uses an average phase voltage and current in the calculation of power. This was considered to potentially lead to greater errors than the direct method, which uses actual phase voltage and currents in the power calculations. Furthermore, the absolute efficiency values of the motors were considered as less important and were merely used to compare trends.

- The energy efficient motors are more efficient than standard motors, and also exhibit relatively flatter efficiency versus load characteristics. The difference between the nominal and partial load efficiency is therefore less pronounced.

- The catalogue efficiency of all the motors given by the supplier showed no correlation with the efficiency results obtained from any of the standards used. The catalogue efficiency can therefore not be considered as the real efficiency of the motor.

- The IP rating of the motor has a significant effect its friction and windage loss. The higher IP rating associated with the energy efficient motors provided better ingress protection, but increases the friction and windage loss up to four times that of the standard motors.

- The energy efficient motors run, on average 18.2°C cooler because they generate less I^2R heat. This results in lower thermal stress on winding insulation.

- Energy efficient motors have lower core loss because of the type of core material used and the thinner laminations. The saturation voltage appears at a higher value and the increase in core loss is less significant with an increase in voltage in EE motors.

- The unregulated terminal voltage of generator and the volt drop across the cables to the motor resulted in the voltage at the test motor to vary with load. The variations in supply voltage to the motor influences its core and hence its efficiency results.

- EE motors operate at lower slip values when retrofitting a standard motor in centrifugal pump load application. This leads to higher output power delivered to the pump load, which could be absorbed by the application in the form of losses or increased productivity. This could lead to marginally less input power drawn from the supply.

- A comprehensive error analysis was carried out using the accuracy of the instruments used in the new test rig. It was found that the RPBE uncertainty associated with the efficiency determined by means of the IEEE112-B is approximately 0.21% for the 3kW motors and 0.24% in the case of the 11kW motors. The IEC60034-2-1 error results were similar. The direct method for determining efficiency has an approximate 0.4% uncertainty associated with the efficiency result. The uncertainty was found to increase with efficiency. A small error in the input and/or output power measurements, especially when these two values are close, can result in a large error in the efficiency result.

- The experimental results show that the efficiency peak shifts to a lower load as the supply voltage decreases and towards a higher load as it increases. With a 10% reduction in average voltage, the efficiency peaks at an approximately 10% lower load with respect to rated voltage. This was found to be the case for all the motors that were tested. However, a 10% increase in the supply voltage resulted in a 20% load shift of the efficiency peak to the right for all the EE motors tested and an approximately 30% shift in the case of the standard motors.

- It was shown that both the EE and STD motors resulted in a drop in efficiency under voltage unbalance supplies. Both types of motors showed a similar decrease in

efficiency at the motor's rated temperature. The decrease in efficiency greatly depends on the temperature of the motor. The results show that there is no shift in the peak of the efficiency curve towards a different load under unbalanced supply conditions. This indicates that the constant and load dependent losses are equal at the same load relative to the balanced case.

- The combined effect of voltage unbalance and under- or overvoltage, was a shift in efficiency to different load and a decrease in efficiency. This indicates that the constant and load dependent losses are not only higher, they also intersect at a different load.

8.2 RECOMMENDATIONS

Based on the conclusions drawn in this thesis the following recommendation can be made:

- A comprehensive study was conducted on the steady-state differences between standard and EE motors. However, a more detailed investigation must be conducted on the transient performance of EE motors. The transient performance issues include start-up current analysis, start-up and breakdown torque performance. Also, a thorough assessment of EE motors supplied with unbalanced voltages during transient operation is necessary. This will ensure that satisfactory transient performance of EE motors are achieved in retrofit application. In particular, the high inrush current drawn by energy efficient motors may cause nuisance tripping of circuit breakers in retrofit applications, which needs to be investigated.

- For the purpose of this thesis four motor sizes were considered. However, to obtain more representative results more motors from more manufacturers should be tested and studied. This would provide a more representative sample of motors which could lead to a better generalisation of the results presented in this thesis.

- The error problem of the power analyser should be assessed in more detail. A possible solution is to apply a correction factor to the current reading in order to improve the current and power accuracies to acceptable limits. Another possibility is to replace the current shunts or the input modules on the power.

- The direct method should only be used, for efficiency estimation, for the comparison of trends of the efficiency vs load characteristic and when the absolute values are considered of less importance. The direct method is very

sensitive to the input variables, especially when the instruments used do not conform to the specification.

- The motor temperature should be allowed to stabilise for efficiency testing at each load and supply condition implemented. The standards require that the efficiency test be carried out at the motors' rated temperature regardless of the load. It was shown that the efficiency of a motor is greatly affected by its operating temperature. Failure to stabilise the temperature at the particular load, could result in an incorrect efficiency estimate. Care should be taken not to damage the motor insulation especially when overloaded and when supplied with unbalance voltages. For the efficiency testing of motors with unbalanced supplies, derating of the load should be considered.

- EE motors operate at a lower slip when retrofitting a standard motor in a centrifugal pump load application. The higher output power delivered to the pump and hence the marginally lower input power drawn from the supply could result in negligible savings to the user. This phenomenon should thoroughly be investigated with several load and EE motor types. This could represent a serious threat to the success of Eskom DSM's EE motor program.

- The operating efficiency of a motor can be optimized by varying the supply voltage. A load requiring say 50% of the rated power of the motor, can be driven more efficiently by lowering the supply voltage by approximately 10%.

- Although motors can be derated to prevent damage to the winding insulation, it is not recommended that motors are operated under unbalanced supplies as this reduces its efficiency.

REFERENCES

[1] "Introduction to Premium Efficiency Motors", [Online] Available: http://www.copper.org/applications/electrical/energy/motor_text.html, Accessed: 22/03/2010

[2] C. T. C. Andrale, R. S. T. Pontes, "Three-Phase Induction Motors Energy Efficiency Standards – A Case Study", [Online] Available: http://www.aedie.org/11chlie-papers/196_andrade.pdf. Accessed: 22/03/2010

[3] "Research project: Efficiency Determination Methods", [Online] Available: www.cemep.org, Accessed: 22/03/2010

[4] "IEC 60034-30 Ed. 1.0 Standard IEC 60034-30: Rotating electrical machines - Part 30: Efficiency classes of single speed, three-phase, cage-induction motors (IE-code)" , IEC 60034-30, 2007

[5] "EE Motors participating suppliers", [Online] Available: http://www.eskomdsm.co.za, Accessed: 22/03/2010

[6] G.C. Paap, "Symmetrical Components in the Time Domain and Their Application to Power Network Calculations", IEEE Transactions On Power Systems, Vol. 15, No. 2, May 2000.

[7] M.M. Berndt and N.L. Schmitz, "Derating of Polyphase Induction Motors Operated with Unbalanced Line Voltages", AIEE Trans. Power Apparatus and Systems, Vol. 81, pp. 680-686, Feb. 1963

[8] W.H. Kersting and H. Phillips," Phase Frame analysis of the Effects of Voltage unbalance on Induction Machines", IEEE Trans. on Industry Applications, Vol. 33, No. 2, March/April 1997.

[9] C.F. Wagmer, R.D. Evans, "Symmetrical Components as applied to the analysis of Unbalanced Electrical Circuits", New York and London, Mc Graw Hill Book Company, Inc. 1933

[10] "Motors and Generators", NEMA Standards Publication no. MG 1-1993.

[11] W. Du Deprez, "Energy Efficiency of induction Machines; A Critical Assessment", PHD thesis, Katholieke Universiteit Leuven, Dec. 2008

[12] "IEEE Standard Test Procedure for Polyphase Induction Motors and Generators", IEEE STD112-2004

[13] "Standard methods for Determining losses and efficiency from tests (excluding machines for traction vehicles)", IEC 60034-2-1, 2007

[14] Nagornyy, A.K. Wallace, A. Von Jouanne, "Stray Load Loss Efficiency Connections", IEEE Industry Applications Magazine, May/June 2004

[15] Parasiliti F., Villani M., Paris C., Walti O., Songini G., Novello A., Rossi T., "Three-Phase Induction Motor Efficiency Improvements With Die-Cast Copper Rotor Cage And Premium Steel", Proceedings of SPEEDAM'04 Symposium, Capri, Italy, 16-18 June 2004.

[16] P. Pillay, P. Hofmann, "Derating of Induction Motors Operating with a Combination of Unbalanced Voltages and Over- or Undervoltages", IEEE Trans. on Industry Applications, 2001

[17] Kueck J.D.,Casada D.A., Otaduy P.J., "A Comparison of Two Energy Efficient Motors", IEEE Trans. on Energy Conversion, Vol. 13, No. 2, June 1998

[18] L. Refoufi, H. Bentarzi, F. Z. Dekandji, "Voltage Unbalance Effects on Induction Motor Performance", 6th WSEAS International Conference on Simulation, Modelling and Optimization, Lisbon, Portugal, Sept 2006.

[19] P. Pillay, M. Manyage "Loss of Life in Induction Machines Operating With Unbalanced Supplies", IEEE Transactions On Energy Conversion, Vol. 21, No. 4, December 2006

[20] "Methods for Determining Losses and Efficiency of Rotating Electrical Machinery from Test", IEC 34-2, 1996.

[21] Boglietti, A. Cavagnino, M. Lazzari, M. Pastorelli, "International Standards for the Induction motor Efficiency Evaluation: A Critical Analysis of the Stray–Load Loss Determination", IEEE Transactions on industry Applications. Vol. 40, No. 5, September/October 2004.

[22] Slaets, P. Van Roy, R. Belmans, K. Hameyer, "Energy Efficiency of Induction Machines", Katholieke Universiteit Leuven, E.E. Dept, Div. ESAT/ELEN, Kardinaal Mercierlaan 94, B-3000, Leuven, Belgium

[23] de Almeida, F. Ferreira, J. Busch, P. Angers," Comparative Analysis of IEE 112-B and IEC 34-2 Efficiency Testing Standards Using Stray load Losses in Low-Voltage Three-

Phase, Cage Induction Motors", IEEE Transactions on industry Applications. Vol. 38, No. 2, March/April 2002.

[24] "Method for determining losses and efficiency of three-phase cage motors.", IEC STD 61972, 2002

[25] J. A. Rice , "Mathematical Statistics, Second Edition" by. Duxbury Press (An imprint of Wadsworth Publishing company). copyright '95

[26] D. B. Pengra and L. T. Dillman, 'Notes on Data Analysis and Experimental Uncertainty', Ohio Wesleyan University, University of Washington,

[27] L. Underhill and D. Bradfield, "Introstat", Department of Statistical Sciences, University of Cape Town. Jan '07

[28] W. Cao, K. J. Bradley, H. Zhang and I. French, 'Experimental Uncertainty in Estimation of the Losses and Efficiency of Induction Motors', 2006 IEEE

[29] Lu, T. G. Habetler and W. Cao, 'Error Analysis of Motor-Efficiency Estimation and Measurement', 2007 IEEE

[30] de Almeida, S. Greenberg, C. Blumstein, "Demand –Side Opprtunities Through The Use of Energy-Efficient Motor Systems", IEEE Transactions On Power Systems, Vol. 5, No. 3, August 1990

[31] E Chiricozzi, F Parasiliti, M Villani, "New Materials and Innovative Technologies to Improve the Efficiency of Three-phase Induction Motors. A Case Study", International Conference on Electrical Machines (ICEM 2004)

[32] Parasiliti F., Villani M., Paris C., Walti O., Songini G., Novello A., Rossi T., "Three-Phase Induction Motor Efficiency Improvements With Die-Cast Copper Rotor Cage And Premium Steel", Proceedings of SPEEDAM'04 Symposium, Capri, Italy, 16-18 June 2004.

[33] Bonnett.A.H, "Understanding Efficiency in Squirel-Cage Induction Motors", IEEE Trans. On Industry Appl., vol IA-16, No.4. July/August 1980

[34] Penrose H.P, "Anatomy of an Energy Efficient Electric Motor Repair", IEEE Electrical Insulation Magazine paper, Feb. 1997

[35] DG Walters, IJ Williams, DC Jackson, B Hansen, "The case for a new generation of high efficiency motors-someproblems and solutions", Electric. Mach. and Drives", 11-13 Sept. 1995, Conference Publication No. 412, IEE 1995

[36] Malinowski J, McCormick J, Dunn K, "Advances in Construction Techniques of AC Induction Motors: Preparation for Super-Premium Efficiency", IEEE Trans. on Ind. Appl., Vol. 40, No. 6, Nov./Dec.2004

[37] Bonett A. H., Yung C, "Increased Efficiency vs Reliability", IEEE Industry Applications Magazine, Jan/Feb 2008

[38] Nagornyy, A.K. Wallace, A. Von Jouanne," Stray Load Loss Efficiency Connections", IEEE Industry Applications Magazine, May/June 2004

[39] P.C. Sen, " Principle of Electric of Machines and Power Electrical" John Wiley & Son, 1997

[40] N. Mohan, T.M. Underland, W.P. Robbins, "Power Electronics Converter, Application, and Design." Third edition, John Wiley & Son, Inc., 2003

[41] "Power Quality and performance Issues with Energy-Efficient motors" Commentary Number 2, November 1998

[42] R.L. Nailen, "Motor Inrush Current: What Does It Really Mean?" *Electrical Apparatus Mag.,* p 12 March 1994

[43] R.G. Bartheld and S.F. Farag, "Energy-Efficient Motor Coordination," *in Conf. Rec. 1985 Annu. Meet. IEEE Pulp and Paper tech*. Conf., pp65-67, (85CH2129-5)

[44] J. Piotrowski, "Shaft alignment handbook: Third Edition"

[45] A. H. *Bonnett* ,"An *Update* on AC *Induction Motor*. Efficiency", IEEE Trans. on Ind. Appl., Vol. 30, No. 5, Sept./Oct.1994

[46] "Guide to the Expression of Uncertainty", Saudi Arabian Standards Association, Draft No.13,200

[47] M. Foroutan, "Protocol for Calculation of Measurement Uncertainty in Analytical Chemistry", Prepared for the National Laboratory for Environmental Testing, Oct.27,2005

[48] EASA, “Understanding Energy Efficient Motors”, [Online] Available: https://smtp.cpuaid.com/easa/resources/cgis/displayitem.cgi?category=2&name=Promotional+Materials&item=5, Accessed: 27/03/2010